Regulation of microtubule attachment at the kinetochore and cell cortex

David M. Kern

ScB Biochemistry and Molecular Biology
Brown University
2009

Submitted to the Department of Biology in partial fulfillment
of the requirements for the degree of

Doctor of Philosophy in Biology
Massachusetts Institute of Technology
February 2016

Signature of the author: Signature redacted

Department of Biology
December 18, 2015

Certified by: Signature redacted

Iain M. Cheeseman
Associate Professor of Biology
Thesis Supervisor

Certified by: Signature redacted

Amy E. Keating
~~Associate~~ Professor of Biology
Chair, Committee for Graduate Students

Regulation of microtubule attachment at the kinetochore and cell cortex

By David M. Kern

Submitted to the Department of Biology on December 18, 2015
in partial fulfillment of the requirements for the degree of
Doctor of Philosophy in Biology

Abstract

During mitosis, the cell divides in two, evenly distributing the genetic material and splitting the rest of cellular contents between the resulting daughter cells. This process is essential, rapid, and complex, requiring precise timing and the collaboration of many proteins. Mistakes made during mitosis can have immediate and catastrophic effects, resulting in cell death. In an organismal context, small mistakes in the relative size of the resulting daughter cells or the angle of division can have compounding consequences for development and function of complex organs, such as the brain. Mitotic chromosome segregation failures and the resulting DNA damage is also a hallmark of human cancers. There are multiple organelles that must work together to acheive a successful mitosis, including the chromosomes, kinetochores, centrosomes, and the microtubule cytoskeleton that forms the mitotic spindle. To assemble the mitotic spindle, the two centrosomes radially nucleate dynamic microtubules that make important connections with kinetochores and the cell cortex. Kinetochores mediate the connection between the chromosomes and microtubule cytoskeleton, whereas the astral microtubules contact the cell cortex and play an important role in positioning the mitotic spindle within the cell. In this thesis, I investigate the establishment and regulation of these two important microtubule-based connections. This work focuses on the kinetochore protein KNL-1, a component of the KMN (KNL-1, Mis12, Ndc80) network, and the kinetochore and microtubule-associated Astrin/SKAP complex. KNL-1 is a kinetochore specific scaffolding protein that I show to have the ability to form large oligomers in nematodes. The Astrin/SKAP complex has the unique property of localizing to diverse mitotic structures, including the kinetochore. I present data that the Astrin/SKAP complex plays multiple roles in mitosis, including kinetochore-microtubule attachment, centrosome integrity, and a previously unknown role in spindle positioning. Together, these results contribute to our understanding of kinetochore protein behavior and regulation and add a new complex to our emerging model of the microtubule connections facilitating mitotic spindle positioning.

Thesis Supervisor: Iain M. Cheeseman
Title: Associate Professor of Biology

Acknowledgements

Thank you Iain for being an awesome mentor. I might hold the record for most time spent in the same lab room as you and I think it is a solid testament to our relationship that we still get along. There are many things that you have taught me scientific and otherwise, but two things, to me, especially exemplify your strengths as a scientist and PI. First, you have taught me by example to conduct science by pursuing interesting questions with curiosity and intensity, without fear of new techniques or scientific hurdles. Second, you lead a lab by enabling the scientific curiosity of its members. This hasn't just been true for me, but for everyone I have seen pass through, and it is impressive. This requires planning, energy, and trust on your part, and it is greatly appreciated.

I spanned what I would call the first and second generation of the Cheeseman Lab and therefore have a lot of members that I have to thank for providing a great environment for conducting research. Jens, thanks for being my rotation mentor and biochemistry bro. Karen, Tomomi, and Julie, thanks for sharing your post-doc wisdom, not killing me, and giving some good and varied examples of how to conduct science. Sasha, hopefully your time in lab was useful and thanks for teaching me about MIT culture. Chelsea, thanks for being my first baymate and teaching me the ropes. Your sterile technique is impeccable. To our multiple Dutch master students Mathijs, Charlotte, and Sanne, thanks for giving me a glimpse into your country, perspective, and lots of orange. Florencia, your fashion advice will stick with me. Every time I wear black and blue together I will know I am a trendsetter. Kara, thanks for always being up for a discussion, on any topic (scientific, pop cultural, philosophical, etc.) and also for helping convince me that cell biology can be cool too. Julie, similar to your bench ancestor Tomomi, you also were a great late night conversation partner and troubleshooter. Keep on representing St. Louis; one day I will get my frozen custard. Scott, thanks for passing on the quick dot blot technique. Tonia, you also taught me a lot about MIT culture and I aspire to your farewell gift giving and egg hiding ability. Kuan-Chung, you were my longest standing baymate, proof of your character, which is matched only by your microscopy and eating abilities. Ian, thanks for teaching me about lawn games, vegas odds, and occasionally bringing me and Laurel our energy drink fix. Zak, it was awesome to have our paths cross again. Nolan, your roller coaster equanimity and your T-shirt collection far surpass my own. Good luck, and hopefully everyone, with Iain's help, will keep the lab motto kicking for years to come.

Thanks to my collaborators. Mike Rigney for helping with electron microscopy, the Desai lab for helping with worm experiments, and Pete for helping with mouse testis experiments and teaching me about Australia.

MIT and the Whitehead are great places to work. Thanks to all the people who make the Institutes tick. Also thanks to all my sources of food and drink in the Kendall area.

The biology graduate program at MIT is excellent, and the students are a big part of that. I was lucky to share a house with Paul and David and have other classmates like Genny, Boris, Ben, Izarys, Daisy, Oksana, Robert, Glenna, Alex, and many more who I got to talk about science, troubleshoot experiments, attend weddings, play Frisbee, and generally have a good time with.

I would like to acknowledge Mark Johnson and Amit Basu for trusting a noob and giving me my first chance to do some science. That first summer really convinced me that this was the thing I wanted to do.

They also originally introduced me to Laurel. She manages to tolerate my personality and actually seems to like it occasionally. She has helped me through scientific slumps, been an awesome friend and companion, lifting bro, and occasionally will let me have some coffee.

My extended family has been supportive, always reminding me that it is time to graduate or find a real job. Thanks to my brother for lots of random conversations, and for being the main family member who can understand enough of biology to not be bored immediately. My parents have been awesome, regardless of where on the scientific rollercoaster I am. They may think research is torture based on our phone conversations, but they also know that I enjoy it. They have taught me a lot about patience and hard work. Also thanks to them for generously allowing me to play a *reasonable* amount of video games. The persistence, creativity, and thumb strength they helped me develop has transferred remarkably well to science.

Finally, thanks to my committee: Bob, Thomas, Terry, and Bruce, for either giving me advice through the years, giving me the opportunities to rotate in your labs, help teach your classes, and/or being available for committee meetings, thesis reading, and defense(s).

Table of Contents

Abstract **3**
Acknowledgements **5**

Table of Contents **8**

Chapter I: Introduction **11**
Mitosis **12**
Microtubules **15**
The mitotic spindle **16**
The kinetochore **18**
The inner kinetochore 19
The outer kinetochore 20
KNL-1 21
The Astrin/SKAP complex **25**
Microtubule binding and plus-end-tracking proteins **26**
Mitotic spindle positioning **28**
Cortical Dynein Regulation at the Cortex 29
Findings Presented in this Thesis **31**
References **36**

Chapter II: The outer kinetochore protein KNL-1 contains a defined oligomerization domain in nematodes **44**
Abstract: **45**
Introduction **46**
Results **48**
The nematode KNL-1 N-terminus oligomerizes 48
The KNL-1 oligomerization domain forms a defined higher-order oligomer 50
The KNL-1 oligomerization domain forms a circular structure when visualized by electron microscopy 53
KNL-1 oligomerization occurs through a small hydrophobic region 54
KNL-1 oligomerization mutants do not dramatically disrupt chromosome segregation 57
Discussion **60**
Materials and Methods **64**

Chapter III: Discovery of the mitotic SKAP isoform reveals a spindle positioning role at astral microtubule plus ends **73**
Abstract **74**
Introduction **75**
Results **78**
SKAP has both mitotic and testis/meiosis-specific isoforms 78
The longer, testis-specific SKAP isoform localizes to elongating spermatids and meiotic cells 82

Short SKAP, but not long SKAP, is fully functional to facilitate mitosis 84
SKAP microtubule binding activity is necessary for Astrin/SKAP spindle localization and chromosome segregation 89
The short SKAP isoform displays robust plus-end-tracking in mitosis 91
Astrin/SKAP localization to microtubule plus ends is necessary for proper spindle positioning 95
The SKAP plus-end-tracking mutant alters astral microtubule behavior at the cell cortex 99
The Astrin/SKAP complex binds and regulates Clasp1 in mitosis 102
Discussion 106
Materials and Methods 112
Acknowledgements 120
References 121

Chapter IV: Discussion and Future Directions 126
Key conclusions of this thesis 127
Nematode KNL-1 forms a defined oligomer in vitro, but does not play a major role in kinetochore structure and function 127
SKAP has a testis-expressed and a novel mitotic isoform 128
SKAP microtubule binding is necessary for Astrin/SKAP complex spindle localization and function 130
The Astrin/SKAP complex is a plus-end tracker which localizes to astral microtubule plus ends 130
The Astrin/SKAP complex plus-end-tracking is needed for metaphase spindle positioning 131
The Astrin/SKAP complex interacts with multiple other spindle positioning proteins and regulates Clasp1 localization in mitosis 132
Unanswered questions and future directions 133
What is the structural role of KNL-1 within the kinetochore? 133
What are the organizing principles governing outer kinetochore architecture? 134
What is the role of the testis isoform of SKAP? 135
Is the Astrin/SKAP complex a mitotic stabilizing factor at centrosomes and kinetochores? 136
What is the mechanism of astral microtubule and cortical dynein force generation? 137
Concluding remarks 138
References 140

Appendix: 144
Kinetochore Structure: Pulling Answers from Yeast 145

Chapter I: Introduction

Mitosis

Mitosis is the process where a cell, having grown in size and replicated its DNA, evenly divides its genetic material and splits its contents between two new cells. Cell division is an important mechanism for the growth and maintenance of single and multi-cellular organisms. The actual process of mitosis is both rapid and highly complex. In a human tissue culture cell, less than five percent the cell cycle (~ 1 hour) is spent performing this critical step (Cheeseman and Desai, 2008). Yet to reach adulthood, the human body must complete mitosis many trillions of times without significant error. A misregulated or defective mitosis can lead to maladies including cancer (Hanahan and Weinberg, 2011) or genetic defects. Therefore, the study of mitosis is essential for understanding the biology of life and disease.

As mitosis is a fundamental process, it is tempting to conclude that the mechanisms of mitosis will be fundamentally conserved. Many model organisms, including yeasts, fruit flies, Xenopus, nematodes, and others have contributed to understanding the kinetochore and mitosis (Gonczy, 2008). However, there are major differences between the cells in these organisms and human cells. These differences must be considered when applying concepts across phylogenetic trees. In the context of this thesis, there are a several key considerations. First of all, the nematode *Caenorhabditis elegans*, the subject of the second chapter of this thesis, is a holocentric organism (Melters et al., 2012), meaning that in mitosis the entire chromosome is coated with a kinetochore assembly. This

places unique structural and regulatory constraints on the kinetochore and spindle that can impact the appearance, sequences, and organization of many mitotic proteins (Cheerambathur et al., 2013; Drinnenberg et al., 2014; Gassmann et al., 2012). Secondly, some proteins, such as the vertebrate specific Astrin/SKAP complex (the focus of the Third Chapter), are only present in certain organisms. Finally, increasing size, complexity, and lifespan place an increasing burden on an organism to perform flawless cell division. Organisms with many necessitate more divisions and compound the detrimental effects of early errors over a large organism and longer lifetime. Therefore, the importance of regulatory networks and redundancy also increases.

In human cells, mitosis begins with the condensation of chromosomes and breakdown of the nuclear envelope (Figure 1). Microtubules grow outward from centrosomes and bind to the kinetochore attachment site on chromosomes. As the cell proceeds from prophase to metaphase, dynamic microtubule polymers and associated proteins align chromosomes at the center of the cell (Cheeseman, 2014; Cheeseman and Desai, 2008). A regulatory system called the spindle assembly checkpoint halts mitotic progression until all chromosomes are aligned at the metaphase plate (Vleugel et al., 2012). When this checkpoint is satisfied, anaphase occurs and the chromosomes separate. Then chromosomes move towards the poles and centrosomes move apart in processes termed anaphase A and B respectively (Sullivan and Morgan, 2007). The final step of mitosis is telophase, when the cell is cleaved in half to physically generate the

daughter cells, chromosomes decondense, and the nuclear envelope is reconstructed. The basic structure that organizes and conducts these mitotic events is called the mitotic spindle (Walczak and Heald, 2008). This structure is composed of microtubules, a highly dynamic cytoskeletal polymer.

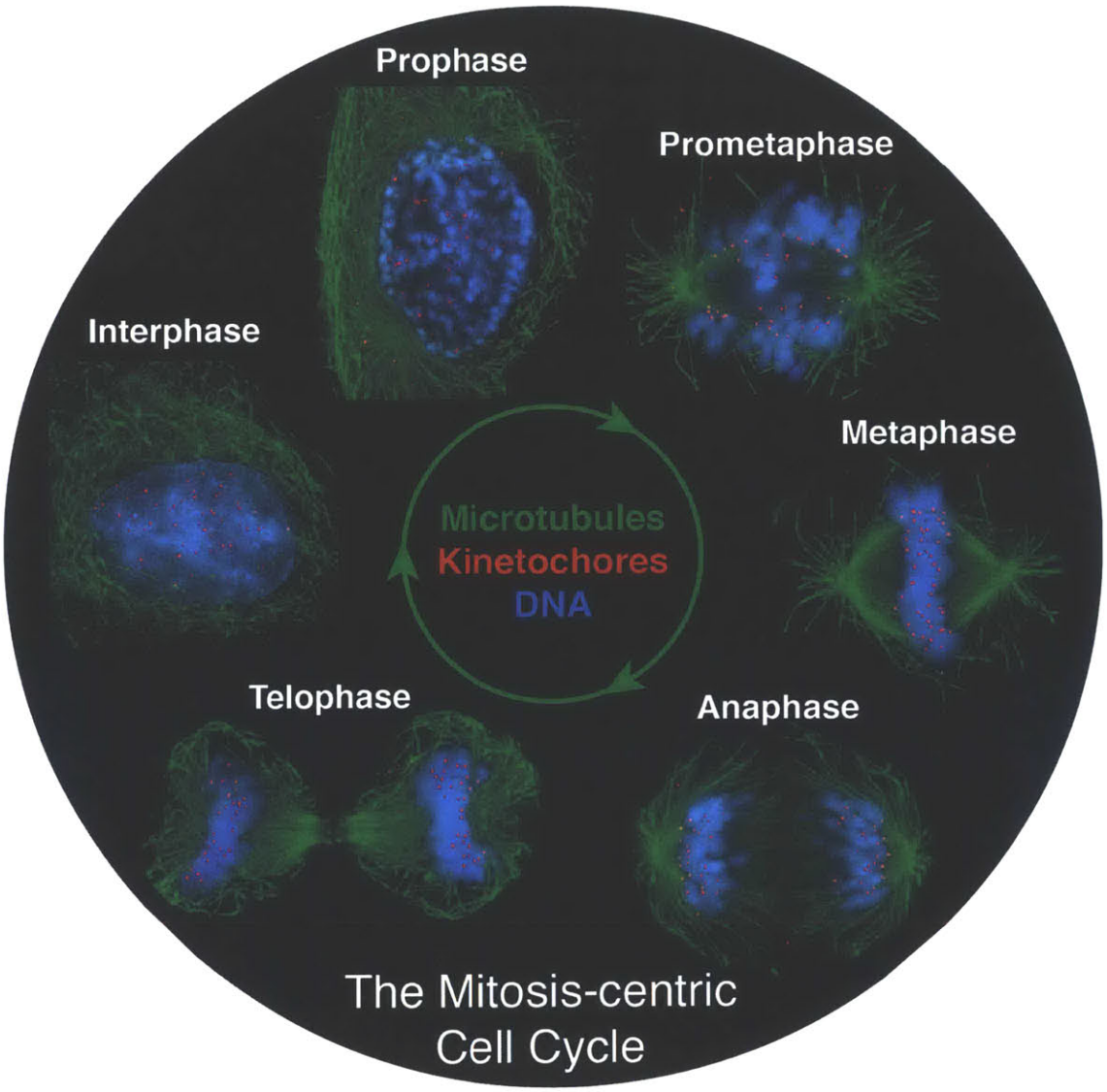

Figure 1. The human, mitosis-centric cell cycle. An interphase human cell and cells in the five stages of mitosis are shown (Adapted from (Cheeseman and Desai, 2008))

Microtubules

Microtubules are one of the major cytoskeletal polymers in the cell, and are made up of polymerized dimers of alpha and beta-tubulin (Figure 2A). Each tubulin subunit can bind GTP, and beta-tubulin has GTPase activity. The tubulin dimer adopts a straight conformation with bound GTP and a slightly curved form when GTP is hydrolyzed by beta-tubulin to GDP. Straight tubulin dimers can assemble into microtubule structures by associating end to end and laterally into a polymer. The asymmetric nature of the dimer gives the microtubule its polarity, with the beta-tubulin end termed the plus end and the alpha-tubulin end termed the minus end. Tubulin dimers preferentially add to the plus end, and in the cell the minus end is generally anchored at the centrosome.

The biochemical properties of tubulin GTP hydrolysis give rise to the special behavior of microtubules, termed dynamic instability (Mitchison and Kirschner, 1984) (Kristofferson et al., 1986). Microtubules can grow as long as new GTP bound (straight) dimers are added to the plus end, but at the same time GTP hydrolysis occurs within the microtubule after tubulin is incorporated. The energy created by this hydrolysis is stored within the polymer, as incorporated GDP dimers cannot convert to the preferred curved conformation within the microtubule lattice. However, if GTP dimers are added too slowly, hydrolysis can catch up with the plus end and incorporated dimers can begin to curve (Desai and Mitchison, 1997). When this occurs the protafilaments (lines of dimers making up the tube) peel back, dimers fall into solution, and the entire

microtubule rapidly depolymerizes in a process called catastrophe. Dynamic instability grants microtubules the ability to grow and shrink quickly, which is essential for mediating the rapid and complex events of mitosis.

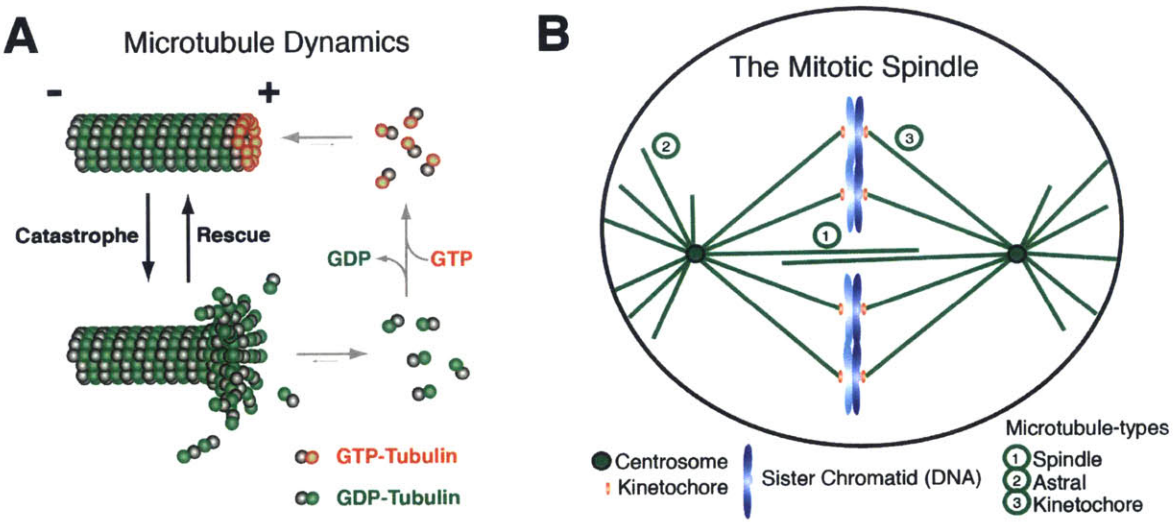

Figure 2. Microtubules and the mitotic spindle. (A) Diagram showing the dynamics of microtubule growth (top) and microtubule decay (bottom). GTP-tubulin adds to the growing plus end of the microtubule. When tubulin dimers are incorporated, they transition from the GTP to GDP bound state. If enough GDP-tubulin is exposed at the plus end, the microtubule will shrink in the process of catastrophe. The microtubule can also begin growth again in a process called rescue. (B) A simplified diagram of the mitotic spindle with microtubules (Spindle, Astral, and Kinetochore), centrosomes, kinetochores, and chromosomes depicted. Spindle microtubules reach across the cell and can be acted on by kinesins at intersection points to lengthen the spindle. Astral microtubules reach out to the cell cortex and are important for positioning the spindle. Kinetochore microtubules connect to the kinetochores, which are situated on the centromeres of chromosomes. (Images adapted from (Cheeseman and Desai, 2008))

The mitotic spindle

The major machine of mitosis is the spindle (Walczak and Heald, 2008), a mega complex that connects centrosomes, kinetochores, and the cell cortex using the dynamic microtubules (Figure 2B). Originating at the centrosomes, the

microtubules radiate outwards and are defined by their orientation and destination. Spindle microtubules grow from the two centrosomes towards the center of the cell. Here microtubules may meet in an antiparallel fashion and specialized kinesin motors use this overlap to slide centrosomes apart (Kapitein et al., 2005). This activity helps create a bipolar spindle early in mitosis and contributes to centrosome separation in anaphase B. Microtubules that grow away from the cell center are called astral microtubules. These are relatively fragile microtubules prone to shrinking, but if they continue to grow they will reach the cell cortex, a region on the inner side of the cell membrane. Once there, these microtubules can transiently bind the microtubule minus-end directed motor dynein, which can pull on astral microtubules to position the spindle (Kiyomitsu, 2015; Kiyomitsu and Cheeseman, 2012). Microtubules that contact chromosomes through the action of chromokinesin proteins act to push chromosomes away from the poles and towards the cell center (Cheeseman and Desai, 2008). Finally, the bundles of microtubules that form stable attachments to kinetochores are called kinetochore microtubules or kinetochore fibers (Rieder, 1981). These microtubules attach to kinetochores on each sister chromatid, which are in turn connected by the cohesin complex. These connections create tension across the centrosome-chromosome-centrosome connection, and this tension is utilized to give shape to the spindle in metaphase and provide force for chromosome separation in anaphase. Thus the cell, using these three microtubule populations and a delicate balance of forces, assembles and

positions the mitotic spindle within the cell. There are multiple critical complexes that make this intricate structure possible, but perhaps the most central is the kinetochore.

The kinetochore

The kinetochore is a macromolecular complex that mediates the connection between chromosomal DNA and microtubule polymers (Cheeseman, 2014; Cheeseman and Desai, 2008) (Figure 3). In humans, the kinetochore is composed of over 100 proteins and, owing to its mitotic role, is highly dynamic. The kinetochore assembles, performs multiple functions, and then disassembles, all within 60 minutes. There are three major classes of kinetochore proteins, which I will loosely classify as the inner kinetochore, the outer kinetochore, and the dynamic kinetochore proteins.

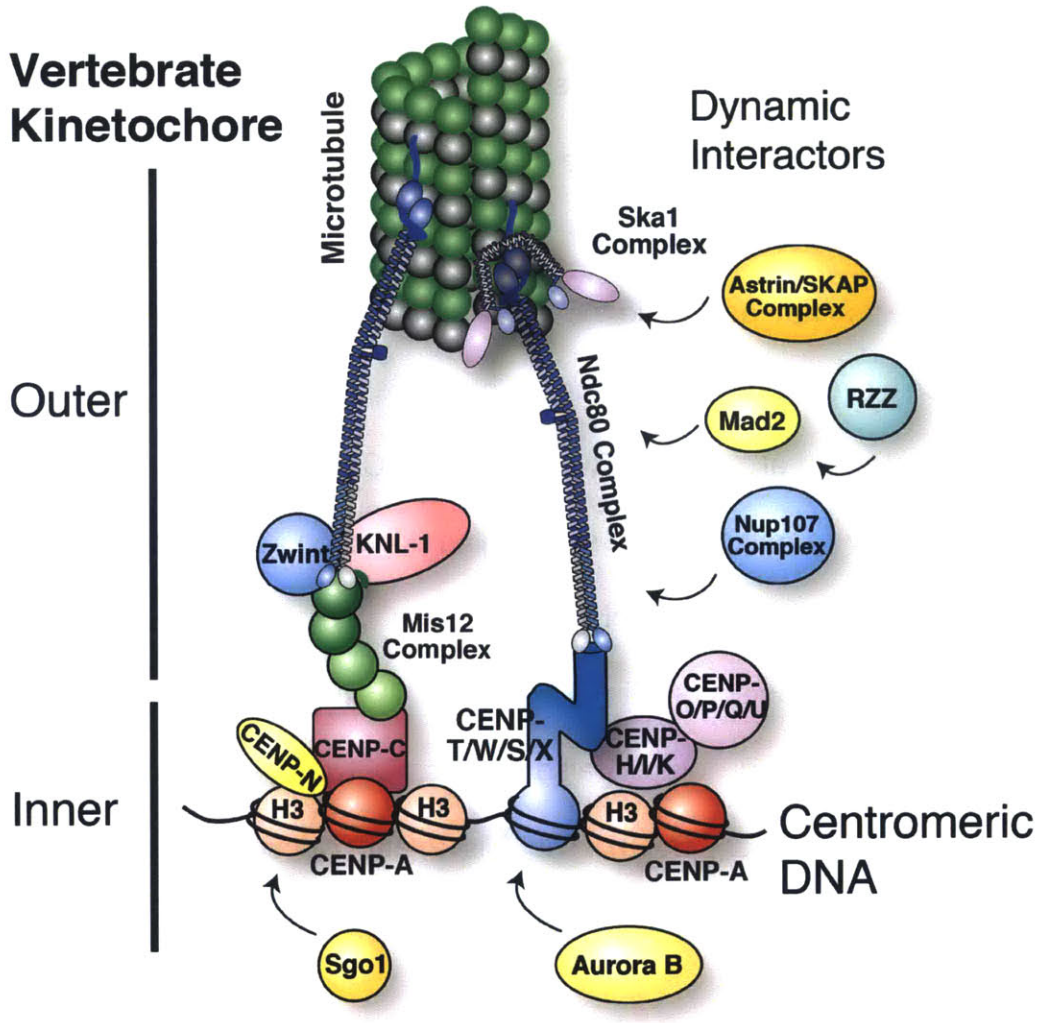

Figure 3. The vertebrate kinetochore. A simplified schematic of the kinetochore depicting the DNA and microtubule attachment sites and the inner and outer protein regions. KNL-1, of the outer kinetochore and the KMN network, is shown in pink and is the subject of Chapter Two. A selection of the dynamic interactors, proteins that localize to the kinetochore without well established binding sites, are shown on the right. The Astrin/SKAP complex, a member of this class, is the subject of Chapter Three. (Image adapted from (Cheeseman, 2014))

The inner kinetochore

The inner kinetochore, responsible for attaching to chromosomes, assembles on a DNA binding region named the centromere (McKinley and Cheeseman, 2015).

The base of the inner kinetochore is a histone H3 variant called CENP-A, which incorporates into specialized nucleosomes found exclusively at the centromere. The placement of CENP-A determines the site of kinetochore assembly, and the stable CENP-A pool is replenished each cell cycle during G1. Together with CENP-A, the proteins that assemble near the DNA interface and are stable throughout the cell cycle are termed the Constitutive Centromere Associated Network or CCAN (Hori et al., 2008) . Two particular CCAN components, CENP-C and CENP-T, play a critical role in bridging kinetochore sub-complexes (Gascoigne et al., 2011). CENP-C, which also binds CENP-A, reaches outward from the CCAN and contacts the Mis12 complex. CENP-T, which contains a nucleosome-like DNA binding domain, also reaches outward and contacts the Ndc80 complex (Nishino et al., 2013). The Mis12 and Ndc80 complexes are important members of the outer kinetochore.

The outer kinetochore

The outer kinetochore is responsible for binding to microtubules, holding on to growing and shrinking microtubules, and sensing and regulating microtubule attachments. Outer kinetochore proteins can be roughly divided into two classes, those that are stable kinetochore members during mitosis and those that dynamically associate with the kinetochore. The former class is primarily comprised of components of the KNL-1, Mis12 complex, Ndc80 complex (KMN) network (Cheeseman et al., 2006). The Ndc80 complex is the conserved microtubule binder of the kinetochore and is made up of four proteins, each with

a globular and a coiled-coil domain (Ciferri et al., 2008; Wigge and Kilmartin, 2001). The Spc24 and Spc25 subunits form the CENP-T or Mis12 binding base of the Ndc80 complex, and the Nuf2 and Ndc80 subunits contact the microtubule. Ndc80 is the largest protein in the complex and contains an additional element; a charged, unstructured N-terminal domain that aids in microtubule binding (Alushin et al., 2012). The Mis12 complex is also composed of four subunits and acts as a central hub for the kinetochore, as it is positioned between the inner kinetochore and the rest of the outer kinetochore components (Goshima et al., 2003; Kline et al., 2006; Obuse et al., 2004). Finally, KNL-1 is a single large protein that plays multiple functions, including acting as a scaffold for many of the dynamic outer kinetochore components. The proteins of the KMN network are present at an estimated number of 8-20 copies per microtubule across many organisms (Lawrimore et al., 2011). In human cells, there are 15-20 microtubules per kinetochore attachment site at the regional centromere (Cheeseman and Desai, 2008). In *C. elegans*, kinetochore proteins coat entire chromosomes. Therefore, to understand kinetochore-microtubule attachment and its mitotic function, it is essential to understand the structure and organization of the KMN network.

KNL-1

KNL-1, or kinetochore null protein 1 (Figure 4), was initially found using an RNAi screen in *Caenorhabditis elegans* (Cheeseman et al., 2008a; Desai et al., 2003). In this organism, loss of KNL-1 leads to a complete lack of kinetochore-

microtubule attachments. However, in other organisms KNL-1 depletion or knockout instead leads to a variety of defects including improper microtubule attachments and a defective spindle assembly checkpoint (Cheeseman et al., 2008b; Kerres et al., 2007; Kiyomitsu et al., 2007; Rosenberg et al., 2011). KNL-1 integrates into the KMN network through a Mis12 binding domain at its C-terminus (Petrovic et al., 2014). The C-terminus also contains a coiled-coil region, which recruits the small protein Zwint in humans and other binding partners in yeasts and *C. elegans* (Pagliuca et al., 2009; Starr et al., 2000; Wang et al., 2004; Zhang et al., 2015). These structured regions are notable in that they are the only stretches of predicted or experimentally proven structure in KNL-1 (Petrovic et al., 2014). KNL-1 is a large protein, ranging from ~1000 amino acids in yeast and *C. elegans* to over 2000 amino acids in humans and over 5000 amino acids in opossum (Uniprot, 2009). Much of this variation in sequence is due to the extension of a repeated sequence element in the middle of the protein. This repeat contains the amino acid sequence "MELT", which has been shown to be the phosphorylation site for the Mps1 checkpoint kinase and a docking site for the checkpoint proteins Bub1, Bub3, and BubR1 (Krenn et al., 2014; Shepperd et al., 2012; Vleugel et al., 2015; Yamagishi et al., 2012). These repeats are predicted to be unstructured, although they can form small structured regions or be clustered through the action of binding checkpoint complexes (Bolanos-Garcia et al., 2009). The extreme N-terminus of KNL-1 contains a region of positive charge, proposed to impart weak microtubule binding to the molecule

(Cheeseman et al., 2006), and a protein phosphatase 1 (PP1) binding domain (Liu et al., 2010). This PP1 recruitment site is essential, as PP1 is necessary to reverse the phosphorylation regulating microtubule binding at the kinetochore (Pinsky et al., 2006; Welburn et al., 2010). Early biochemical work on KNL-1 and KMN network reconstitution was performed using *C. elegans* proteins. In these experiments, KNL-1 appeared to have an oligomerization behavior, which was proposed to organize the many proteins that make up the KMN network at a kinetochore. To assess this hypothesis, I characterized the biochemistry, conservation, and function of KNL-1 oligomerization, which is the subject of Chapter Two of this thesis.

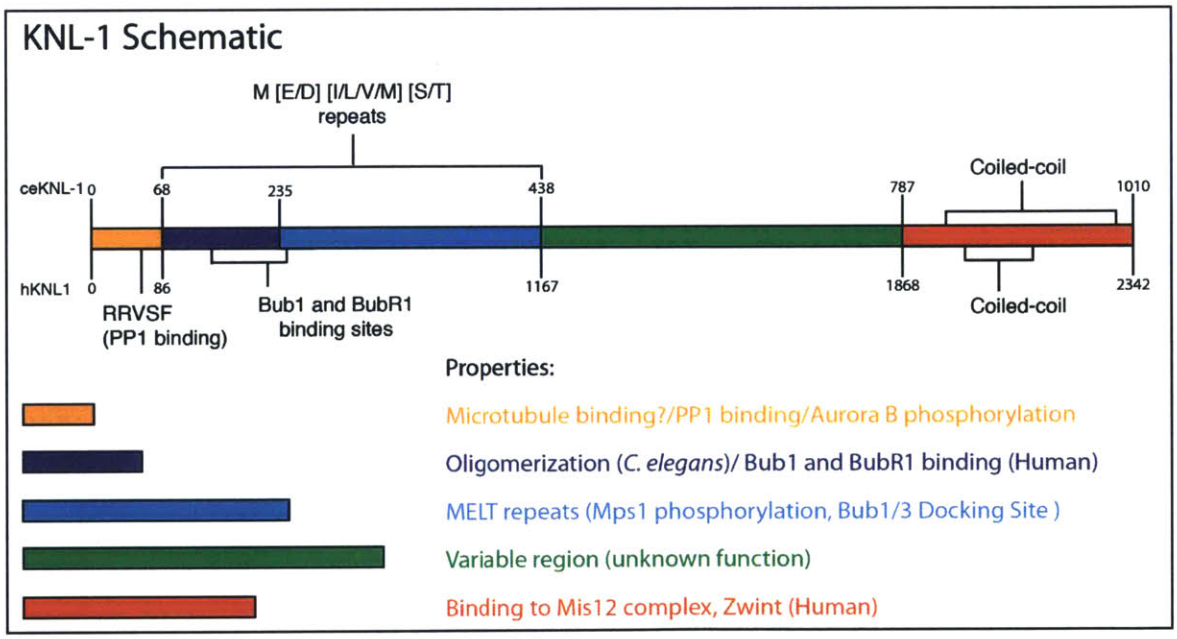

Figure 4. KNL-1. An annotated diagram of KNL-1 with residues relative domain locations for the human and *C. elegans* protein. The *C. elegans* oligomerization domain, shown in dark blue, is the subject of Chapter Two.

Dynamic kinetochore proteins

The third class of kinetochore components consists of the many proteins that dynamically localize to the kinetochore. Unlike the DNA-binding inner kinetochore proteins that localize throughout the cell cycle, or the structural and microtubule binding proteins of the outer kinetochore that localize for the duration of mitosis, dynamic kinetochore proteins have roles at specific time points. These dynamic proteins have characteristically weaker interactions with the kinetochore that are generally regulated by phosphorylation, competition, or a conformational change. Some of the most studied proteins in this class are the components of the spindle assembly checkpoint (Musacchio and Salmon, 2007). These proteins localize to the kinetochore in prophase, prior to the formation of stable kinetochore-microtubule attachments. Once these connections are made, checkpoint proteins disappear from the kinetochore. Intriguingly, dynamic localization is also shared by components of the nuclear pore complex, which resides at the kinetochore briefly during mitosis until anaphase onset (Orjalo et al., 2006; Zuccolo et al., 2007). These localization dynamics are often controlled by phosphorylation (Gascoigne and Cheeseman, 2011). Multiple mitotic kinases and phosphatases are also among the dynamic kinetochore proteins and play roles in regulating kinetochore assembly (CDK1) (Gascoigne et al., 2011), regulating microtubule attachment state (Aurora B and PP1) (Liu et al., 2010; Welburn et al., 2010), or establishing the spindle assembly checkpoint (Mps1) (Hiruma et al., 2015; Ji et al., 2015), among others. There are also multiple dynamic kinetochore proteins

that play roles in controlling microtubule dynamics, including the microtubule stabilizer Clasp1 (Maffini et al., 2009; Maiato et al., 2003) and the microtubule depolymerase MCAK (Andrews et al., 2004; Howard and Hyman, 2007). Finally, there are dynamic proteins that have been proposed to play a part in mediating the connection between kinetochores and microtubules, including the Ska1 complex (Schmidt et al., 2012; Welburn et al., 2009) and the Astrin/SKAP complex (Schmidt et al., 2010).

The Astrin/SKAP complex

The vertebrate specific Astrin (Mack and Compton, 2001) and SKAP (Fang et al., 2009) proteins, as well as the dynein light chain LC8 (Kardon and Vale, 2009; Schmidt et al., 2010), combine to form a dynamic kinetochore and microtubule interacting complex. Astrin was originally discovered in a proteomic screen of microtubule-associated proteins (MAPs) (Mack and Compton, 2001) and shown to have a role in human cells through depletion experiments (Gruber et al., 2002; Thein et al., 2007). SKAP was discovered later as a kinetochore localizing protein (Fang et al., 2009) and binding partner of Astrin along with LC8 (Dunsch et al., 2011; Schmidt et al., 2010). The Astrin/SKAP complex has a unique kinetochore localization, which is essentially the opposite of the spindle assembly checkpoint proteins, with Astrin/SKAP only fully localizing to kinetochores with proper microtubule attachments and tension. To achieve this, Astrin/SKAP localization is antagonized by the tension-sensing kinase Aurora B

(Schmidt et al., 2010). This metaphase and anaphase localization timing, coupled with chromosome misalignment and mitotic delay phenotypes, has led to the hypothesis that the Astrin/SKAP complex plays a role in kinetochore-microtubule attachments and anaphase onset. Together with this role at kinetochores, Astrin/SKAP have been implicated in maintaining centrosome cohesion (Thein et al., 2007), as depletions also lead to spindle multipolarity (greater than two microtubule organizing centers in mitosis) (Logarinho et al., 2012). However, previous studies on the Astrin/SKAP complex have not agreed on precise nature of its depletion phenotypes, and these have largely not been rescued. Furthermore, due to the pleiotropic nature of these phenotypes and transient and numerous Astrin/SKAP complex interactions, this complex has remained poorly understood. In Chapter 3, I focus on the Astrin/SKAP complex, particularly on its interactions with microtubules.

Microtubule binding and plus-end-tracking proteins

Microtubules have multiple associated proteins that take advantage of diverse microtubule properties to mediate their interactions. Tubulin has a negatively charged tail termed the E-hook, and grooves that proteins can use to dock along the microtubule. Therefore, proteins that bind to microtubules generally have positively charged domains or folds that utilize the exposed grooves of a microtubule. Classes of microtubule binding proteins include molecular motors, such as dynein (Kardon and Vale, 2009) and kinesin (Hirokawa et al., 2009), microtubule-associated proteins that associate along the microtubule lattice,

specialized kinetochore microtubule interactors, such as the Ndc80 complex (Ciferri et al., 2008), and a unique class of proteins called plus-end trackers (+TIPs) that associate with microtubule plus ends (Akhmanova and Steinmetz, 2015).

The major microtubule plus-end-binding proteins are the EB (End-binding) family of proteins that preferentially associate with the GTP-bound tubulin dimers at the growing end of a microtubule. When visualized in cells, these proteins have a characteristic comet tail appearance, with the trailing tail representing the region of GTP hydrolysis. As microtubules are continuously nucleated from centrosomes during mitosis, EB proteins give the characteristic appearance of fireworks marking all of the plus ends in a cell. Proteins that bind to EB proteins, using a motif containing the amino acids Sx(I/L)P, themselves acquire end-binding ability (Akhmanova and Steinmetz, 2015; Honnappa et al., 2009; Tamura et al., 2015). Plus-end-tracking is useful for proteins that modulate microtubule dynamics, as the simplest way to influence polymerization, depolymerization, or stability is at the microtubule tip. For example, both the microtubule stabilizer Clasp1 (Mimori-Kiyosue et al., 2005) and the microtubule depolymerase MCAK (Moore et al., 2005) are targeted to plus ends through their interactions with EB proteins. Therefore modifying or regulating the composition of proteins at the plus end confers can confer unique properties to different microtubule populations (Akhmanova and Steinmetz, 2015). For example, the stability of kinetochore microtubules is due to the end-on binding and anchoring of the plus end. On the

other hand, decreasing pro-growth factors or increasing microtubule-destabilizing factors can create highly dynamic populations, such as astral microtubules. The properties and control of microtubules are critical for the proper execution of the many steps of mitosis.

Mitotic spindle positioning

The position of the mitotic spindle is critical for cell division, as the placement of the metaphase plate helps to set the site of cell cleavage (Gonczy, 2008; Kiyomitsu, 2015; Knoblich, 2010; Siller and Doe, 2009). Individual cells generally favor a symmetrical division, as this distributes cellular contents evenly and gives each daughter cell a good chance to survive. In an organismal context, asymmetric divisions can occur as growing cells differentiate or form complex shapes. Furthermore, properly setting the angle of division is crucial for placing daughter cells in the correct location in a developing tissue (Bergstralh and St Johnston, 2014). Spindle and kinetochore microtubules help create the length, shape, and tension that define a mitotic spindle. The combined action of astral microtubules and cortically anchored dynein motor can then pull the spindle back and forth within the cell (Carminati and Stearns, 1997; Kiyomitsu and Cheeseman, 2012). As dynein is a minus-end directed motor (Cianfrocco et al., 2015), when it binds to an astral microtubule (Redwine et al., 2012), it can walk towards the centrosomes and impart a pulling force, tugging the spindle to that side of the cell (Figure 5A). Depending on organism and cell type, astral microtubule connections can be more or less stable. If a cell needs to perform an

asymmetric division, such as those in the *C. elegans* early embryo, astral microtubule connections on one side of the cell need to be strong and persistent (Gonczy, 2008). However, in human tissue culture cells, these interactions last for only a few seconds before astral microtubules depolymerize (Samora et al., 2011). This brief moment of attachment, when dynein generates its pulling force, remains poorly understood. This is partly due to the instability of astral microtubules and transient nature of the connection. Furthermore, the molecular players have not been fully identified. With all the complexity that underlies microtubule attachment at kinetochores, it is tempting to hypothesize that more proteins than just dynein and tubulin are involved at the cortex. As the contact point for astral microtubules is the plus end, including plus-end-tracking proteins, it is possible that many of these proteins play a role upon cortical contact. Indeed, one plus-end tracker, Clasp1, has been proposed to play a role in this process (Samora et al., 2011). However, generating a full picture of astral microtubule behavior and cortical dynein force generation remains an important goal. In Chapter Three of this thesis, I present evidence that the Astrin/SKAP complex has an important role in the astral microtubule spindle-positioning pathway.

Cortical Dynein Regulation at the Cortex

The other side of the spindle positioning is the role of cortical dynein. During metaphase, dynein binds to the NuMA protein, which in turn binds to LGN, with LGN bound to the membrane through the membrane tethered Gαi protein (Kiyomitsu and Cheeseman, 2012). In anaphase, the Gαi pathway is assisted by

another pathway utilizing the 4.1G and R proteins (Kiyomitsu and Cheeseman, 2013). Cortical force generation occurs if an astral microtubule makes contact with dynein at the cell cortex, and more astral microtubules will make cortical contact if they nucleate from a close centrosome. Considering only these two points, cortical dynein force would act in this scenario to further misposition a misplaced spindle. Therefore, regulation of the cortical dynein force must occur to achieve a robust pathway for spindle centering. Recent papers have shown that one way to regulate this pathway is by controlling the level of dynein bound to its cortical receptors (Kiyomitsu and Cheeseman, 2012). Cortical dynein localization is antagonized by two different regulatory gradients emanating from chromosomes and spindle poles respectively (Figure 5B). First, for restricting dynein localization to either side of the cell and determining spindle angle, a gradient of RAN-GTP generated at chromosomes negatively regulates dynein localization at the top and bottom of the metaphase plate (Bird et al., 2013; Kiyomitsu and Cheeseman, 2012). Second, for controlling side-to-side motion of the spindle, centrosome localized Polo-like kinase 1 (Plk1) delocalizes dynein from cell cortex if a centrosome gets too close. Using these two mechanisms, the cell can first orient and subsequently center its spindle in a regulated game of tug of war between dynein at each cortex. However, it is possible that more regulation, including that of astral microtubules (Akhmanova and Steinmetz, 2015), contributes to a robust spindle positioning pathway.

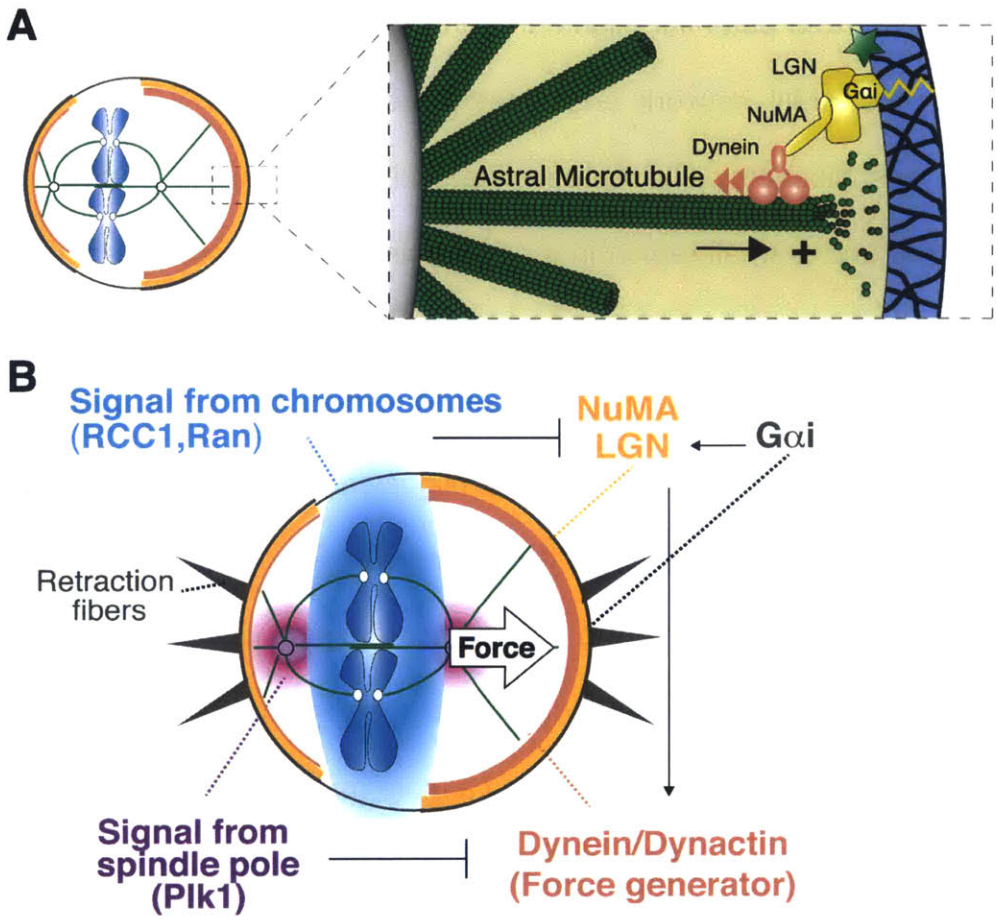

Figure 5. Mitotic spindle positioning. (A) Schematic of the astral microtubule-cortical dynein interaction site. Dynein, in complex with NuMA, is recruited to the cortex by an interaction with LGN, which is itself bound to the membrane tethered Gαi protein. (Adapted from (Siller and Doe, 2009)) (B) Model for cortical dynein regulation for spindle positioning. Localization of LGN is guided by cell retraction fibers and negatively regulated by a chromosome-derived Ran gradient to help set the spindle angle. A centrosome-derived Plk1 gradient negatively regulates dynein regulation. If a centrosome gets too close to cortex, cortical dynein pulling force from that side will weaken and force from the opposite side will get stronger, effectively pulling the spindle back to center. This setup is similar to a tug-of-war game where astral microtubules are the rope (and everyone wins). (Adapted from (Kiyomitsu and Cheeseman, 2012))

Findings Presented in this Thesis

During my graduate work, I focused on two key sites of microtubule attachment in mitotic cells, the kinetochore and the cell cortex. I first investigated the

biochemical behavior and potential oligomerization of KNL-1. Due to the central role of KNL1 in the KMN network and kinetochore structure, I asked if this oligomerization was biochemically reproducible and physiologically relevant. I truncated KNL-1 to find a small region in the N-terminus was responsible for the oligomerization behavior and found that the protein oligomerizes into a precise decameric assembly. By removing this domain, or mutating a small region of hydrophobic amino acids, I could ablate the oligomerization activity. As this region did not show clear conservation outside of nematodes, I collaborated with the Desai Lab to test the contribution to *C. elegans* division. However, they did not find any major organismal or cellular defects for the oligomerization mutants. We speculate that the oligomerization may play a more minor role in organization of the N-terminus of nematode KNL-1, perhaps in clustering checkpoint-signaling molecules in these holocentric organisms. This study is the subject of Chapter Two of this thesis.

Next, I studied the Astrin/SKAP complex to determine its mitotic functions. Previous studies on SKAP had reported differing depletion phenotypes, and no prior study had rescued SKAP depletion. I found that the isoform of SKAP used in previous mitotic studies is, surprisingly, only expressed in mammalian testes. The true mitotic form had remained hidden as a shorter isoform generated from an alternative transcriptional start. Using this correct isoform, I was able to rescue SKAP depletion and verify two of SKAP's mitotic phenotypes: chromosome misalignment and loss of spindle and centrosome integrity. I also

characterized the microtubule-binding domain of SKAP, and showed that it is essential for Astrin/SKAP complex microtubule localization and mitotic function. The novel mitotic SKAP isoform, unlike the longer testis isoform, displayed clear plus-end-tracking activity. I show that a SKAP mutant unable to plus-end track was able to rescue the chromosome and centrosome defects of SKAP depletion. However, many of these cells exhibited a novel phenotype with drastically mispositioned metaphase spindles.

By conducting a proteomic analysis of Astrin and SKAP, I found that they interact with dynein, NuMA Clasp1, and Plk1, all proteins that play important roles in spindle positioning. To narrow down the protein interactions directly responsible for the SKAP plus-end tracking mutant phenotype, I tested the behavior of these candidates in the mutant context. I found that dynein localization and regulation was not perturbed. However, the Clasp1 protein localization was strongly reduced on microtubule plus ends in mitosis. Combining this data with evidence from previous literature, I propose a model where both the Astrin/SKAP complex and Clasp1 play roles in mediating the interaction between astral microtubules and cortical dynein. Misregulation of this system leads to side-to-side metaphase spindle positioning defections. Taken together, in this work I demonstrate the proper mitotic form of SKAP, better characterize the mitotic behavior and phenotypes of the Astrin/SKAP complex, and uncover a new spindle positioning role for Astrin/SKAP at astral microtubule plus ends. These discoveries solve some previous mysteries about SKAP function and

provide a useful list of mitotic molecular interactions for the Astrin/SKAP complex. Furthermore, they open up new questions about the role of SKAP in testes and the process of astral microtubule docking on cortical dynein. The Astrin/SKAP complex is the subject of Chapter Three of this thesis.

References

Akhmanova, A., and M.O. Steinmetz. 2015. Control of microtubule organization and dynamics: two ends in the limelight. *Nature Reviews Molecular Cell Biology*. 16:711-726.

Alushin, G.M., V. Musinipally, D. Matson, J. Tooley, P.T. Stukenberg, and E. Nogales. 2012. Multimodal microtubule binding by the Ndc80 kinetochore complex. *Nature Structural & Molecular Biology*. 19:1161-1167.

Andrews, P.D., Y. Ovechkina, N. Morrice, M. Wagenbach, K. Duncan, L. Wordeman, and J.R. Swedlow. 2004. Aurora B regulates MCAK at the mitotic centromere. *Developmental Cell*. 6:253-268.

Bergstralh, D.T., and D. St Johnston. 2014. Spindle orientation: what if it goes wrong? *Seminars in Cell & Developmental Biology*. 34:140-145.

Bird, S.L., R. Heald, and K. Weis. 2013. RanGTP and CLASP1 cooperate to position the mitotic spindle. *Molecular Biology of the Cell*. 24:2506-2514.

Bolanos-Garcia, V.M., T. Kiyomitsu, S. D'Arcy, D.Y. Chirgadze, J.G. Grossmann, D. Matak-Vinkovic, A.R. Venkitaraman, M. Yanagida, C.V. Robinson, and T.L. Blundell. 2009. The crystal structure of the N-terminal region of BUB1 provides insight into the mechanism of BUB1 recruitment to kinetochores. *Structure*. 17:105-116.

Carminati, J.L., and T. Stearns. 1997. Microtubules orient the mitotic spindle in yeast through dynein-dependent interactions with the cell cortex. *Journal of Cell Biology*. 138:629-641.

Cheerambathur, D.K., R. Gassmann, B. Cook, K. Oegema, and A. Desai. 2013. Crosstalk between microtubule attachment complexes ensures accurate chromosome segregation. *Science*. 342:1239-1242.

Cheeseman, I.M. 2014. The kinetochore. *Cold Spring Harbor Perspectives in Biology*. 6:a015826.

Cheeseman, I.M., J.S. Chappie, E.M. Wilson-Kubalek, and A. Desai. 2006. The conserved KMN network constitutes the core microtubule-binding site of the kinetochore. *Cell*. 127:983-997.

Cheeseman, I.M., and A. Desai. 2008. Molecular architecture of the kinetochore-microtubule interface. *Nature Reviews Molecular Cell Biology*. 9:33-46.

Cheeseman, I.M., T. Hori, T. Fukagawa, and A. Desai. 2008a. KNL1 and the CENP-H/I/K Complex Coordinately Direct Kinetochore Assembly in Vertebrates. *The Journal of Cell Biology*. 19:587-594.

Cheeseman, I.M., T. Hori, T. Fukagawa, and A. Desai. 2008b. KNL1 and the CENP-H/I/K complex coordinately direct kinetochore assembly in vertebrates. *Molecular Biology of the Cell*. 19:587-594.

Cianfrocco, M.A., M.E. DeSantis, A.E. Leschziner, and S.L. Reck-Peterson. 2015. Mechanism and Regulation of Cytoplasmic Dynein.Annual Review of Cell and Developmental Biology. 31:83-108.

Ciferri, C., S. Pasqualato, E. Screpanti, G. Varetti, S. Santaguida, G. Dos Reis, A. Maiolica, J. Polka, J.G. De Luca, P. De Wulf, M. Salek, J. Rappsilber, C.A.

Moores, E.D. Salmon, and A. Musacchio. 2008. Implications for kinetochore-microtubule attachment from the structure of an engineered Ndc80 complex. *Cell*. 133:427-439.

Desai, A., and T.J. Mitchison. 1997. Microtubule polymerization dynamics.Annual Review of Cell and Developmental Biology. 13:83-117.

Desai, A., S. Rybina, T. Muller-Reichert, A. Shevchenko, A. Shevchenko, A. Hyman, and K. Oegema. 2003. KNL-1 directs assembly of the microtubule-binding interface of the kinetochore in C. elegans. *Genes and Development*. 17:2421-2435.

Drinnenberg, I.A., D. deYoung, S. Henikoff, and H.S. Malik. 2014. Recurrent loss of CenH3 is associated with independent transitions to holocentricity in insects. *eLife*. 3.

Dunsch, A.K., E. Linnane, F.A. Barr, and U. Gruneberg. 2011. The astrin-kinastrin/SKAP complex localizes to microtubule plus ends and facilitates chromosome alignment. *The Journal of Cell Biology*. 192:959-968.

Fang, L., A. Seki, and G. Fang. 2009. SKAP associates with kinetochores and promotes the metaphase-to-anaphase transition. *Cell Cycle*. 8:2819-2827.

Gascoigne, K.E., and I.M. Cheeseman. 2011. Kinetochore assembly: if you build it, they will come. *Current Opinion in Cell Biology*. 23:102-108.

Gascoigne, K.E., K. Takeuchi, A. Suzuki, T. Hori, T. Fukagawa, and I.M. Cheeseman. 2011. Induced ectopic kinetochore assembly bypasses the requirement for CENP-A nucleosomes. *Cell*. 145:410-422.

Gassmann, R., A. Rechtsteiner, K.W. Yuen, A. Muroyama, T. Egelhofer, L. Gaydos, F. Barron, P. Maddox, A. Essex, J. Monen, S. Ercan, J.D. Lieb, K. Oegema, S. Strome, and A. Desai. 2012. An inverse relationship to germline transcription defines centromeric chromatin in C. elegans. *Nature*. 484:534-537.

Gonczy, P. 2008. Mechanisms of asymmetric cell division: flies and worms pave the way. *Nature Reviews Molecular Cell Biology*. 9:355-366.

Goshima, G., T. Kiyomitsu, K. Yoda, and M. Yanagida. 2003. Human centromere chromatin protein hMis12, essential for equal segregation, is independent of CENP-A loading pathway. *The Journal of Cell Biology*. 160:25-39.

Gruber, J., J. Harborth, J. Schnabel, K. Weber, and M. Hatzfeld. 2002. The mitotic-spindle-associated protein astrin is essential for progression through mitosis. *Journal of Cell Science*. 115:4053-4059.

Hanahan, D., and R.A. Weinberg. 2011. Hallmarks of cancer: the next generation. *Cell*. 144:646-674.

Hirokawa, N., Y. Noda, Y. Tanaka, and S. Niwa. 2009. Kinesin superfamily motor proteins and intracellular transport. *Nature Reviews Molecular Cell Biology*. 10:682-696.

Hiruma, Y., C. Sacristan, S.T. Pachis, A. Adamopoulos, T. Kuijt, M. Ubbink, E. von Castelmur, A. Perrakis, and G.J. Kops. 2015. Competition between MPS1 and microtubules at kinetochores regulates spindle checkpoint signaling. *Science*. 348:1264-1267.

Honnappa, S., S.M. Gouveia, A. Weisbrich, F.F. Damberger, N.S. Bhavesh, H. Jawhari, I. Grigoriev, F.J. van Rijssel, R.M. Buey, A. Lawera, I. Jelesarov, F.K. Winkler, K. Wuthrich, A. Akhmanova, and M.O. Steinmetz. 2009. An EB1-binding motif acts as a microtubule tip localization signal. *Cell.* 138:366-376.

Hori, T., M. Amano, A. Suzuki, C.B. Backer, J.P. Welburn, Y. Dong, B.F. McEwen, W.H. Shang, E. Suzuki, K. Okawa, I.M. Cheeseman, and T. Fukagawa. 2008. CCAN makes multiple contacts with centromeric DNA to provide distinct pathways to the outer kinetochore. *Cell.* 135:1039-1052.

Howard, J., and A.A. Hyman. 2007. Microtubule polymerases and depolymerases. *Current Opinion in Cell Biology.* 19:31-35.

Ji, Z., H. Gao, and H. Yu. 2015. Kinetochore attachment sensed by competitive Mps1 and microtubule binding to Ndc80C. *Science.* 348:1260-1264.

Kapitein, L.C., E.J. Peterman, B.H. Kwok, J.H. Kim, T.M. Kapoor, and C.F. Schmidt. 2005. The bipolar mitotic kinesin Eg5 moves on both microtubules that it crosslinks. *Nature.* 435:114-118.

Kardon, J.R., and R.D. Vale. 2009. Regulators of the cytoplasmic dynein motor. *Nature Reviews Molecular Cell Biology.* 10:854-865.

Kerres, A., V. Jakopec, and U. Fleig. 2007. The Conserved Spc7 Protein Is Required for Spindle Integrity and Links Kinetochore Complexes in Fission Yeast. *Molecular Biology of the Cell.* 18:2441-2454.

Kiyomitsu, T. 2015. Mechanisms of daughter cell-size control during cell division. *Trends in Cell Biology.* 25:286-295.

Kiyomitsu, T., and I.M. Cheeseman. 2012a. Chromosome- and spindle-pole-derived signals generate an intrinsic code for spindle position and orientation. *Nature Cell Biology.* 14:311-317.

Kiyomitsu, T., and I.M. Cheeseman. 2013. Cortical dynein and asymmetric membrane elongation coordinately position the spindle in anaphase. *Cell.* 154:391-402.

Kiyomitsu, T., C. Obuse, and M. Yanagida. 2007. Human Blinkin/AF15q14 Is Required for Chromosome Alignment and the Mitotic Checkpoint through Direct Interaction with Bub1 and BubR1. *Developmental Cell.* 13:663-676.

Kline, S.L., I.M. Cheeseman, T. Hori, T. Fukagawa, and A. Desai. 2006. The human Mis12 complex is required for kinetochore assembly and proper chromosome segregation. *The Journal of Cell Biology.* 173:9-17.

Knoblich, J.A. 2010. Asymmetric cell division: recent developments and their implications for tumour biology. *Nature Reviews Molecular Cell Biology.* 11:849-860.

Krenn, V., K. Overlack, I. Primorac, S. van Gerwen, and A. Musacchio. 2014. KI motifs of human Knl1 enhance assembly of comprehensive spindle checkpoint complexes around MELT repeats. *Current Biology.* 24:29-39.

Kristofferson, D., T. Mitchison, and M. Kirschner. 1986. Direct observation of steady-state microtubule dynamics. *The Journal of Cell Biology.* 102:1007-1019.

Lawrimore, J., Bloom, K.S., and Salmon, E.D. (2011). Point centromeres contain more than a single centromere-specific Cse4 (CENP-A) nucleosome. *The Journal of Cell Biology. 195*, 573-582.

Liu, D., M. Vleugel, C.B. Backer, T. Hori, T. Fukagawa, I.M. Cheeseman, and M.A. Lampson. 2010. Regulated targeting of protein phosphatase 1 to the outer kinetochore by KNL1 opposes Aurora B kinase. *The Journal of Cell Biology*. 188:809-820.

Logarinho, E., S. Maffini, M. Barisic, A. Marques, A. Toso, P. Meraldi, and H. Maiato. 2012. CLASPs prevent irreversible multipolarity by ensuring spindle-pole resistance to traction forces during chromosome alignment. *Nature Cell Biology*. 14:295-303.

Mack, G.J., and D.A. Compton. 2001. Analysis of mitotic microtubule-associated proteins using mass spectrometry identifies astrin, a spindle-associated protein. *Proceedings of the National Academy of Sciences of the United States of America*. 98:14434-14439.

Maffini, S., A.R. Maia, A.L. Manning, Z. Maliga, A.L. Pereira, M. Junqueira, A. Shevchenko, A. Hyman, J.R. Yates, 3rd, N. Galjart, D.A. Compton, and H. Maiato. 2009. Motor-independent targeting of CLASPs to kinetochores by CENP-E promotes microtubule turnover and poleward flux. *Current Biology*. 19:1566-1572.

Maiato, H., E.A. Fairley, C.L. Rieder, J.R. Swedlow, C.E. Sunkel, and W.C. Earnshaw. 2003. Human CLASP1 is an outer kinetochore component that regulates spindle microtubule dynamics. *Cell*. 113:891-904.

McKinley, K.L., and I.M. Cheeseman. 2015. The molecular basis for centromere identity and function. *Nature Reviews Molecular Cell Biology. 60(6):886-98.*

Melters, D.P., L.V. Paliulis, I.F. Korf, and S.W. Chan. 2012. Holocentric chromosomes: convergent evolution, meiotic adaptations, and genomic analysis. *Chromosome Research*. 20:579-593.

Mimori-Kiyosue, Y., I. Grigoriev, G. Lansbergen, H. Sasaki, C. Matsui, F. Severin, N. Galjart, F. Grosveld, I. Vorobjev, S. Tsukita, and A. Akhmanova. 2005. CLASP1 and CLASP2 bind to EB1 and regulate microtubule plus-end dynamics at the cell cortex. *The Journal of Cell Biology*. 168:141-153.

Mitchison, T., and M.W. Kirschner. 1984. Dynamic instability of microtubule growth. *Nature*. 312:237-242.

Moore, A.T., K.E. Rankin, G. von Dassow, L. Peris, M. Wagenbach, Y. Ovechkina, A. Andrieux, D. Job, and L. Wordeman. 2005. MCAK associates with the tips of polymerizing microtubules. *The Journal of Cell Biology*. 169:391-397.

Musacchio, A., and E.D. Salmon. 2007. The spindle-assembly checkpoint in space and time. *Nature Reviews Molecular and Cellular Biology*. 8:379-393.

Nishino, T., F. Rago, T. Hori, K. Tomii, I.M. Cheeseman, and T. Fukagawa. 2013. CENP-T provides a structural platform for outer kinetochore assembly. *The EMBO Journal*. 32:424-436.

Obuse, C., O. Iwasaki, T. Kiyomitsu, G. Goshima, Y. Toyoda, and M. Yanagida. 2004. A conserved Mis12 centromere complex is linked to heterochromatic HP1 and outer kinetochore protein Zwint-1. *Nature Cell Biology*. 6:1135-1141.

Orjalo, A.V., A. Arnaoutov, Z. Shen, Y. Boyarchuk, S.G. Zeitlin, B. Fontoura, S. Briggs, M. Dasso, and D.J. Forbes. 2006. The Nup107-160 Nucleoporin Complex Is Required for Correct Bipolar Spindle Assembly. *Molecular Biology of the Cell*. 17:3806-3818.

Pagliuca, C., V.M. Draviam, E. Marco, P.K. Sorger, and P. De Wulf. 2009. Roles for the conserved spc105p/kre28p complex in kinetochore-microtubule binding and the spindle assembly checkpoint. *PloS One*. 4:e7640.

Petrovic, A., S. Mosalaganti, J. Keller, M. Mattiuzzo, K. Overlack, V. Krenn, A. De Antoni, S. Wohlgemuth, V. Cecatiello, S. Pasqualato, S. Raunser, and A. Musacchio. 2014. Modular assembly of RWD domains on the Mis12 complex underlies outer kinetochore organization. *Molecular Cell*. 53:591-605.

Pinsky, B.A., C.V. Kotwaliwale, S.Y. Tatsutani, C.A. Breed, and S. Biggins. 2006. Glc7/protein phosphatase 1 regulatory subunits can oppose the Ipl1/aurora protein kinase by redistributing Glc7. *Molecular and Cellular Biology*. 26:2648-2660.

Redwine, W.B., R. Hernandez-Lopez, S. Zou, J. Huang, S.L. Reck-Peterson, and A.E. Leschziner. 2012. Structural basis for microtubule binding and release by dynein. *Science*. 337:1532-1536.

Rieder, C.L. 1981. The structure of the cold-stable kinetochore fiber in metaphase PtK1 cells. *Chromosoma*. 84:145-158.

Rosenberg, J.S., F.R. Cross, and H. Funabiki. 2011. KNL1/Spc105 recruits PP1 to silence the spindle assembly checkpoint. *Current Biology*. 21:942-947.

Samora, C.P., B. Mogessie, L. Conway, J.L. Ross, A. Straube, and A.D. McAinsh. 2011. MAP4 and CLASP1 operate as a safety mechanism to maintain a stable spindle position in mitosis. *Nature Cell Biology*. 13:1040-1050.

Schmidt, J.C., H. Arthanari, A. Boeszoermenyi, N.M. Dashkevich, E.M. Wilson-Kubalek, N. Monnier, M. Markus, M. Oberer, R.A. Milligan, M. Bathe, G. Wagner, E.L. Grishchuk, and I.M. Cheeseman. 2012. The kinetochore-bound Ska1 complex tracks depolymerizing microtubules and binds to curved protofilaments. *Developmental Cell*. 23:968-980.

Schmidt, J.C., T. Kiyomitsu, T. Hori, C.B. Backer, T. Fukagawa, and I.M. Cheeseman. 2010. Aurora B kinase controls the targeting of the Astrin-SKAP complex to bioriented kinetochores. *The Journal of Cell Biology*. 191:269-280.

Shepperd, L.A., J.C. Meadows, A.M. Sochaj, T.C. Lancaster, J. Zou, G.J. Buttrick, J. Rappsilber, K.G. Hardwick, and J.B. Millar. 2012. Phosphodependent recruitment of Bub1 and Bub3 to Spc7/KNL1 by Mph1 kinase maintains the spindle checkpoint. *Current Biology*. 22:891-899.

Siller, K.H., and C.Q. Doe. 2009. Spindle orientation during asymmetric cell division. *Nature Cell Biology*. 11:365-374.

Starr, D.A., R. Saffery, Z. Li, A.E. Simpson, K.H. Choo, T.J. Yen, and M.L. Goldberg. 2000. HZwint-1, a novel human kinetochore component that interacts with HZW10. *Journal of Cell Science*. 113 (Pt 11):1939-1950.

Sullivan, M., and D.O. Morgan. 2007. Finishing mitosis, one step at a time. *Nature Reviews Molecular Cell Biology*. 8:894-903.

Tamura, N., J.E. Simon, A. Nayak, R. Shenoy, N. Hiroi, V. Boilot, A. Funahashi, and V.M. Draviam. 2015. A proteomic study of mitotic phase-specific interactors of EB1 reveals a role for SXIP-mediated protein interactions in anaphase onset. *Biology Open*. 4:155-169.

Thein, K.H., J. Kleylein-Sohn, E.A. Nigg, and U. Gruneberg. 2007. Astrin is required for the maintenance of sister chromatid cohesion and centrosome integrity. *The Journal of Cell Biology*. 178:345-354.

Vleugel, M., E. Hoogendoorn, B. Snel, and G.J. Kops. 2012. Evolution and function of the mitotic checkpoint. *Developmental Cell*. 23:239-250.

Vleugel, M., M. Omerzu, V. Groenewold, M.A. Hadders, S.M. Lens, and G.J. Kops. 2015. Sequential multisite phospho-regulation of KNL1-BUB3 interfaces at mitotic kinetochores. *Molecular Cell*. 57:824-835.

Walczak, C.E., and R. Heald. 2008. Mechanisms of mitotic spindle assembly and function. *International review of cytology*. 265:111-158.

Wang, H., X. Hu, X. Ding, Z. Dou, Z. Yang, A.W. Shaw, M. Teng, D.W. Cleveland, M.L. Goldberg, L. Niu, and X. Yao. 2004. Human Zwint-1 specifies localization of Zeste White 10 to kinetochores and is essential for mitotic checkpoint signaling. *The Journal of Biological Chemistry*
. 279:54590-54598.

Welburn, J.P., E.L. Grishchuk, C.B. Backer, E.M. Wilson-Kubalek, J.R. Yates, 3rd, and I.M. Cheeseman. 2009. The human kinetochore Ska1 complex facilitates microtubule depolymerization-coupled motility. *Developmental Cell*. 16:374-385.

Welburn, J.P., M. Vleugel, D. Liu, J.R. Yates, 3rd, M.A. Lampson, T. Fukagawa, and I.M. Cheeseman. 2010a. Aurora B phosphorylates spatially distinct targets to differentially regulate the kinetochore-microtubule interface. *Molecular Cell*. 38:383-392.

Wigge, P.A., and J.V. Kilmartin. 2001. The Ndc80p complex from Saccharomyces cerevisiae contains conserved centromere components and has a function in chromosome segregation. *Journal of Cell Biology*. 152:349-360.

Yamagishi, Y., C.H. Yang, Y. Tanno, and Y. Watanabe. 2012. MPS1/Mph1 phosphorylates the kinetochore protein KNL1/Spc7 to recruit SAC components. *Nature Cell Biology*. 14:746-752.

Zhang, G., T. Lischetti, D.G. Hayward, and J. Nilsson. 2015. Distinct domains in Bub1 localize RZZ and BubR1 to kinetochores to regulate the checkpoint. *Nature Communications*. 6:7162.

Zuccolo, M., A. Alves, V. Galy, S. Bolhy, E. Formstecher, V. Racine, J.B. Sibarita, T. Fukagawa, R. Shiekhattar, T. Yen, and V. Doye. 2007. The human Nup107-160 nuclear pore subcomplex contributes to proper kinetochore functions. *The EMBO Journal*. 26:1853-1864.

Chapter II: The outer kinetochore protein KNL-1 contains a defined oligomerization domain in nematodes

Reprinted from the American Society for Cell Biology journal Molecular Biology of the Cell with permission:

The outer kinetochore protein KNL-1 contains a defined oligomerization domain in nematodes. Kern DM, Kim T, Rigney M, Hattersley N, Desai A, Cheeseman IM.
Mol Biol Cell. 2015 Jan 15;26(2):229-37.

Taekyung Kim and Neil Hattersley conducted the C. elegans viability and division experiments. Mike Rigney performed the electron microscopy.

Abstract:

The kinetochore is a large, macromolecular assembly that is essential for connecting chromosomes to microtubules during mitosis. Despite the recent identification of multiple kinetochore components, the nature and organization of the higher order kinetochore structure remain unknown. The outer kinetochore KNL-1/Mis12 complex/Ndc80 complex (KMN) network plays a key role in generating and sensing microtubule attachments. Here, we demonstrate that *Caenorhabditis elegans* KNL-1 exists as an oligomer and we identify a specific domain in KNL-1 responsible for this activity. An N-terminal KNL-1 domain from both *C. elegans* and the related nematode C. *remanei* oligomerizes into a decameric assembly that appears roughly circular when visualized by electron microscopy. Based on sequence and mutational analysis, we identify a small hydrophobic region as responsible for this oligomerization activity. However, mutants that precisely disrupt KNL-1 oligomerization did not alter KNL-1 localization or result in the loss of embryonic viability based on gene replacements in *C. elegans*. In *C. elegans*, KNL-1 oligomerization may coordinate with other kinetochore activities to ensure the proper organization, function, and sensory capabilities of the kinetochore-microtubule attachment.

Introduction

The kinetochore is a macromolecular protein assembly that forms the primary connection between chromosomes and spindle microtubules (Cheeseman and Desai, 2008). The major group of proteins responsible for the ability of the kinetochore to capture a microtubule is the conserved KNL-1/Mis12 complex/Ndc80 complex (KMN) network (Cheeseman *et al.*, 2004; Cheeseman *et al.*, 2006). The Ndc80 complex acts as the critical microtubule-binding element within the KMN network (Cheeseman *et al.*, 2006; DeLuca *et al.*, 2006; Wei *et al.*, 2007; Ciferri *et al.*, 2008), with the Mis12 complex acting to connect the KMN network to the inner kinetochore (Gascoigne *et al.*, 2011; Przewloka *et al.*, 2011; Screpanti *et al.*, 2011). Finally, KNL-1 is a large protein that is required to assemble the KMN network (Cheeseman *et al.*, 2006). KNL-1 possesses a weak microtubule binding activity (Cheeseman *et al.*, 2006; Welburn *et al.*, 2010; Espeut *et al.*, 2012), and provides a scaffold for multiple signaling proteins at kinetochores including PP1 (Liu *et al.*, 2010), Bub1, and Bub3 (Kiyomitsu *et al.*, 2007; Kiyomitsu *et al.*, 2011; Krenn *et al.*, 2012; Caldas *et al.*, 2013; Vleugel *et al.*, 2013; Zhang *et al.*, 2014).

Although the protein components at the kinetochore have been largely identified, there is limited data on how these proteins assemble into a productive higher order conformation to facilitate microtubule interactions and kinetochore integrity. As prior studies have demonstrated that at least ~8-20 copies of the KMN network proteins are bound to each microtubule at kinetochores (Joglekar *et al.*, 2006; Joglekar *et al.*, 2008; Lawrimore *et al.*, 2011), the organization of these multiple complexes is a critical task. One possibility is that the microtubule itself imparts a higher-order organization to the kinetochore elements that bind the microtubule lattice. This could occur through the intrinsic symmetry of the microtubule or simply due to spatial constraints in binding sites. Alternatively, a

subset of kinetochore proteins may act to organize kinetochore proteins into the higher-order structure. For example, at centrioles, the oligomerization of the central hub element Sas6 provides the organization and 9-fold symmetry to the centriole barrel (Kitagawa *et al.*, 2011; van Breugel *et al.*, 2011). In this way, a single component of a complex could organize the remaining components to bring them into close proximity. However, it not known whether any kinetochore components self associate in a defined way that would provide such an organization to the kinetochore. Our prior work reconstituting the *C. elegans* KMN network found that KNL-1 behaved as a much larger species than would be expected based on its molecular weight (Cheeseman *et al.*, 2006). We interpreted this as a potential oligomerization for KNL-1, but the basis for and nature of this behavior was unclear.

Here, we investigated this apparent KNL-1 oligomerization activity. Our work demonstrates that nematode KNL-1 oligomerizes to a defined state at physiologically relevant concentrations. The oligomeric region forms a roughly circular structure when visualized by electron microscopy. Biochemical experiments and sequence analysis identified a small region that is conserved in nematodes as containing the oligomerization activity. However, interfering with KNL-1 oligomerization by deletion of this region or specific point mutants did not result in dramatic defects in *C. elegans* replacement experiments. We propose that nematode KNL-1 oligomerization may act in concert with other unidentified organizational elements within the kinetochore to generate a higher order kinetochore structure to organize the microtubule binding interface or signaling networks at kinetochores.

Results

The nematode KNL-1 N-terminus oligomerizes

We found previously that recombinant, full-length *C. elegans* KNL-1 behaved as a much larger species than expected based on its predicted molecular weight in size exclusion chromatography (SEC; see Fig. 1A) and sucrose gradients (Cheeseman *et al.*, 2006). We reasoned that this behavior could be due to a combination of possibilities: 1) KNL-1 aggregates non-specifically, 2) KNL-1 is highly elongated, or 3) KNL-1 oligomerizes in a structurally specific manner. To investigate the basis for this behavior, we began by creating truncations for *C. elegans* KNL-1 (see Supplemental Fig. 1A and 1B). Based on the migration of these truncations by SEC, we found that the N-terminal half of KNL-1 was sufficient to display this large apparent behavior (Fig. 1B). The N-terminus of KNL-1 acted as a single large species as revealed by both defined peaks in SEC and low polydispersity as assessed by Dynamic Light Scattering (DLS) (Fig. 1B). We further refined the region responsible for this activity to a small ~150 amino acid domain in the N-terminus of KNL-1, which we will refer to as the "oligomerization domain". This 150 amino acid construct was well-behaved biochemically, but acted as a much larger assembly (8.6 nm Stokes radius) than expected based on its predicted molecular weight (20 kDa). For comparison, the globular thyroglobulin size standard has a similar Stokes radius of 8.5 nm, but a molecular mass of 670 kDa. To test whether this apparent KNL-1 oligomerization activity was conserved in diverse nematode species, we analyzed the behavior of the *C. remanei* KNL-1 protein, which has diverged significantly from *C. elegans* KNL-1 (31% amino acid identity along the entire length), but displays clear homology including in the N-terminal oligomerization domain (Fig. 1C). Following purification of a recombinant *C. remanei* KNL-1 fragment with homology to the *C.*

elegans oligomerization domain, we found that the *C. remanei* protein was also oligomeric based on SEC and DLS (Fig. 1B), with the 17.6 kDa domain of C. *remanei* KNL-1 behaving as a 7.6 nm species. Thus, both C. *elegans* and C. *remanei* KNL-1 display an apparent oligomerization behavior in this conserved N-terminal region.

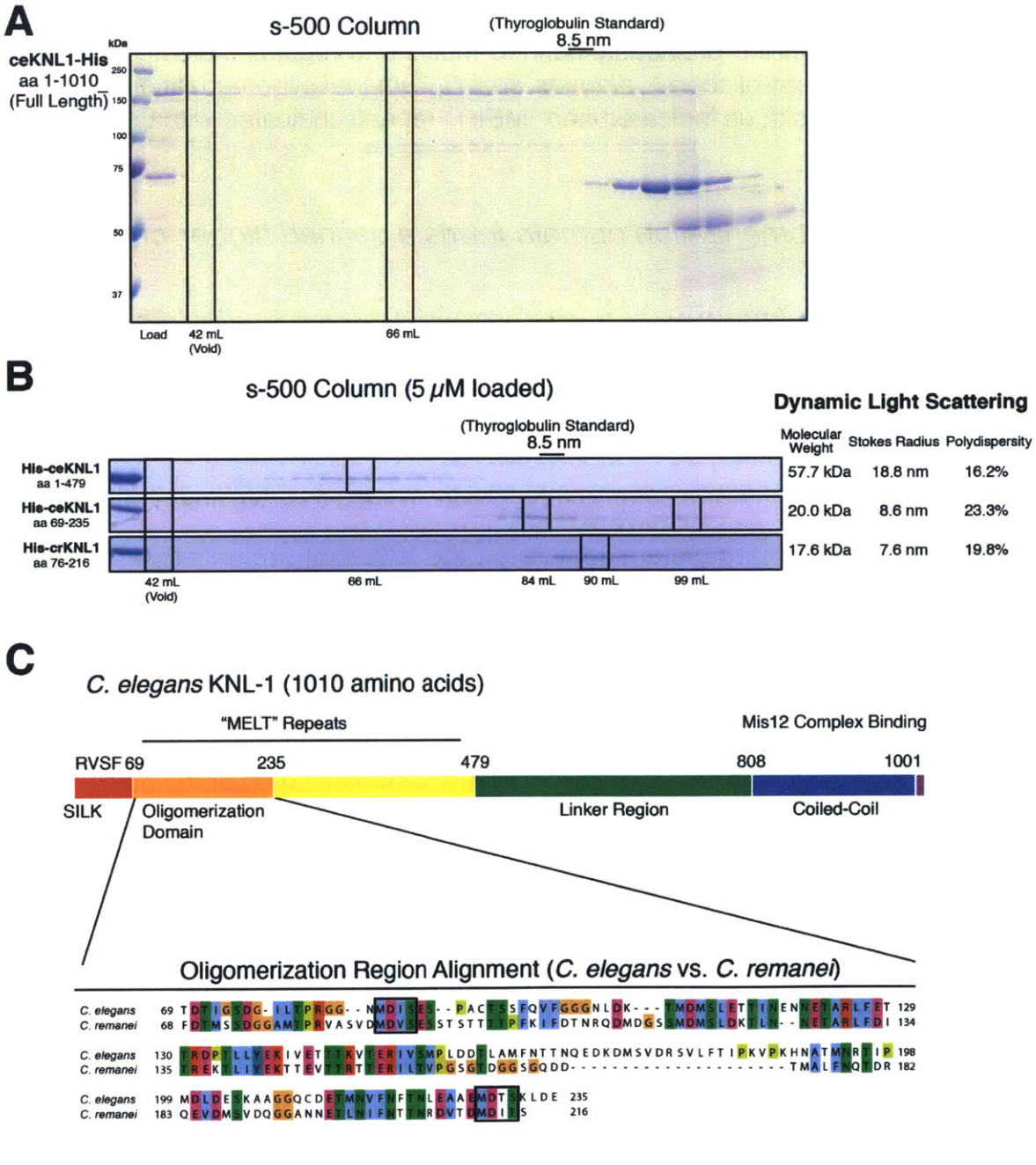

Figure 1. Identification of an N-terminal oligomerization domain in nematode KNL-1. (A) Coomassie-stained SDS-PAGE gel showing size exclusion chromatography analysis for full length ceKNL-1 purified from bacteria. The load volume is shown as is, but fractions were TCA precipitated and re-suspended to concentrate the samples prior to gel loading. (B) Coomassie-stained SDS-PAGE gels showing fractions from size exclusion chromatography analysis of *C. elegans* and *C. remanei* KNL-1 protein fragments. 5 μM concentrations of the indicated proteins were loaded on a s-500 column, with the relative elution volumes indicated. The predicted molecular weights, and the stokes radii and % polydispersity measured by Dynamic Light Scattering are indicated to the right. (C) Top, diagram showing a schematic of the *C. elegans* KNL-1 protein, with the previously defined motifs and regions indicated. Bottom, sequence alignment of the *C. elegans* and *C. remanei* oligomerization domains with conserved residues indicated and "MELT" repeats indicated with boxes.

The KNL-1 oligomerization domain forms a defined higher-order oligomer

As both the *C. elegans* and *C. remanei* KNL-1 oligomerization domains behaved similarly as large defined species, we sought to determine whether this large size was due to specific higher-order oligomerization, or whether the protein has a highly elongated shape or is aggregation prone. To test this, we first analyzed the effect of the cross-linker glutaraldehyde on the KNL-1 oligomerization domains. At appropriate protein concentrations and time scales, glutaraldehyde will generate covalent linkages (usually between lysine residues), but only between proteins that are present in close proximity (<7.5 Å; Wine *et al.*, 2007). We found that both the *C. elegans* and *C. remanei* KNL-1 oligomerization domains could be readily cross-linked with glutaraldehyde (Fig. 2A). At high glutaraldehyde concentrations, the proteins were almost completely cross-linked into a single large species that likely corresponds to the fully cross-linked oligomer. However, at lower glutaraldehyde concentrations, we observed incompletely cross-linked species. Based on the migration of these cross-linked forms in SDS-PAGE gels, we were able to detect the presence of a ladder of incompletely cross-linked

species with clear bands detected for dimers and trimers of KNL-1. Due to the apparent large size of the cross-linked domains observed by SDS-PAGE, we sought to ensure that the glutaraldehyde was not artificially generating a large oligomer through spurious interactions. To test this, we cross-linked each domain using glutaraldehyde and compared the behavior of control and cross-linked proteins by SEC (Fig. 2B). Importantly, the cross-linked KNL-1 proteins migrated similarly to the non-cross-linked proteins by SEC, and we did not observe any large cross-linked aggregates in the void volume of the column. These crosslinking experiments demonstrate that KNL-1 subunits are in close proximity and self-associate into a higher order complex.

We next sought to determine the stoichiometry of the KNL-1 oligomer using Sedimentation Velocity Analytical Ultracentrifugation (SV-AUC). For this analysis, we observed the best fit and behavior for a larger N-terminal fragment of C. *remanei* KNL-1. The SV-AUC analysis indicated C. *remanei* KNL-1 formed a decamer, as well as having a monomeric form (Fig. 2C). Although this protein behaved primarily as a single defined species, we observed some apparent disassociation of the larger assembly during the sedimentation run based on the spread of the oligomeric peak and the fitted frictional coefficient of ~2. We also analyzed the *C. elegans* KNL-1 oligomerization domain by AUC, but we were unable to obtain a consistent fit for this protein due to a larger spread of the primary peak (data not shown), likely due to its disassociation during the assay. Based on the combination of this SV-AUC data, together with the SEC and DLS analysis, we conclude that nematode KNL-1 N-terminus forms a defined high order oligomer composed of approximately 10 subunits.

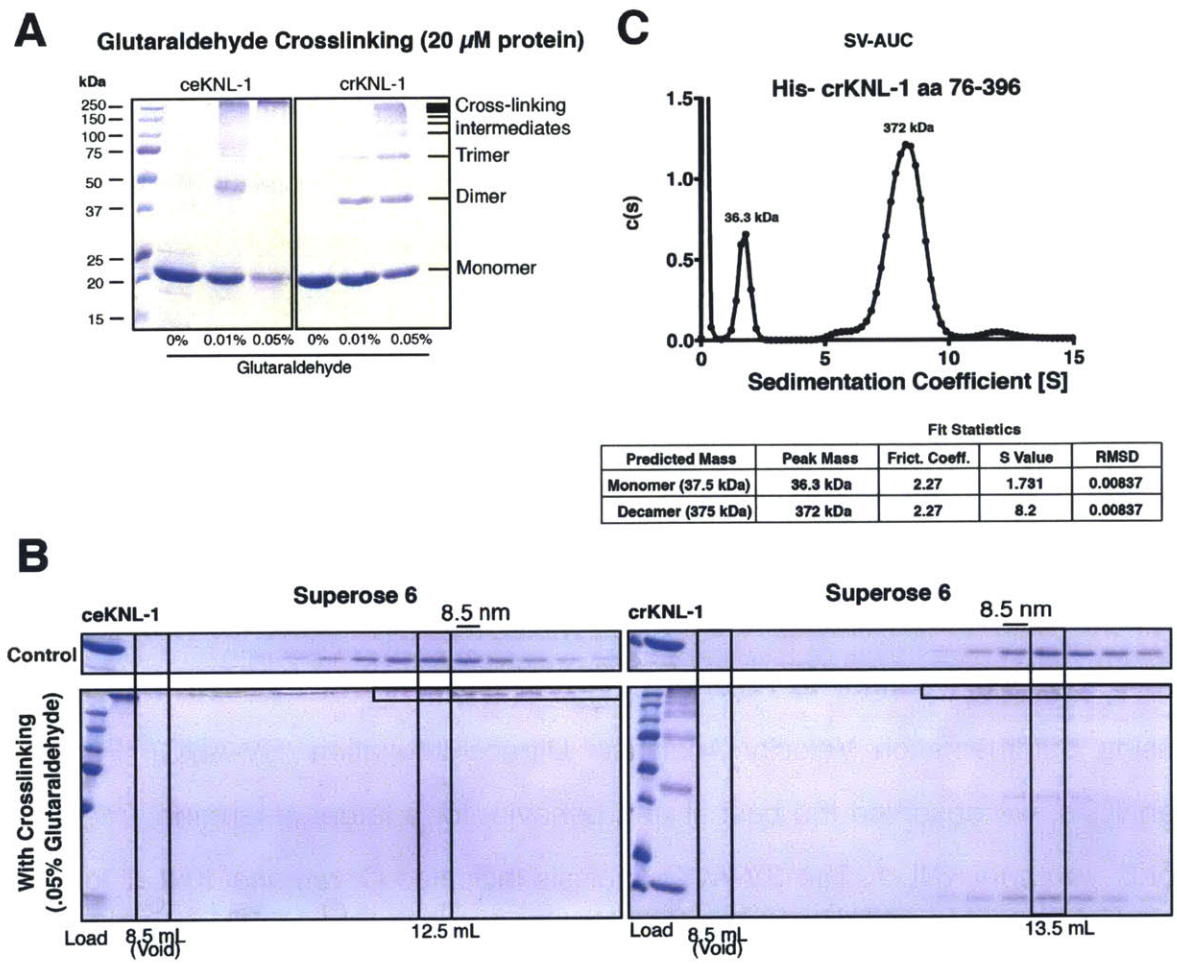

Figure 2. The KNL-1 N-terminal domain oligomerizes into a decameric assembly. (A) Coomassie-stained SDS-PAGE gels showing the *C. elegans* and *C. remanei* KNL-1 oligomerization domains (at a concentration of 20 μM) treated with the indicated concentrations of the crosslinking agent glutaraldehyde. The shift in migration SDS-PAGE gel reflects the formation of multimeric crosslinked assemblies, as indicated on the right. (B) Coomassie-stained SDS-PAGE gels showing fractions from the size exclusion chromatography analysis of the *C. elegans* and *C. remanei* oligomerization domains. The native oligomerization domains (top) and the domains crosslinked using .05% glutaraldehyde (bottom) display similar migration indicating that this treatment does not result in protein aggregation. We note that cross-linking appears to make the oligomers slightly smaller, potentially from stabilizing disordered regions of protein. The fully crosslinked *C. elegans* protein migrates just below the stacking gel. (C) Trace from the SV-AUC analysis of *C. remanei* KNL-1 aa 76-396. Fitting of the migration behavior (bottom) is consistent with the presence of a monomeric and decameric form.

The KNL-1 oligomerization domain forms a circular structure when visualized by electron microscopy

To directly visualize KNL-1 oligomerization, we analyzed the *C. elegans* and C. *remanei* oligomerization domains by negative stain transmission electron microscopy (TEM). We found that KNL-1 was present as particles of roughly similar size and shape. Although there was some variability in individual particles, the *C. elegans* KNL-1 oligomerization domain formed a low-resolution circular or ring-like structure with a diameter of ~15 nm (Fig. 3). Similarly, the *C. remanei* oligomerization domain was present as a circular structure with a diameter of ~11 nm (Fig. 3). Thus, the KNL-1 N-terminus oligomerizes into a particle with a roughly cylindrical shape.

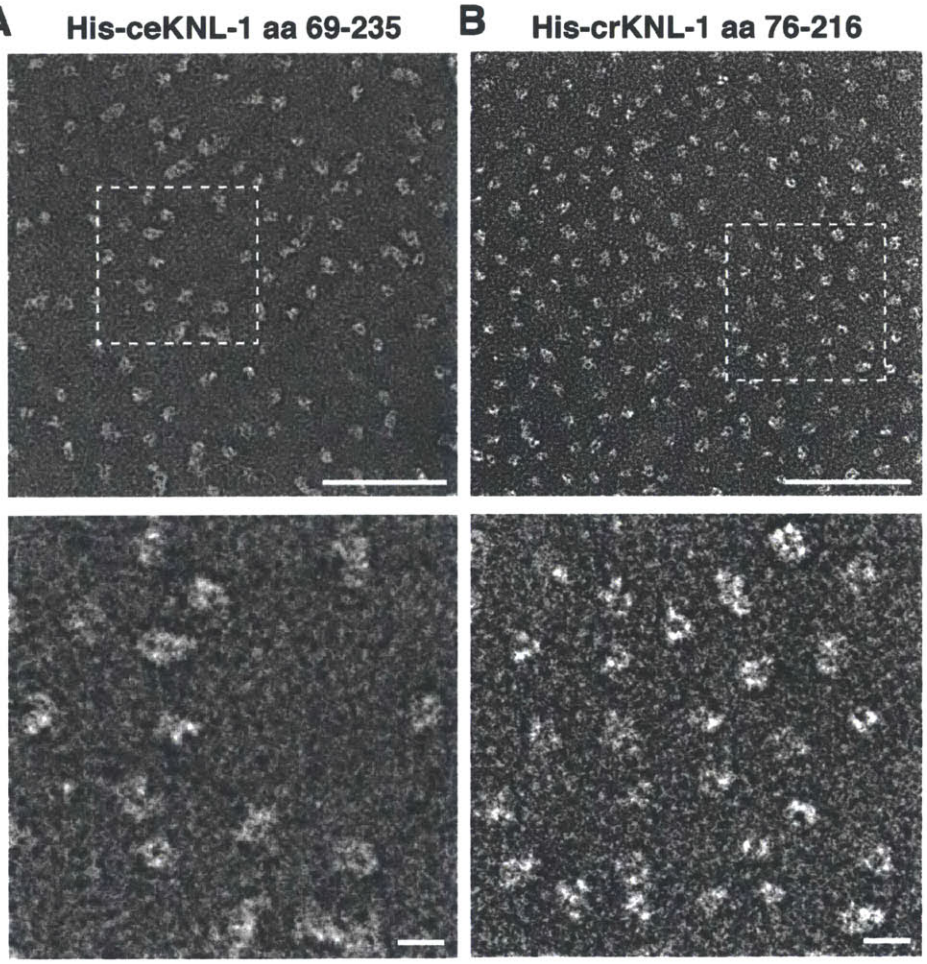

Figure 3. Visualization of the KNL-1 oligomerization domain by transmission electron microscopy. (A) Top, a field of ceKNL-1 oligomerization domain particles detected using transmssion electron microscopy with negative staining. Scale bar, 100 nm. Bottom, a zoomed-in view from the boxed region above. Scale bar, 20 nm. (B) Top, a field of crKNL-1 oligomerization domain particles. Scale bar, 100 nm. Bottom, zoomed-in view from the boxed region above. Scale bar, 20 nm.

KNL-1 oligomerization occurs through a small hydrophobic region

We next sought to determine the structural basis and specific residues required for the oligomerization of the KNL-1 N-terminal domain. We reasoned that KNL-1 self-association could occur through hydrogen bonding, charge-charge interactions, or hydrophobic interactions. To test this, we analyzed behavior of the *C. elegans* oligomerization domain by SEC under high salt conditions (1 M NaCl). Such conditions will negate charge-charge interactions, but strengthen hydrophobic interactions. Importantly, we found that KNL-1 self-association was enhanced in 1 M NaCl (Fig. 4A), suggesting that it is dependent on hydrophobic interactions. Through sequence analysis, we identified a small region within KNL-1 that contains multiple hydrophobic residues and is conserved amongst *Caenorhabitis* species (Fig. 4C). Mutating the combination of the hydrophobic residues in this region to alanine (KNL-1 8A) abolished the oligomerization activity based on altered migration in size exclusion chromatography (Fig. 4A). Mutation of a single conserved tyrosine residue (Y137A) within this hydrophobic region strongly reduced KNL-1 oligomerization without an obvious effect on protein expression or behavior (Fig. 4A).

Furthermore, we found that when our larger N-terminal ceKNL-1 construct (aa 1-479) was tagged with superfolder GFP (sfGFP; Pedelacq *et al.*, 2006) at its C-terminus, we obtained dramatically higher protein expression compared to the

untagged version (Supplemental Fig. 1C). At these high protein concentrations, we found that the KNL-1 protein formed a gel-like material after bead elution that pelleted efficiently in a centrifuge tube (Fig. 4B) and expanded the apparent bead volume during its purification (Supplemental Fig. 1C). The formation of this gel-like material as well as the observed increase in bead volume was disrupted by the KNL-1 8A mutation (Fig. 4B and Supplemental Fig. 1C). Therefore, nematode KNL-1 oligomerizes using specific residues in a small conserved hydrophobic protein region.

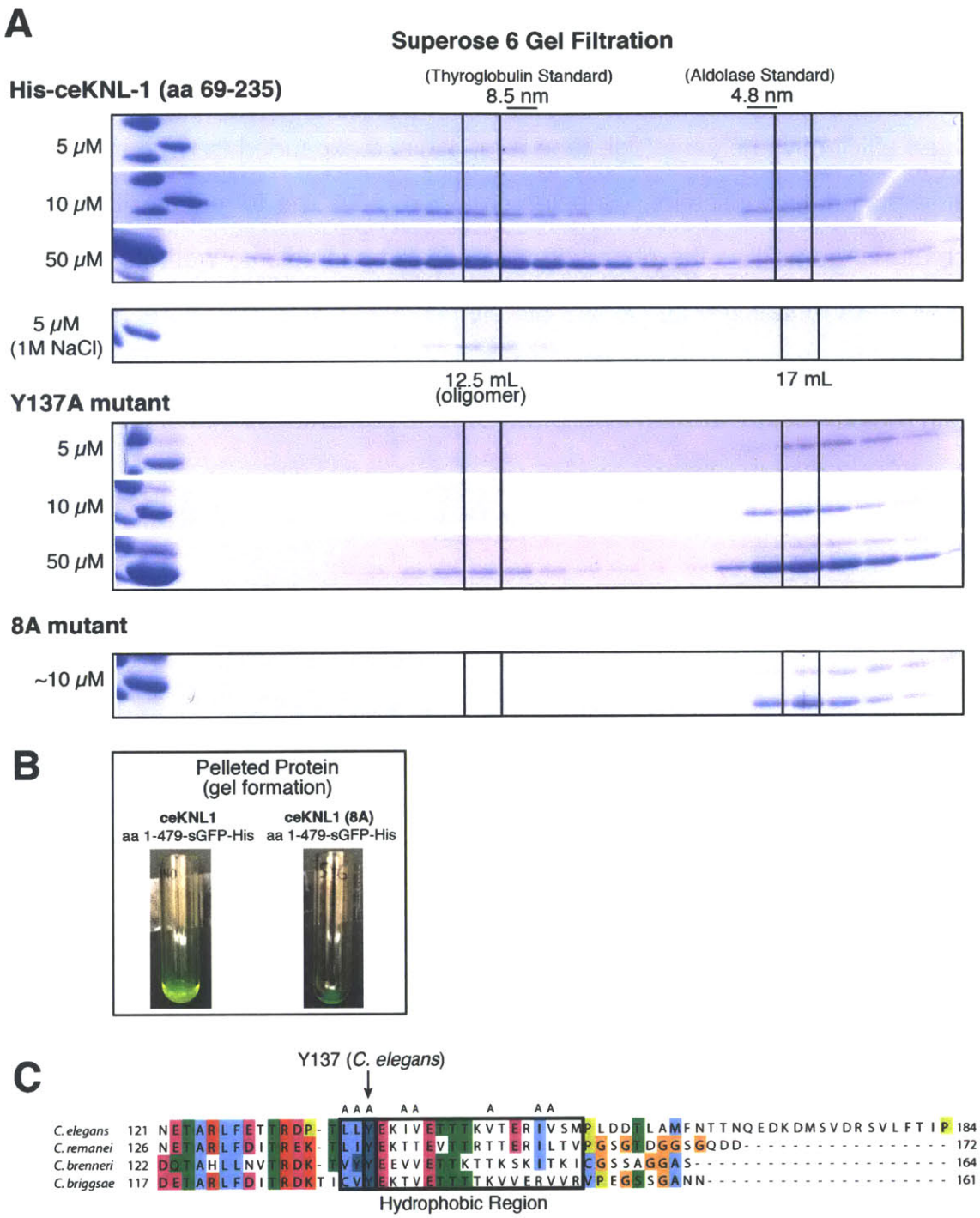

Figure 4. KNL-1 oligomerization requires a conserved, hydrophobic patch. (A) Coomassie-stained SDS-PAGE gels showing fractions from size exclusion chromatography analysis of the *C. elegans* KNL-1 oligomerization domain tested at increasing concentrations, or in the presence of 1 M NaCl as indicated. Top, migration behavior of the wild-type oligomerization domain. Middle, migration behavior of the Y137A mutant, which severely compromises the oligomerization

activity. Bottom, migration behavior of the 8A mutant construct (concentration is approximate due to the presence of a contaminating protein). (B) Pellets from the wild-type and 8A mutant superfolder GFP tagged proteins. The wild-type protein produces a substantial amount of a protein gel substance after nickel bead elution. This gel can be pelleted at low speed (22,000 g, not shown) and high speed (100,000 g, shown here). (C) Alignment of *Caenorhabditis* KNL-1 proteins showing the conservation of the residues in the oligomerization domain, highlighting the presence of a hydrophobic patch and the presence of the conserved tryptophan residue. Mutations included in the 8A mutant are indicated by A's above the residues.

KNL-1 oligomerization mutants do not dramatically disrupt chromosome segregation

Based on the biochemical analyses above, nematode KNL-1 proteins undergo oligomerization. To test the contributions of this oligomerization domain to kinetochore function, we analyzed the effect of these mutants in vivo. For these experiments, we generated transgenic *C. elegans* strains using single copy *mos* insertions expressing RNAi-resistant wild-type KNL-1-mCherry (see Espeut *et al.*, 2012) or mutants designed to disrupt the KNL-1 oligomerization. This includes mutations in the hydrophobic residues that are required for KNL-1 oligomerization (KNL-1 8A) or a deletion of the defined oligomerization domain (Δ102-236). Each of these KNL-1 mutants localized to the holocentric *C. elegans* kinetochores during mitosis similar to wild-type KNL-1 (Fig. 5A). To test the effects of these mutants, we depleted endogenous KNL-1 by RNAi in the transgenic strains. In the absence of transgene expression, KNL-1 depletion resulted in penetrant embryonic lethality (Fig. 5B), and eliminated kinetochore-microtubule interactions based on the rapid and premature separation of spindle poles (Fig. 5C; Desai *et al.*, 2003; Cheeseman *et al.*, 2004). Expression of wild-type KNL-1-mCherry was able to fully rescue embryonic lethality (Fig. 5B) and mitotic spindle elongation behavior (Fig. 5C). Despite the significant defects in oligomerization observed in our biochemical assays, expression of the KNL-1 8A hydrophobic mutant did not

result in obvious defects in embryonic lethality (Fig. 5B) or spindle pole elongation (Fig. 5C). Deletion of the entire oligomerization domain in KNL-1 (Δ102-236) did not result in embryonic lethality (Fig. 5B), but did display a small, but reproducible delay in spindle pole elongation (Fig. 5C). We note that the Δ102-236 deletion likely also reduces BUB-1 recruitment (Moyle *et al.*, 2014), in addition to perturbing KNL-1 oligomerization. Finally, to test whether oligomerization activity is required for the function of KNL-1 as a signaling scaffold, we generated KNL-1 mutants that disrupt both oligomerization (8A mutant) and diminish BUB-1 recruitment through mutation of the MELT sequence repeats (Moyle *et al.*, 2014). However, the 8A+MELT double mutant displayed normal embryonic viability (Fig. 5B). Overall, these data suggest that the KNL-1 oligomerization domain is not essential. However, we speculate that this activity may synergize with other unidentified features of the nematode kinetochore to promote proper chromosome segregation.

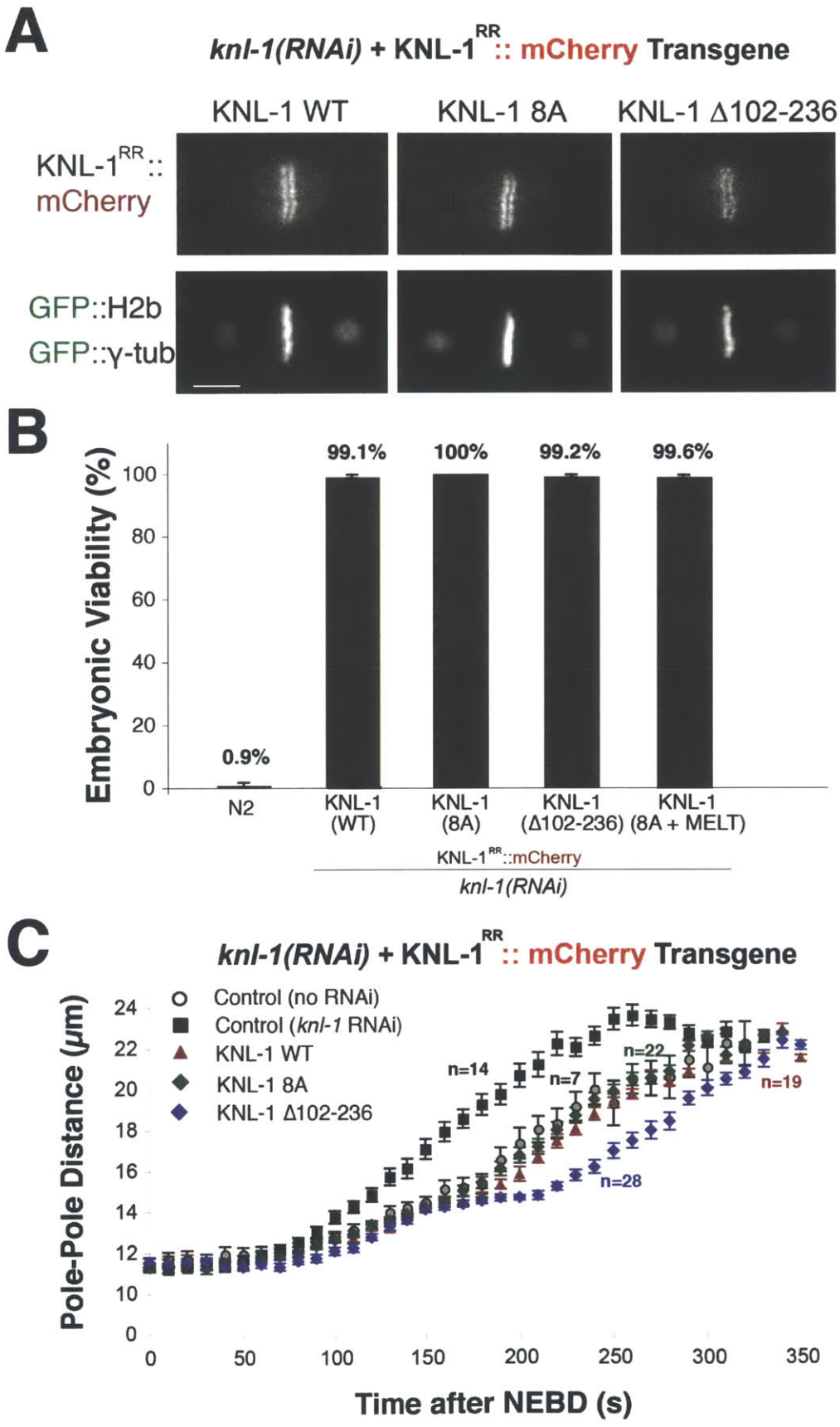
A
knl-1(RNAi) + KNL-1RR:: mCherry Transgene
KNL-1 WT
KNL-1 8A
KNL-1 Δ102-236
KNL-1RR:: mCherry
GFP::H2b
GFP::γ-tub
B
Embryonic Viability (%)
99.1%
100%
99.2%
99.6%
0.9%
N2
KNL-1 (WT)
KNL-1 (8A)
KNL-1 (Δ102-236)
KNL-1 (8A + MELT)
KNL-1RR::mCherry
knl-1(RNAi)
C
knl-1(RNAi) + KNL-1RR:: mCherry Transgene
Control (no RNAi)
Control (knl-1 RNAi)
KNL-1 WT
KNL-1 8A
KNL-1 Δ102-236
n=14
n=7
n=22
n=19
n=28
Pole-Pole Distance (μm)
Time after NEBD (s)

Figure 5. KNL-1 oligomerization is not essential for *C. elegans* viability. (A) Fluorescence images showing the localization of the mCherry-KNL-1 proteins (wild type or the indicated mutants) expressed in the first cell division *C. elegans* embryo. The bar-like localization reflects localization to the holocentric *C. elegans* kinetochores. Scale bar, 5 μm. (B) Graph indicating the embryonic viability following KNL-1 RNAi for N2 worms (n = 7 worms and 1512 embryos), or worms stably expressing wild-type KNL-1 (n = 7 worms and 733 embryos), KNL-1 8A (n = 10 worms and 1041 embryos), KNL-1 Δ102-236 (n = 6 worms and 676 embryos), and KNL-1 8A + MELT (n = 13 worms and 1269 embryos). The graph shows the percent viability +/- standard error. (C) Graph showing spindle pole separation over time during the first embyronic cell division for control embryos (Control (no RNAi); n = 7), or KNL-1 RNAi embryos (Control (KNL-1 RNAi); n = 14), or KNL-1 RNAi embryos expressing KNL-1 wild type (n = 19), KNL-1 8A (n = 22), or KNL-1 Δ102-236 (n = 28). Error bars represent standard error. The curves are aligned with respect to nuclear envelope breakdown (NEBD).

Discussion

Our prior work suggested a potential self-association for KNL-1 (Cheeseman *et al.*, 2006). Here, we demonstrated that an N-terminal domain of nematode KNL-1 oligomerizes as a defined decameric assembly. Although this oligomerization activity is not essential for viability in *C. elegans*, it may function coordinately with additional factors to organize elements of the kinetochore. Although the oligomerization region we identified is conserved in nematode species, we did not detect obvious conservation of this domain in other organisms. We note that recent work on the human KNL1 protein has suggested the potential for its self-association through its N-terminal region based on immunoprecipitation from cells (Petrovic *et al.*, 2014). This self-interaction may indicate the binding of hKNL1 to itself, or may be mediated by one of its binding partners such as Bub1. Importantly, we note that the oligomerization that we have defined is early within the "MELT" repeat region of nematode KNL-1 (Fig. 1C), similar to the position of the Bub1-interacting "KI" motifs in human KNL1 (Kiyomitsu *et al.*, 2011). In both cases, this suggests the formation of a higher order complex of KNL1 and its

spindle assembly checkpoint-binding partners at its N-terminus. Different organisms may also have distinct requirements for these features of kinetochore organization and function. For example, we note that in contrast with the human kinetochore, in *C. elegans* the Ska1 complex and the N-terminal tail of Ndc80 are dispensable for kinetochore function (Schmidt *et al.*, 2012; Cheerambathur *et al.*, 2013). It is also possible that other kinetochore proteins may self-associate, such as has been proposed for CENP-Q (Amaro *et al.*, 2010), to contribute to kinetochore organization.

We propose that there are three principal functions for self-association of kinetochore components. First, interactions between kinetochore components may be critical for the structural integrity of kinetochores. Second, self-association of kinetochore components may be important to organize the microtubule interface. Finally, such a self-association may help to cluster signaling molecules at kinetochores. We hypothesize that the observed oligomerization for the *C. elegans* KNL-1 may play a role in organizing the N-terminus of the protein. The N-terminus of KNL-1 in all organisms is predicted to be largely disordered (Caldas and DeLuca, 2014; our unpublished analysis). Recent work has demonstrated that KNL-1 binds to Bub1 using its "MELT" repeats in this region (Krenn *et al.*, 2012; Caldas *et al.*, 2013; Vleugel *et al.*, 2013; Zhang *et al.*, 2014). As multiple repeats are present throughout the N-terminus of KNL-1, this may allow a single molecule of KNL-1 to recruit multiple Bub1 proteins (Vleugel *et al.*, 2013). Self-association of KNL-1 would act to further locally concentrate Bub1, potentially amplifying this signal for its roles in the spindle assembly checkpoint and recruiting Aurora B to centromeres. Generating a focus of signaling activity may be especially important in a holocentric kinetochore since a diffuse kinetochore poses different signaling requirements compared to a localized kinetochore. It is likely that other

kinetochore components possess properties or behaviors that promote kinetochore structure and organization in parallel to KNL-1.

A

ceKNL-1 residues	Molecular Weight (kDa)	Approximate Stokes Radius (nm)
69-479	46.9	14
69-266	23.6	9
270-479	24.6	3.5
69-235 (Figure 1b)	20	8.6
69-203	16.6	7.5
69-188	14.8	Forms aggregates
103-235	16.6	Forms aggregates

B

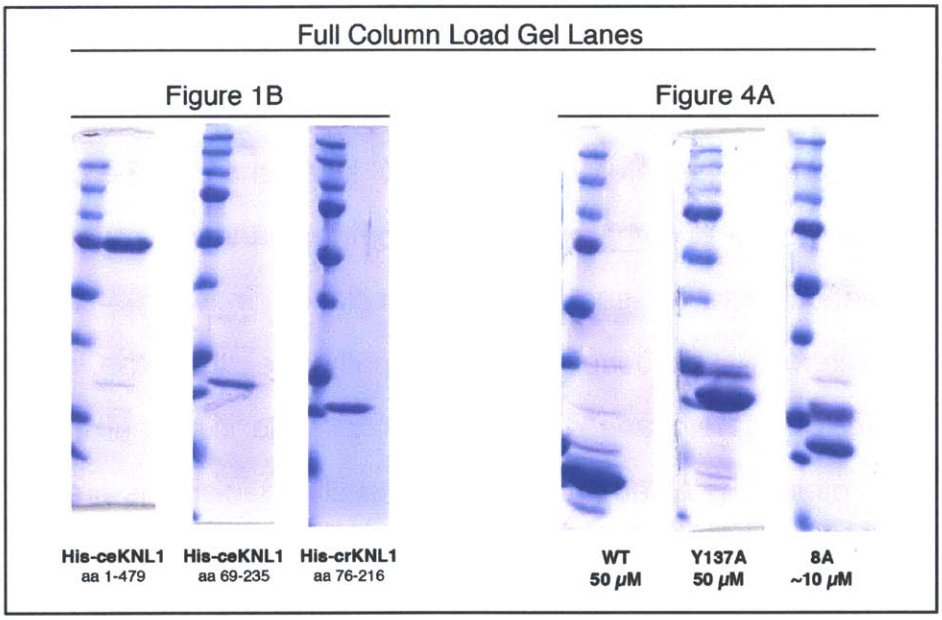

C

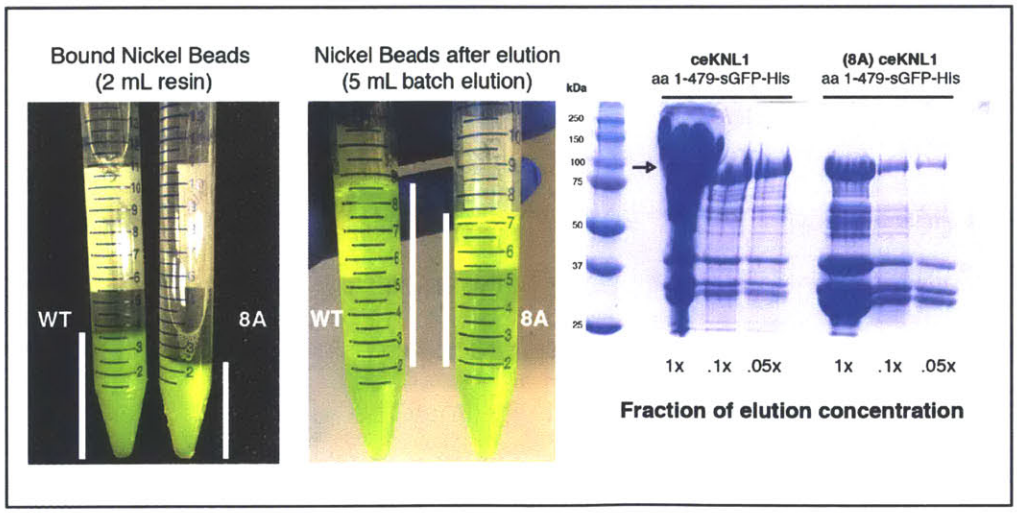

Supplemental Figure 1. Analysis of the KNL-1 oligomerization domain (A) Table showing the behavior of ceKNL1 truncations. All constructs have an N-terminal His-tag (MRGSHHHHHHGMAS-). The stokes radii are approximated from superpose 6 sizing column runs except where noted. Aggregated proteins ran in the void of the column. (B) The uncropped gel lanes for the highest concentrations of proteins used in Figure 1B and Figure 4A. (C) Purification of wild-type and 8A mutant ceKNL-1 1-479-superfolderGFP-His fusions. From left to right (1) Apparent nickel bead volume is increased from 2 mL to 3.5 mL when bound to wild-type protein. (2) When eluted overnight with 5 mL of elution buffer, the extra bead volume moves to the elution. (3). Superfolder fusions (indicated with arrow) express at high levels as shown by Coomassie gel.

Supplemental Tables

Table S1. *C. elegans* strains used in this study

Strain Number	Genotype
N2(ancestral)	
TH32	unc-119(ed3) III; ruIs32[pAZ132; pie-1/GFP::histone H2B] III; ddIs6 [GFP::tbg-1; unc-119(+)] V
OD334	*unc-119(ed3) III; ltSi1[pOD809/pJE110; Pknl-1::KNL-1reencoded::mCherry; cb-unc-119(+)]II*
OD388	ltSi1[pOD809/pJE110; Pknl-1::KNL-1reencoded::mCherry; cb-unc-119(+)]II;unc-119(ed3) III?;I; ruIs32[pAZ132; pie-1/GFP::histone H2B] III; ddIs6 [GFP::tbg-1; unc-119(+)] V
OD710	ltSi1[pDK(ic80?); Pknl-1::KNL-1reencoded::mCherry(Δ102-236); cb-unc-119(+)]II;unc-119(ed3) III?;I; ruIs32[pAZ132; pie-1/GFP::histone H2B] III; ddIs6 [GFP::tbg-1; unc-119(+)] V
OD1378	*unc-119(ed3) III; ltSi1[pDK329; Pknl-1::KNL-1reencoded::mCherry(8A); cb-unc-119(+)]II*
OD1618	*ltSi1[pDK329; Pknl-1::KNL-1reencoded::mCherry(8A); cb-unc-119(+)]II;unc-119(ed3) III?;I; ruIs32[pAZ132; pie-1/GFP::histone H2B] III; ddIs6 [GFP::tbg-1; unc-119(+)] V*
OD2030	unc-119(ed3) III; ltSi1[pDK471; Pknl-1::KNL-1reencoded::mCherry(8A+MELT mutants); cb-unc-119(+)]II

Table S2. Oligos and template used for dsRNA production

Gene	Oligonucleotide #1	Oligonucleotide #2	Template	mg/mL
C02F5.1 (knl-1)	5'-AATTAACCCTCACTAAAGGAATCTCGAATCACCGAAATGTC-3'	5'-TAATACGACTCACTATAGGTTCACAAACTTGGAAGCCGCTG-3'	N2 cDNA	1.5

Materials and Methods

Plasmids

6xHis *E. coli* expression constructs for the KNL-1 oligomerization domains (His-ceKNL-1 amino acids 69-235, His-crKNL-1 amino acids 76-216, and His-crKNL-1 amino acids 76-396) were amplified from *C. elegans* cDNA or synthesized by Genewiz and cloned into pRSETa to add an N-terminal His-tag (MRGSHHHHHHGMAS-). The 6xHis-ceKNL-1 1-479 expression constructs was generated using a modified pET3aTr vector to add a PreScission cleavable, N-terminal His-tag (MRGSHHHHHHGMASMTGGQQMGRDLYDDDDKLEVLFQGPH-).

SuperfolderGFP constructs were cloned with a custom C-terminal superfolderGFP-His tag. Mutations for ceKNL-1 constructs were introduced using PCR.

Protein Production and Purification

Proteins were produced using 3-12 L of BL21 (DE3) *E. coli*. Generally, bacteria was grown to OD 0.6-1 at 30°C in LB media containing antibiotic and 0.4% glucose. The temperature was reduced to 18°C and protein production was induced with 100 mM IPTG. The bacteria was harvested 6 hours post-induction (20 hours for GFP constructs) with Lysis Buffer (50 mM Sodium Phosphate pH 8, 300 mM NaCl, 40 mM Imidazole) and frozen at -80°C. The bacterial pellet was then thawed and lysed using 1 mg/mL lysozyme and sonication. 10 mM Beta-mercaptoethanol was then added. The lysate was pelleted at 40,000 x g for 30 minutes. The supernatant was bound to Ni-NTA resin (Qiagen) for 1 hour at 4°C. The resin was washed with Wash Buffer (50 mM Sodium Phosphate pH 8, 500 mM NaCl, 40 mM Imidazole, 10 mM BME, 0.1% Tween-20). Bound protein was

then eluted with Elution Buffer (50 mM Sodium Phosphate pH 7, 500 mM NaCl, 250 mM Imidazole, 10 mM BME). Elutions were loaded onto Superose 6 or Superdex 200 columns for gel filtration into Schwartz Buffer (20 mM Sodium Phosphate pH 7, 150 mM NaCl, 1 mM DTT). Peak fractions were checked using SDS-PAGE gels stained with Coomassie. The peak fractions were then pooled and spin concentrated (Vivaspin; GE Healthcare). Protein concentrations were determined using the Biorad Assay kit. Protein was used fresh (within a few days on ice and never freeze/thawed) for all experiments.

Gel Filtration

Proteins were loaded at indicated concentrations onto either a Sephacryl S-500 HR 16/60 column or a Superose 6 10/30 GL column equilibrated in Schwartz Buffer. Size standards run with matching loading volumes are marked as indicated in figures. Runs were analyzed using representative fractions spanning the column runs with SDS-PAGE gels stained with Coomassie. Note: Due to the low absorption coefficient at 280 nm for the KNL-1 protein fragments we used large Coomassie-stained gels, instead of UV traces, for visualization.

Dynamic Light Scattering

Measurements were taken using a Protein Solutions Dynapro instrument and Dynamics V6 software. The measurements were taken using 10 reads each with a 10 second averaging time.

Glutaraldehyde cross-linking

Proteins were cross-linked at the indicated concentrations of protein. Glutaraldehyde (70% stock solution, EM grade, Sigma-Aldrich) was diluted in ddH_2O to 0.2% or 1% (1% was also used for Superose 6 runs) and mixed with

protein at 1:20 to the indicated final concentrations. Mock cross-linking was performed using the equivalent volume of ddH_2O. The proteins were cross-linked for 10 minutes at room temperature and then quenched with 1:10 volume of 1M Tris pH 8. For Figure 2A, the protein was loaded onto a 12% SDS-PAGE gel for visualization with Coomassie. For Figure 2B, following the quenching, the proteins were pelleted at 18,000 g and then loaded onto the Superose 6 gel filtration column in Schwartz Buffer and runs were visualized using 12% SDS-PAGE gels stained with Coomassie.

Analytical Ultracentrifugation

The sedimentation-velocity (SV) experiment for the His-crKNL-1 76-396 construct was conducted using purified protein at ~20 μM in Schwartz Buffer using a Beckman Optima XL-I analytical ultracentrifuge in interference mode (MIT Biophysical Instrumentation Facility, MIT-BIF). Data was collected at 20°C at 25,000 rpm. The data was fit using SEDFIT to a model for continuous sedimentation coefficient distribution, assuming a single frictional coefficient. The molecular weights were estimated using the best-fit frictional coefficients.

Election Microscopy

To prevent disassembly of the oligomers under the conditions used for EM, His-ceKNL-1 69-235 and His-crKNL-1 76-216 were cross-linked at ~5 μM and ~10 μM respectively using a final concentration of 0.1% Glutaraldehyde. Following quenching, protein was dialyzed into EM Buffer (20 mM Tris pH 7.5, 150 mM NaCl, 1 mM DTT) for 5 hours at 4°C. Samples were then kept on ice until grid preparation. For grid preparation, 4 μl samples were applied to freshly glow-discharged continuous carbon grids and stained with 0.75% uranyl formate. Images were collected on an FEI Tecnai F-20 electron microscope with a Gatan

US4000 CCD detector using a nominal magnification of 62,000x (83,701x at detector) and a -3 μm defocus.

Sequence Analysis

Sequences were aligned using ClustalX and Jalview software.

Worm strains

The worm strains used in this study are listed in Table S1. The KNL-1 mutations were engineered into a vector expressing KNL-1::mCherry (Espeut *et al.*, 2012). Plasmids were injected into strain EG4322 to obtain stable single-copy integrants (Frokjaer-Jensen *et al.*, 2008). Integration of transgenes was confirmed by PCR. For live imaging, transgenes were crossed into a strain expressing GFP::H2b/GFP::γ-tubulin and the transgene as well as both markers were homozygosed prior to analysis.

RNA-mediated Interference

Double-stranded RNAs used in this study are listed in Table S2. All RNAi was performed by microinjection. L4 worms were injected with dsRNAs and incubated for 38–43 h at 20°C before imaging of the embryos. For lethality assays, L4 worms were injected with dsRNA and singled onto plates at 24 hours post-injection; adult worms were removed from the plates at 48 hours post-injection and hatched larvae and unhatched embryos were counted at 72 hours post-injection.

Time-lapse microscopy

For imaging of chromosomes and pole tracking analysis, images were acquired on a deconvolution microscope (DeltaVision; Applied Precision) equipped with a

charge-coupled device camera (CoolSnap; Roper Scientific) with 5 x 2 μm z-stacks, 2x2 binning, and a 60x 1.3 NA U-planApo objective (Olympus) at 10 sec intervals and 100 ms exposure at 18°C. Spindle pole separation was quantified as described (Desai *et al.*, 2003).

For KNL-1 localization, embryos expressing GFP::H2b/GFP::γ-tubulin/KNL-1::mCherry were filmed every 20 sec with 5 x 2 μm z-stacks on an Andor Revolution XD Confocal System (Andor Technology) and a confocal scanner unit (CSU-10; Yokogawa) mounted on an inverted microscope (TE2000-E; Nikon) equipped with 100x, 1.4 NA Plan Apochromat lens and outfitted with an electron multiplication back-thinned charge-coupled device camera (iXon, Andor Technology, binning 1x1) at 20°C. Exposure was 100 ms for GFP and 300 ms for mCherry.

Acknowledgements

Debby Pheasant and the Biophysical Instrumentation Facility for the Study of Complex Macromolecular Systems (NSF-007031) are gratefully acknowledged. We thank Nikolaus Grigorieff, Mathijs Vleugel, Bob Sauer, Thomas Schwartz, Ellen Kloss, and members of the Cheeseman laboratory for their support, input, and helpful discussions. This work was supported by a Scholar award to IMC from the Leukemia & Lymphoma Society, grants from the NIH/National Institute of General Medical Sciences to IMC (GM088313), AD (GM074215), and a Research Scholar Grant to IC (121776) from the American Cancer Society. M.R. was supported by funding from HHMI to Nikolaus Grigorieff.

References

Amaro, A.C., Samora, C.P., Holtackers, R., Wang, E., Kingston, I.J., Alonso, M., Lampson, M., McAinsh, A.D., and Meraldi, P. (2010). Molecular control of

kinetochore-microtubule dynamics and chromosome oscillations. Nat Cell Biol *12*, 319-329.

Caldas, G.V., and DeLuca, J.G. (2014). KNL1: bringing order to the kinetochore. Chromosoma *123*, 169-181.

Caldas, G.V., DeLuca, K.F., and DeLuca, J.G. (2013). KNL1 facilitates phosphorylation of outer kinetochore proteins by promoting Aurora B kinase activity. J Cell Biol *203*, 957-969.

Cheerambathur, D.K., Gassmann, R., Cook, B., Oegema, K., and Desai, A. (2013). Crosstalk between microtubule attachment complexes ensures accurate chromosome segregation. Science *342*, 1239-1242.

Cheeseman, I.M., Chappie, J.S., Wilson-Kubalek, E.M., and Desai, A. (2006). The Conserved KMN Network Constitutes the Core Microtubule-Binding Site of the Kinetochore. Cell *127*, 983-997.

Cheeseman, I.M., and Desai, A. (2008). Molecular Architecture of the Kinetochore-Microtubule Interface. Nat Rev Mol Cell Biol *9*, 33-46.

Cheeseman, I.M., Niessen, S., Anderson, S., Hyndman, F., Yates, J.R., III, Oegema, K., and Desai, A. (2004). A conserved protein network controls assembly of the outer kinetochore and its ability to sustain tension. Genes Dev. *18*, 2255-2268.

Ciferri, C., Pasqualato, S., Screpanti, E., Varetti, G., Santaguida, S., Dos Reis, G., Maiolica, A., Polka, J., De Luca, J.G., De Wulf, P., Salek, M., Rappsilber, J., Moores, C.A., Salmon, E.D., and Musacchio, A. (2008). Implications for kinetochore-microtubule attachment from the structure of an engineered Ndc80 complex. Cell *133*, 427-439.

DeLuca, J.G., Gall, W.E., Ciferri, C., Cimini, D., Musacchio, A., and Salmon, E.D. (2006). Kinetochore Microtubule Dynamics and Attachment Stability Are Regulated by Hec1. Cell *127*, 969-982.

Desai, A., Rybina, S., Muller-Reichert, T., Shevchenko, A., Shevchenko, A., Hyman, A., and Oegema, K. (2003). KNL-1 directs assembly of the microtubule-binding interface of the kinetochore in C. elegans. Genes Dev. *17*, 2421-2435.

Espeut, J., Cheerambathur, D.K., Krenning, L., Oegema, K., and Desai, A. (2012). Microtubule binding by KNL-1 contributes to spindle checkpoint silencing at the kinetochore. J Cell Biol *196*, 469-482.

Frokjaer-Jensen, C., Davis, M.W., Hopkins, C.E., Newman, B.J., Thummel, J.M., Olesen, S.P., Grunnet, M., and Jorgensen, E.M. (2008). Single-copy insertion of transgenes in Caenorhabditis elegans. Nat Genet *40*, 1375-1383.

Gascoigne, K.E., Takeuchi, K., Suzuki, A., Hori, T., Fukagawa, T., and Cheeseman, I.M. (2011). Induced ectopic kinetochore assembly bypasses the requirement for CENP-A nucleosomes. Cell *145*, 410-422.

Joglekar, A.P., Bouck, D., Finley, K., Liu, X., Wan, Y., Berman, J., He, X., Salmon, E.D., and Bloom, K.S. (2008). Molecular architecture of the kinetochore-microtubule attachment site is conserved between point and regional centromeres. J Cell Biol *181*, 587-594.

Joglekar, A.P., Bouck, D.C., Molk, J.N., Bloom, K.S., and Salmon, E.D. (2006). Molecular architecture of a kinetochore-microtubule attachment site. Nat Cell Biol *8*, 581-585.

Kitagawa, D., Vakonakis, I., Olieric, N., Hilbert, M., Keller, D., Olieric, V., Bortfeld, M., Erat, M.C., Fluckiger, I., Gonczy, P., and Steinmetz, M.O. (2011). Structural basis of the 9-fold symmetry of centrioles. Cell *144*, 364-375.

Kiyomitsu, T., Murakami, H., and Yanagida, M. (2011). Protein interaction domain mapping of human kinetochore protein Blinkin reveals a consensus motif for binding of spindle assembly checkpoint proteins Bub1 and BubR1. Mol Cell Biol *31*, 998-1011.

Kiyomitsu, T., Obuse, C., and Yanagida, M. (2007). Human Blinkin/AF15q14 Is Required for Chromosome Alignment and the Mitotic Checkpoint through Direct Interaction with Bub1 and BubR1. Dev Cell *13*, 663-676.

Krenn, V., Wehenkel, A., Li, X., Santaguida, S., and Musacchio, A. (2012). Structural analysis reveals features of the spindle checkpoint kinase Bub1-kinetochore subunit Knl1 interaction. J Cell Biol *196*, 451-467.

Lawrimore, J., Bloom, K.S., and Salmon, E.D. (2011). Point centromeres contain more than a single centromere-specific Cse4 (CENP-A) nucleosome. J Cell Biol *195*, 573-582.

Liu, D., Vleugel, M., Backer, C.B., Hori, T., Fukagawa, T., Cheeseman, I.M., and Lampson, M.A. (2010). Regulated targeting of protein phosphatase 1 to the outer kinetochore by KNL1 opposes Aurora B kinase. J Cell Biol *188*, 809-820.

Moyle, M.W., Kim, T., Hattersley, N., Espeut, J., Cheerambathur, D.K., Oegema, K., and Desai, A. (2014). A Bub1-Mad1 interaction targets the Mad1-Mad2 complex to unattached kinetochores to initiate the spindle checkpoint. J Cell Biol *204*, 647-657.

Pedelacq, J.D., Cabantous, S., Tran, T., Terwilliger, T.C., and Waldo, G.S. (2006). Engineering and characterization of a superfolder green fluorescent protein. Nat Biotechnol *24*, 79-88.

Petrovic, A., Mosalaganti, S., Keller, J., Mattiuzzo, M., Overlack, K., Krenn, V., De Antoni, A., Wohlgemuth, S., Cecatiello, V., Pasqualato, S., Raunser, S., and Musacchio, A. (2014). Modular assembly of RWD domains on the Mis12 complex underlies outer kinetochore organization. Mol Cell *53*, 591-605.

Przewloka, M.R., Venkei, Z., Bolanos-Garcia, V.M., Debski, J., Dadlez, M., and Glover, D.M. (2011). CENP-C is a structural platform for kinetochore assembly. Current Biology *21*, 399-405.

Schmidt, J.C., Arthanari, H., Boeszoermenyi, A., Dashkevich, N.M., Wilson-Kubalek, E.M., Monnier, N., Markus, M., Oberer, M., Milligan, R.A., Bathe, M., Wagner, G., Grishchuk, E.L., and Cheeseman, I.M. (2012). The kinetochore-bound Ska1 complex tracks depolymerizing microtubules and binds to curved protofilaments. Dev Cell *23*, 968-980.

Screpanti, E., De Antoni, A., Alushin, G.M., Petrovic, A., Melis, T., Nogales, E., and Musacchio, A. (2011). Direct binding of Cenp-C to the Mis12 complex joins the inner and outer kinetochore. Current Biology *21*, 391-398.

van Breugel, M., Hirono, M., Andreeva, A., Yanagisawa, H.A., Yamaguchi, S., Nakazawa, Y., Morgner, N., Petrovich, M., Ebong, I.O., Robinson, C.V., Johnson, C.M., Veprintsev, D., and Zuber, B. (2011). Structures of SAS-6 suggest its organization in centrioles. Science *331*, 1196-1199.

Vleugel, M., Tromer, E., Omerzu, M., Groenewold, V., Nijenhuis, W., Snel, B., and Kops, G.J. (2013). Arrayed BUB recruitment modules in the kinetochore scaffold KNL1 promote accurate chromosome segregation. J Cell Biol *203*, 943-955.

Wei, R.R., Al-Bassam, J., and Harrison, S.C. (2007). The Ndc80/HEC1 complex is a contact point for kinetochore-microtubule attachment. Nat Struct Mol Biol *14*, 54-59.

Welburn, J.P., Vleugel, M., Liu, D., Yates, J.R., 3rd, Lampson, M.A., Fukagawa, T., and Cheeseman, I.M. (2010). Aurora B phosphorylates spatially distinct targets to differentially regulate the kinetochore-microtubule interface. Mol Cell *38*, 383-392.

Wine, Y., Cohen-Hadar, N., Freeman, A., and Frolow, F. (2007). Elucidation of the mechanism and end products of glutaraldehyde crosslinking reaction by X-ray structure analysis. Biotechnology and bioengineering *98*, 711-718.

Zhang, G., Lischetti, T., and Nilsson, J. (2014). A minimal number of MELT repeats supports all the functions of KNL1 in chromosome segregation. J Cell Sci *127*, 871-884.

Chapter III: Discovery of the mitotic SKAP isoform reveals a spindle positioning role at astral microtubule plus ends

David M. Kern, Peter K. Nicholls, David C. Page, Iain M. Cheeseman

Peter K. Nicholls carried out mouse tissue harvesting, preparation of tissue sections, and scanning confocal imaging of sections.

Abstract

The Astrin/SKAP complex plays important roles in mitotic chromosome alignment and centrosome integrity, but previous work found conflicting results for SKAP function. Here, we demonstrate that SKAP is expressed as two distinct transcriptional isoforms in mammals; a longer testis-specific isoform that was used for previous studies in mitotic cells, and a novel shorter mitotic isoform. Unlike the longer isoform, short SKAP rescues SKAP depletion in mitosis and displays robust microtubule plus-end tracking, including localization to astral microtubules. Eliminating SKAP microtubule binding results in severe chromosome segregation defects. In contrast, SKAP mutants defective specifically for plus-end tracking facilitate proper chromosome segregation, but cause dramatic spindle positioning defects. We find that SKAP plus-end-tracking mutant cells show a reduction in Clasp1 localization to microtubules, and display increased lateral microtubule contacts with the cell cortex, which result in unbalanced cortical dynein pulling forces. Our work reveals an unappreciated role for the Astrin/SKAP complex as an astral microtubule mediator of mitotic spindle positioning.

Introduction

Mitosis requires the assembly of the microtubule-based mitotic spindle to provide the structure and forces for cell division. Multiple molecular players associate with the cell division apparatus to facilitate spindle assembly and chromosome segregation. Previous work from our lab and others has identified the Astrin/SKAP complex, which localizes to kinetochores and the mitotic spindle where it plays multiple important roles, including in chromosome alignment and the maintenance of spindle bipolarity (Dunsch et al., 2011; Gruber et al., 2002; Mack and Compton, 2001; Manning et al., 2010; Schmidt et al., 2010; Thein et al., 2007). The Astrin/SKAP complex (Dunsch et al., 2011; Schmidt et al., 2010) is a comprised of the dynein light chain LC8, the large protein Astrin (also referred to as Spag5), and the Small Kinetochore-Associated Protein, SKAP (Fang et al., 2009); also referred to as C15orf23, Traf4af1, or Kinastrin). Although SKAP plays a central role within this complex, previous work has found conflicting results for its contributions and behavior. Here, we find that the SKAP isoform that was used in all previous studies of the human protein is exclusively expressed in mammalian testes, whereas mitotic cells instead express a shorter isoform of SKAP. Our analysis of the mitotic SKAP isoform reveals a striking localization of this protein both along the length of spindle microtubules and to microtubule plus ends, including to astral microtubules, suggesting potential roles for this complex beyond its previously defined functions in chromosome segregation.

Microtubules emanating from the spindle poles interact with two major subcellular sites: kinetochores and the cell cortex. Whereas kinetochores link microtubules to chromosomal DNA to direct chromosome segregation, the cell cortex anchors astral microtubules to the plasma membrane to generate cortical pulling forces that direct spindle positioning and orientation. Spindle positioning is

critical for organismal development and cellular viability (Gonczy, 2008; Knoblich, 2010; Siller and Doe, 2009). The position of the mitotic spindle within a dividing cell establishes the cell division plane and the site of the cytokinetic furrow, thereby defining the relative sizes of the two daughter cells. The force to move the spindle within a cell is generated by the interaction of astral microtubule plus ends with the microtubule-based motor cytoplasmic dynein, which is localized to the cell cortex (Kiyomitsu, 2015; Kiyomitsu and Cheeseman, 2012; Kotak et al., 2012; McNally, 2013). Astral microtubules are a unique mitotic population of highly dynamic microtubules that emanate from the centrosome and grow towards the cell cortex. When astral microtubules contact the cortex, dynein is thought to establish an "end-on" attachment and generate pulling force to move the spindle towards the cell cortex (Hendricks et al., 2012; Laan et al., 2012). The amount of pulling force on each side of the spindle is regulated through dynamic changes in the relative levels of cortical dynein (Collins et al., 2012; Kiyomitsu and Cheeseman, 2012). As a cell progresses from pro-metaphase into metaphase, the dynein motors on each side of the cell engage in a brief "tug-of-war" until the spindle is positioned at the cell center. In human cells, mitotic spindle position is controlled by both extrinsic and intrinsic cues (Fink et al., 2011; Kiyomitsu and Cheeseman, 2012). Much of the work on spindle positioning has focused on external or cortical factors, leaving important open questions regarding the function of astral microtubules. Although several microtubule plus-end proteins have been proposed to play roles in spindle positioning, including the end-binding (EB) proteins and Clasp1 (Bird et al., 2013; Green et al., 2005; Rogers et al., 2002; Samora et al., 2011), it remains unclear what protein components and properties of astral microtubule plus ends are required for proper interactions with cortical dynein.

Our analysis reveals that the Astrin/SKAP complex plays an important role as astral microtubule plus-end-tracking proteins for mediating proper spindle positioning. In cells with a plus-end-tracking mutant of SKAP, chromosome segregation occurs normally, but metaphase spindles are dramatically mispositioned within the cell. We demonstrate that this spindle mispositioning occurs through an imbalance of forces generated by dynein localized to the cell cortex. SKAP plus-end-tracking mutants display an accumulation of lateral interactions between astral microtubules and cell cortex. We propose that the Astrin/SKAP complex mediates the proper connection between astral microtubule plus ends and cortical dynein.

Results

SKAP has both mitotic and testis/meiosis-specific isoforms

All previous studies on SKAP have utilized a consensus annotated database protein sequence (ID: Q9Y448-1) with a predicted molecular weight of 34.5 kDa. However, in analyzing the behavior of SKAP in human tissue culture cells, our affinity purified anti-SKAP antibody detected a protein of ~27 kDa following SDS-PAGE and Western blotting (Fig. 1A). To investigate this discrepancy, we pooled data from our immunoprecipitations of the SKAP-associated protein Astrin from mitotic HeLa cells and assessed the peptides detected for endogenous SKAP. Although we obtained significant coverage from the C terminal regions of the protein, we were unable to detect peptides from a large region of the N terminus for the annotated protein (Fig. 1B). To determine the origin of the apparent differences in the SKAP protein sequence, we examined RNA-seq data from the Human BodyMap 2.0 database (Fig. 1C). We found that the only tissue with reads spanning the entire annotated SKAP sequence was testis. In all other tissues, transcriptional initiation began within the first annotated exon resulting in an mRNA lacking the previously defined start codon. Instead, the first in-frame, coding methionine appeared within the previously defined exon 2. We conclude that the mitotic form of SKAP observed in HeLa cells is generated from this alternative transcriptional start site leading to translation at the second annotated methionine. This shorter SKAP isoform has a predicted molecular weight of 26.9 kDa, consistent with our mass spectrometry and Western blot analysis (Fig. 1A, 1B and Fig. S1A).

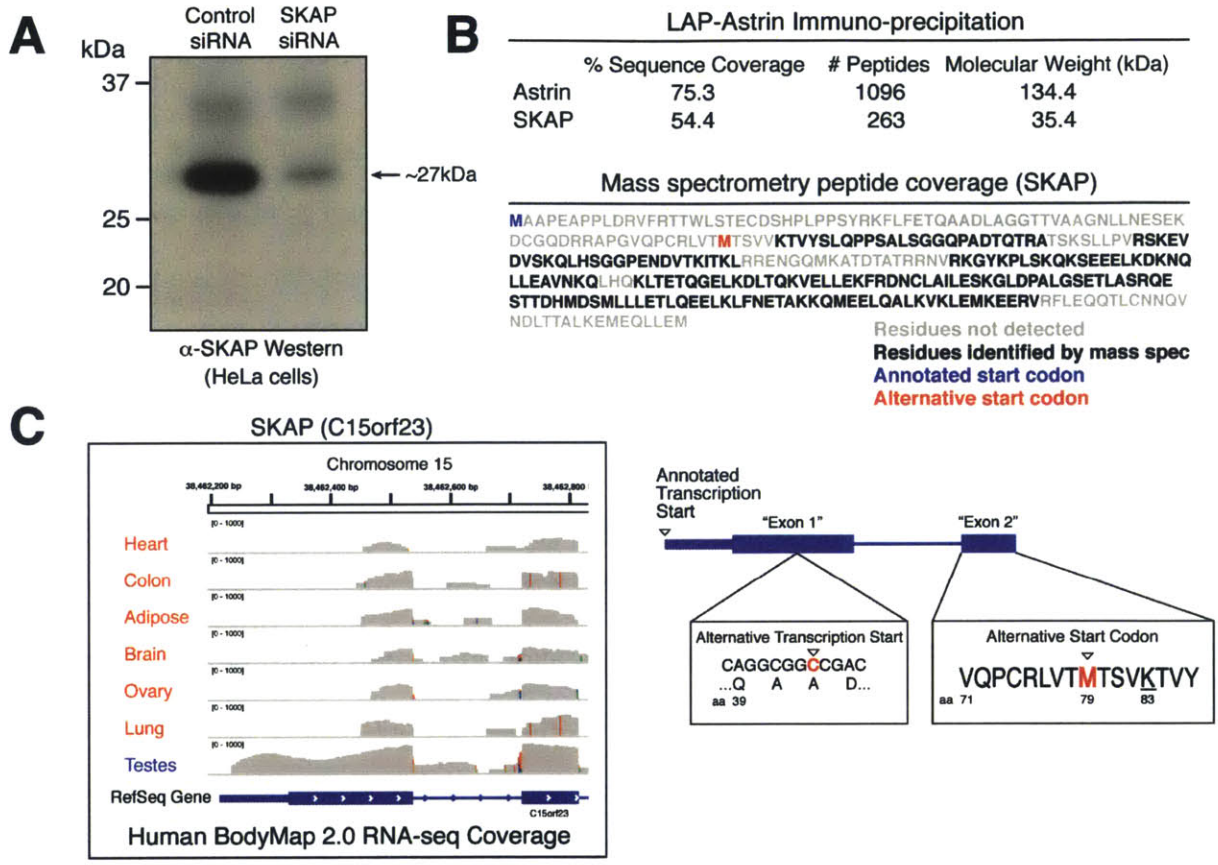

Figure 1. SKAP has distinct mitotic and testis-specific isoforms. (A) Western blot showing the molecular weight of endogenous SKAP from HeLa cells assessed by protein marker migration. (B) Top: Immunoprecipitation Mass Spectrometry (IP-MS) data pooled from LAP-Astrin IPs analyzed for Astrin and SKAP peptides. Bottom: Identified SKAP peptides mapped against SKAP amino acid sequence. (ID: Q9Y448-1) (C) Left: Map of the 5' end of the SKAP locus with RNA-seq reads from Human BodyMap 2.0. Right: Schematic of the transcript for the short (mitotic) SKAP isoform. Underlined lysine indicates the first peptide identifiable in a tryptic digest for short SKAP.

SKAP and its binding partner Astrin are conserved throughout vertebrates (Fig. S1B), but lack obvious orthologues in fungi, insects, and nematodes. In contrast, the longer, testis-specific SKAP isoform shows a unique phylogeny, with this form only appearing recently in eutherian mammals. The N-terminal extension does not appear in birds (aves) or metatherian mammals (marsupials)

and shows greater sequence divergence than the rest of the protein. The N terminal regions of the human and mouse SKAP proteins have only 46% identity, compared to 75% identity for the remainder of the protein (Fig. S1A and S1B). Thus, in eutherian mammals, SKAP is expressed as two isoforms with distinct transcriptional start sites, resulting in a shorter mitotic form (which we will refer to as "short SKAP") and a longer testis-specific form (which we will refer to as "long SKAP").

We previously generated an antibody that detects both isoforms of the human SKAP protein (Schmidt et al., 2010). Using this antibody, we observed SKAP localization to kinetochores and spindle microtubules in metaphase mouse 3T3 cells (Fig. S1C), similar to its localization in human HeLa cells (Schmidt et al., 2010). To specifically investigate the expression and localization of the longer SKAP isoform, we additionally generated an antibody against the testis-specific N-terminal extension of the mouse SKAP protein (Fig. S1A). Western blotting indicated that the short SKAP isoform was present in mitotic (nocodazole-arrested) mouse 3T3 cells, juvenile (6 day old) mouse testis, and adult (70 day old) mouse testis, which represent cells or tissues with mitotic populations (Fig. S1D). In contrast, we found that the long SKAP isoform was only present in adult mouse testis (Fig. S1D). Consistent with this, immunoprecipitation of SKAP from adult mouse testes identified peptides corresponding to the N-terminal region that was absent in mitotic cells, as well as co-purifying peptides from Astrin (Fig. 2A). Therefore, both the long SKAP and short SKAP proteins are produced in mice, with testis-specific and mitotic expression respectively.

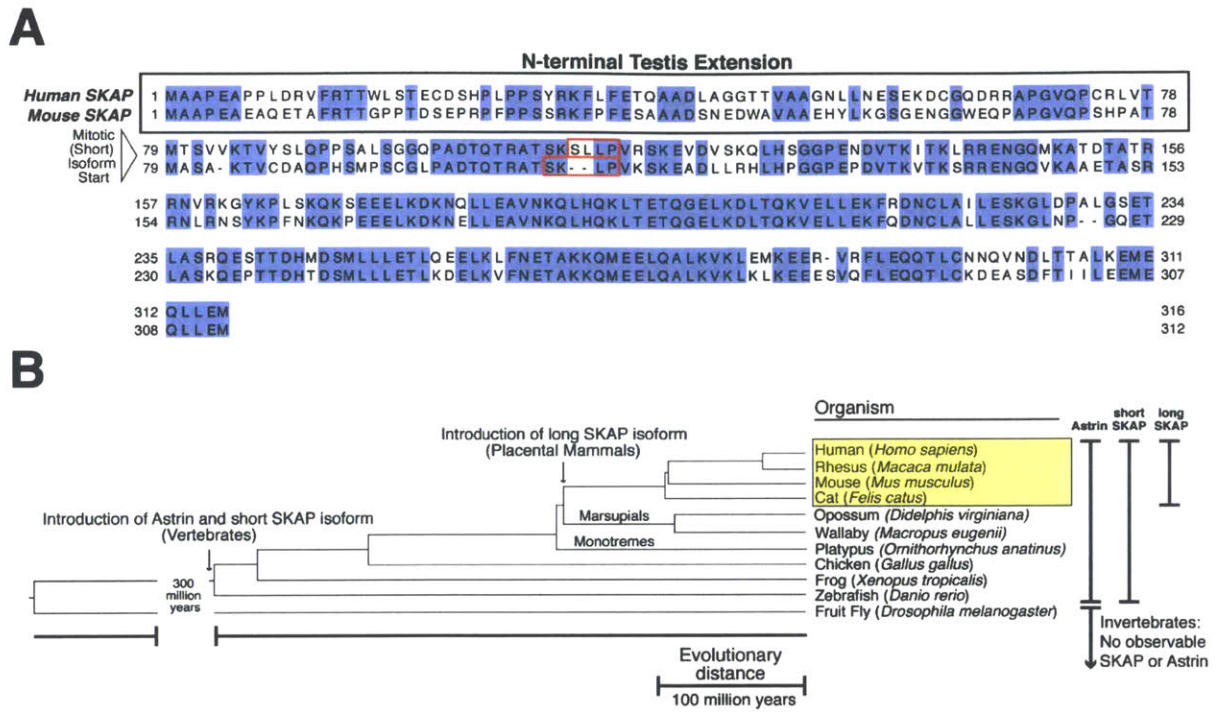

Figure S1. Alignment and Phylogeny for SKAP and its isoforms and characterization of SKAP isoforms in mouse cells and tissues. (A) Alignment of human vs. mouse SKAP proteins using Jalview software. Identity is shown in blue. The N-terminal testis extension is boxed in black and the start of the mitotic isoform is marked with an arrow. The SX[I/L]P motif in each protein is boxed in red. (B) Phylogeny for SKAP derived from TimeTree species divergence data. Astrin and the short (mitotic) form of SKAP are first visible in vertebrates. The long (testis-specific) isoform is first detectable in placental (eutherian) mammals (highlighted in yellow). (C) Immunofluorescence of the human full length SKAP antibody in a metaphase mouse 3T3 cell. The image represents a maximal intensity projection. SKAP localizes to kinetochores and the mitotic spindle. Scale bar, 5 μm. (D) Western blot showing the presence of the SKAP long and short isoforms in the indicated cells and tissues. The short form is

present in mitotic cells and tissues. The long (testis-specific) form appears in adult mouse testis. Tubulin is shown as a relative control for loading levels. Tubulin displays a shift in its mobililty due to its increasing post-translational modifications state from left to right. * indicate non-specific bands.

The longer, testis-specific SKAP isoform localizes to elongating spermatids and meiotic cells

To visualize the expression and localization of the long SKAP isoform, we immuno-stained mouse testes. In adult mice, we observed extremely strong localization in elongating spermatids within the seminiferous epithelium (Fig. 2B). This localization began as a punctate pattern throughout the DNA (Fig. 2C) in testis developmental stage X (Russell et al., 1990), then spread to the cytoplasm and increased in levels though stages XI and XII, persisting in stages I and II, before decreasing in stages III and IV (data not shown). In addition to the high levels of expression during late spermatogenesis, immunohistochemistry revealed localization of the testis-specific SKAP isoform to meiosis I spindles (Fig. 2D) and weaker localization to meiosis II spindles (data not shown) in stage XI diplotene and stage XII secondary spermatocytes, respectively. We did not detect localization of the testis-specific SKAP isoform in mitotic cells of the testis, attesting to both the timing of the localization and specificity of the antibody. We also note that recent work from the de Massy laboratory (Grey et al., submitted; personal communication) found that in SKAP knockout mice, both the short and long SKAP isoforms detected by Western blotting were abolished. This further establishes the existence of both isoforms and validates the long SKAP antibody described here. In summary, our work demonstrates that the testis-specific SKAP isoform localizes to meiotic cells, DNA localized puncta in stage X, and is expressed at a high level in elongated spermatids, consistent with multiple potential roles in spermatogenesis.

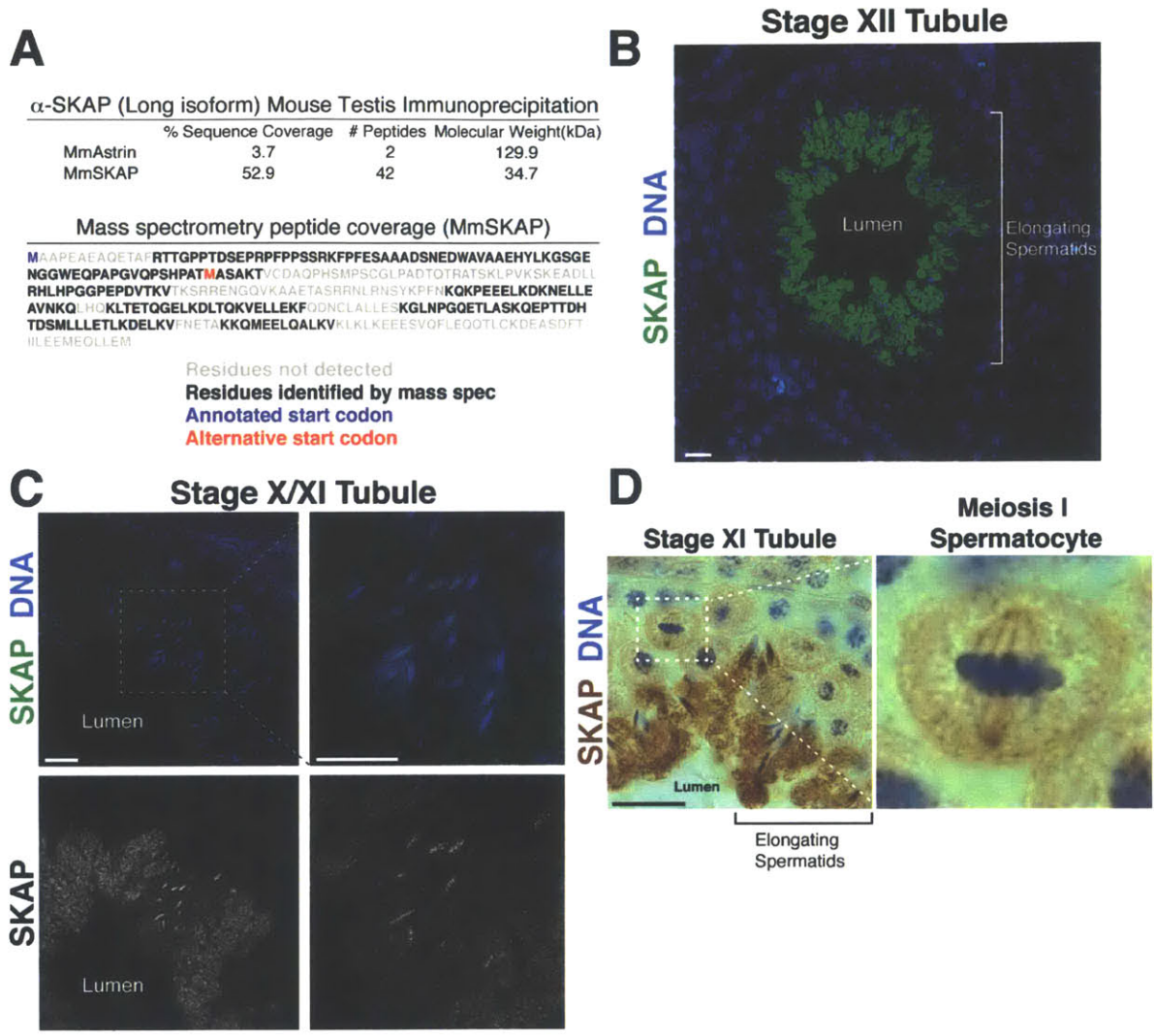

Figure 2. The long testis-specific SKAP isoform localizes to elongating spermatids and meiotic spindles. (A) Top: IP-MS data using an antibody to the long form of mouse SKAP from mouse testes analyzed for Astrin and SKAP peptides. Bottom: Identified SKAP peptides mapped against SKAP amino acid sequence. (ID: Q9Y448-1) (B) Confocal image of long (testis) SKAP immunofluorescent localization to elongating spermatids in a mouse seminiferous tubule. The seminiferious tubule lumen is indicated throughout this figure. (C) Testis sections showing immunofluorescent SKAP localization to elongating spermatids in a mouse seminiferous tubule transitioning from developmental Stage X to XI. Left: Region imaged with a 40X objective. Right: Region imaged with a 100X objective. (D) Testis visualized for SKAP using immunohistochemistry stain imaged with a brightfield microscope using a 100X objective. Left: Image of a region of a mouse tubule. Right: Zoom of a meiotic cell showing SKAP staining. Scale bars, 20 μm.

Short SKAP, but not long SKAP, is fully functional to facilitate mitosis

Prior studies on SKAP function in mitosis have relied on unrescued RNAi depletions (Schmidt et al., 2010) or ectopic expression of long SKAP (Lee et al., 2014; Tamura et al., 2015). With knowledge of these two SKAP isoforms, we next tested the functionality of each isoform in mitotic human cells by conducting rescue experiments. Following SKAP depletion by RNAi (Fig. 3A; Fig. S2A), we observed dramatic defects in mitosis, including cells with highly misaligned chromosomes, disorganized spindles, and multi-polar spindles that are a result of premature centriole splitting based on centrin localization (Fig. 3B-E). Expression of an RNAi-resistant version of the long (testis-specific) SKAP isoform was unable to rescue these defects (Fig 3B, C, E, and Fig. S2B, C; see Materials and Methods). In contrast, expression of the short SKAP isoform fully rescued SKAP depletion as assessed by proper SKAP localization (Fig. 3B), chromosome alignment (Fig. 3B, C), bipolar spindle assembly, and mitotic timing from nuclear envelope breakdown (NEBD) to anaphase (Fig. 3E and Fig. S2B). Therefore, the short (mitotic) isoform, but not the long (testis) isoform, rescues SKAP depletion defects in mitosis, demonstrating that these isoforms represent functionally distinct proteins.

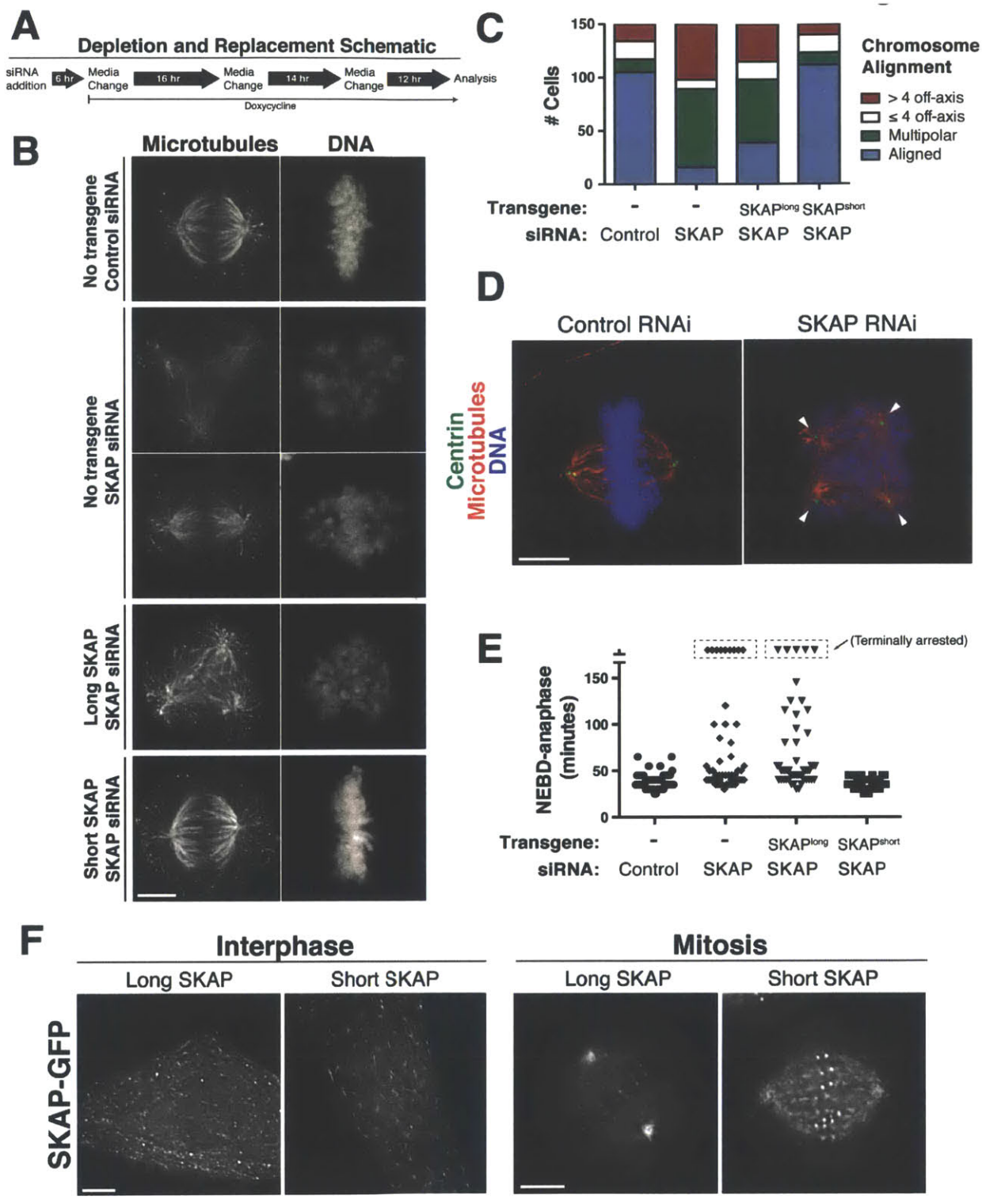

Figure 3. The long and short SKAP isoforms display distinct mitotic functionality. (A) Schematic of SKAP depletion and replacement protocol. Also see Fig. S2A for a Western blot analyzing the efficiency of depletion and replacment. (B) Immunofluorescence images showing tubulin and DNA

localization for the phenotypes exhibited during SKAP depletion and rescue experiments. From top to bottom: aligned, multipolar, misaligned (off-axis) chromosomes, multipolar, and aligned. Images represent maximal intensity projections. (C) Quantification of mitotic chromosome alignment for SKAP depletion and rescue experiments from part B. Cells were quantified by observing DNA and spindle morphology by immunofluorescence. Cells were quantified for a phenotype if they displayed GFP reporter expression (if applicable) and showed chromosome alignment, spindle and cell shape morphology indicative of a metaphase or multipolar mitotic cell. (D) Immunofluoresence images showing a control cell with a bipolar spindle paired centrioles and a SKAP-depleted multipolar cell with prematurely separated centrioles. (E) Quantification of mitotic timing (NEBD-anaphase) as assessed from time-lapse movies at 40 hours post-siRNA addition (see Materials and Methods). NEBD and anaphase were scored using DNA and cell morphology. Cells were counted if they entered mitosis during the course of filming. Cells that arrested for greater than 3 hours or reached a terminal mitotic phenotype are boxed at the top of the graph. N = 52 cells per condition. Note: this analysis excludes cells in the depletion and long SKAP experiments that were arrested at the start of the movie, and thus likely underpresents the extent of the mitotic arrest. (F) Live cell imaging showing GFP-tagged SKAP cell lines for the two SKAP isoforms in interphase and mitosis. Scale bars, 5 μm.

To investigate the basis for this functional difference, we analyzed the associations and subcellular localization of the two SKAP isoforms as exogenously expressed GFP fusions. We found that both long and short SKAP displayed largely similar interacting partners, including the other Astrin/SKAP complex components (Fig. S2D). However, despite these similar interactions, these SKAP isoforms displayed distinct localization (Fig. 3F). In interphase cells, long SKAP-GFP displayed weak microtubule localization, as well as localization to punctate foci throughout the cytoplasm. In contrast, short SKAP-GFP displayed clear localization to microtubule plus ends in interphase cells. In mitosis, a GFP fusion to the long SKAP isoform localized to kinetochores, centrosomes, and spindle microtubules (Fig. 3F), consistent with previous work (Schmidt et al., 2010). The short isoform of SKAP also localized to aligned kinetochores, spindle microtubules, and centrosomes in mitotic cells. However, the spindle localization of short SKAP was more intense along microtubule

lengths and additionally displayed a speckled pattern typical of plus-end-tracking proteins, consistent with the interphase data. As the testes-specific long SKAP isoform is able to associate with the other components of the Astrin/SKAP complex when expressed ectopically, but displays distinct localization behavior, long SKAP could act in a dominant manner by replacing endogenous short SKAP in the Astrin/SKAP complex explaining the defects reported previously for the ectopic expression of long SKAP (Lee et al., 2014; Tamura et al., 2015). Together, these analyses demonstrate that the two SKAP isoforms exhibit differential localization in mitotic cells, and only the shorter SKAP isoform is fully functional to facilitate the multiple roles of SKAP during mitosis.

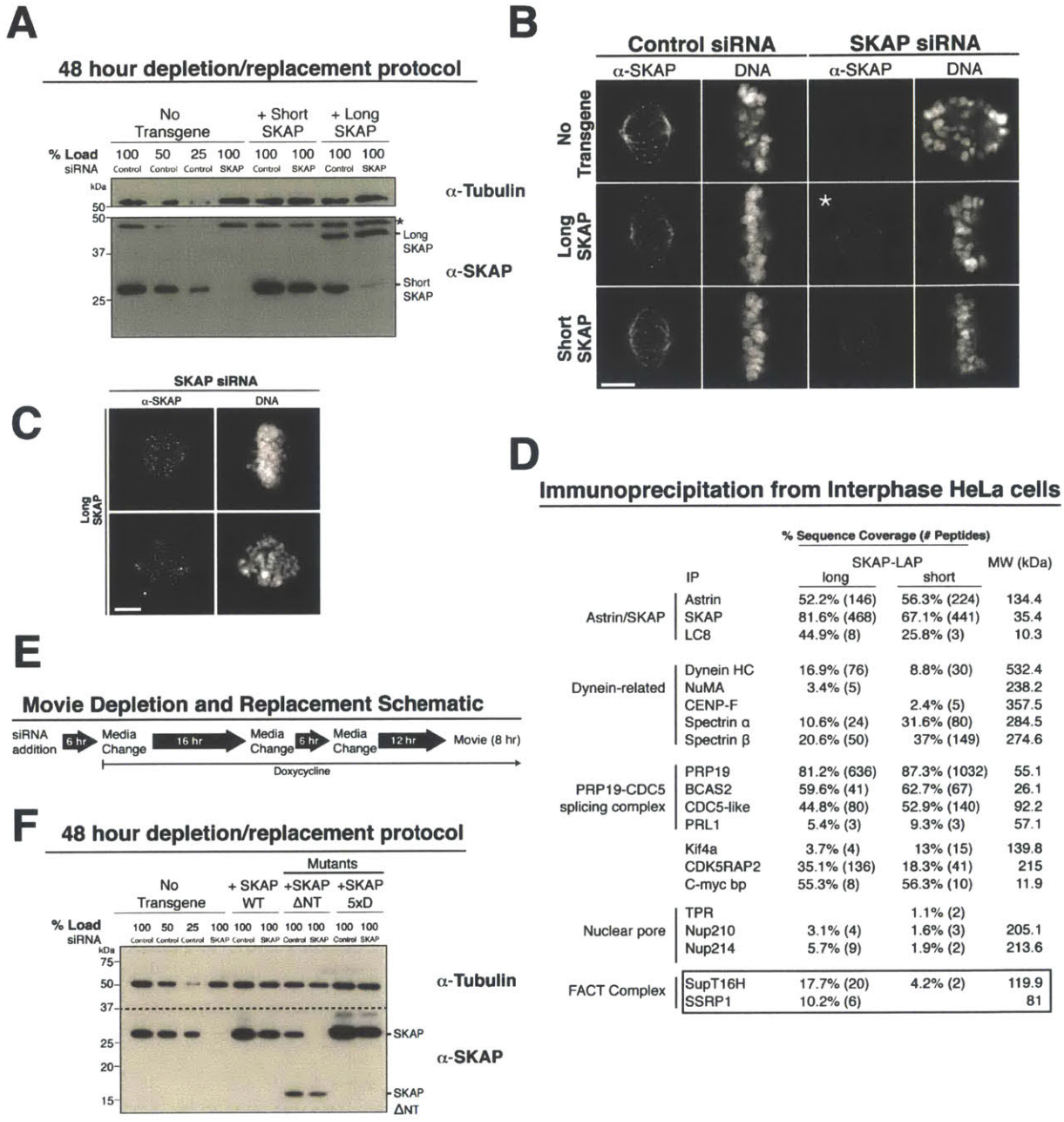

Figure S2. SKAP interphase interactions and validation of the SKAP depletion and replacement protocols. A) Western blot for the 48 hour depletion and SKAP replacement protocol. Tubulin was used as a loading control. The membrane was cut to probe with the SKAP and tubulin antibodies as indicated. *marks a non-specific band. (B) SKAP immunofluorescence for SKAP depletion and rescue experiments. *indicates that this cell with aligned chromosomes was a rare in this condition, but is included to show SKAP localization to aligned kinetochores and the slight reduction in spindle localization. For localization representing the spindle morphology in the majority of cells in this condition, see part C. (C) Immunofluorescence showing SKAP

localization in cells in which the long SKAP isoform replaces endogenous SKAP. These images are included to highlight SKAP localization in cells with misaligned chromosomes, which are more typical of this condition and are scaled individually. (D) Interphase interactions for SKAP-LAP showing the mass spectrometry sequence coverage obtained for affinity purifications of the long and short forms. LAP-preps were performed using the same reagents on the same day and 300 mM KCl was used in buffers for both bead binding and washing. (E) Schematic showing protocol for phenotype movies. (F) Western blot for the 48 hour depletion and SKAP replacement protocol for SKAP microtubule binding mutants. The membrane was cut as indicated by dotted line to probe with the different antibodies. Scale bars, 5 μm.

SKAP microtubule binding activity is necessary for Astrin/SKAP spindle localization and chromosome segregation

The short, mitosis-specific SKAP isoform displays localization both along the length of microtubules and to microtubule plus ends. To dissect the contributions of this localization to SKAP function, we first sought to eliminate SKAP's microtubule binding activity. SKAP contains a C-terminal coiled coil region (Fig. 4A), which we predicted would be responsible for SKAP to associate with the Astrin/SKAP complex, and an N-terminal region with a patch of positively charged residues immediately preceding the coiled coil that is well suited for associating with negatively charged microtubules. Eliminating the entire N-terminal region to generate a construct containing only the coiled coil region (SKAP ΔNT) disrupted SKAP microtubule localization, but did not prevent SKAP localization to kinetochores (Fig. 4B, C). Similarly, a more specific mutant in which a cluster of 5 positively charged residues was targeted to reverse these charges (SKAP 5xD; Fig. 4A), also compromised SKAP localization to microtubules, but not kinetochores (Fig. 4B, C). Expression of these mutants, at levels similar to the endogenous protein (Fig. S2F), also reduced the microtubule localization of endogenous SKAP, indicating that these mutants act in a dominant fashion likely through the formation of mixed Astrin/SKAP complexes (Fig. 4C).

Cells in which endogenous SKAP was replaced by these SKAP ΔNT and 5xD mutants displayed severe defects in chromosome alignment and spindle assembly (Fig. 4D, E), similar to those observed following SKAP depletion. Together, these data indicate that SKAP contains the major microtubule binding activity of the Astrin/SKAP complex, and that this microtubule binding is critical for the localization and function of this complex.

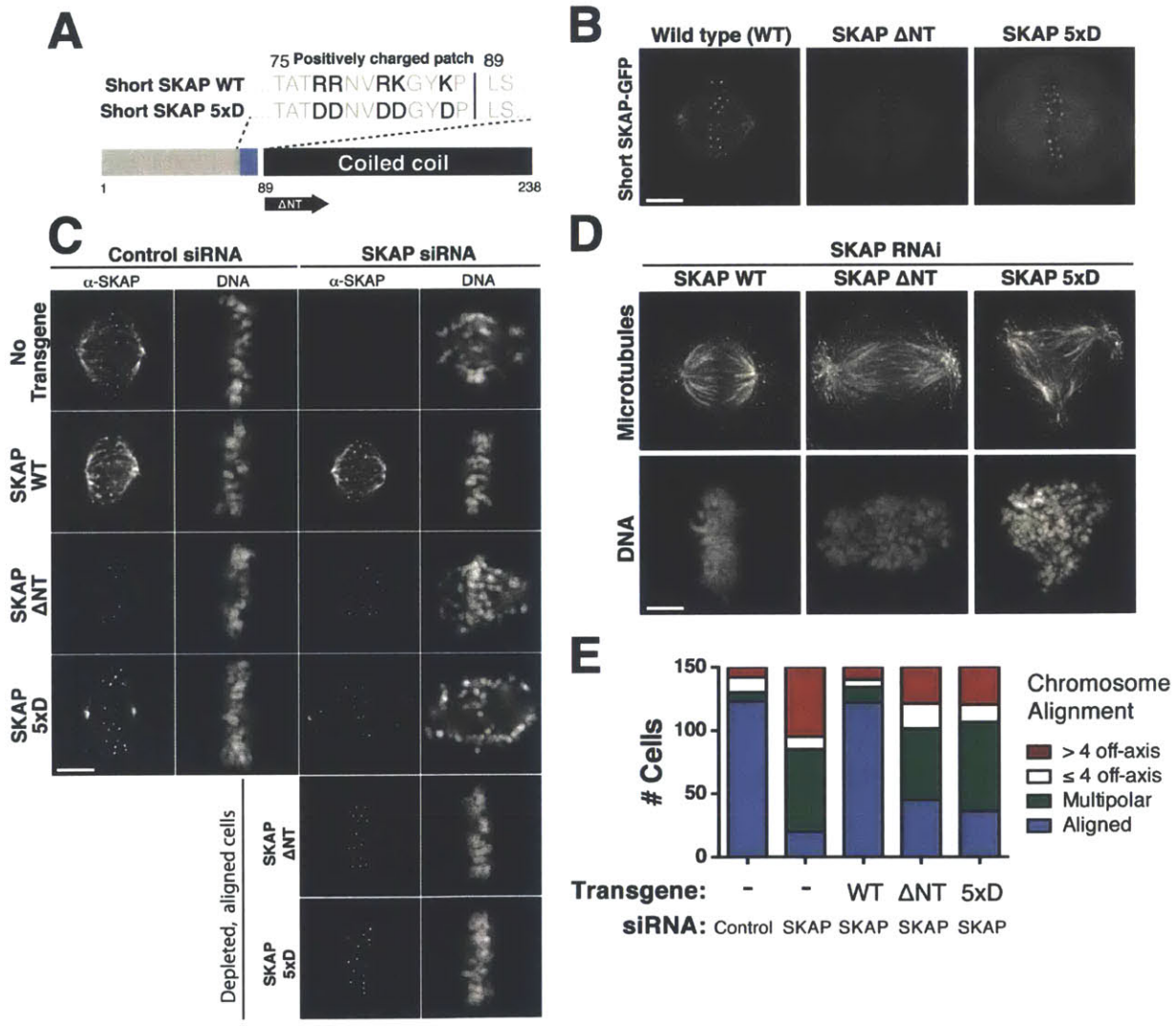

Figure 4. SKAP microtubule binding mutants prevent Astrin/SKAP complex microtubule localization and display defects similar to SKAP depletion. (A) Diagram of SKAP microtubule binding mutants: a mutant with 5 positive charged

amino acids changed to aspartate (SKAP 5xD) and mutant removing the N-terminus to leave only the SKAP coiled-coil (SKAP ΔNT). (B) Fluorescent images showing SKAP-GFP localization in cells expressing wild-type (WT) SKAP or the indicated SKAP microtubule binding mutants. (C) Immunofluorescence images showing SKAP and DNA localization in the indicated SKAP microtubule binding mutants. Although most mutant cells display defective chromosome alignment, the cells at the bottom are included to highlight the ability of SKAP to localize to kinetochores, but not microtubules, in cells with aligned chromosomes. DNA is scaled independently for each image. (D) Immunofluorescence images showing examples of cells with aligned chromosomes, many off-axis chromosomes, and a multipolar spindle from experiments with SKAP WT, ΔNT, and 5xD respectively. Images represent maximal intensity projections. (E) Quantification of SKAP mutant cell phenotypes performed as in Fig. 3C and D. Scale bars, 5 μm.

The short SKAP isoform displays robust plus-end-tracking in mitosis

We next sought to precisely analyze the plus-end-tracking activity of SKAP. Prior studies on the Astrin/SKAP complex reported plus-end-tracking for GFP-Astrin expressed in interphase cells (Dunsch et al., 2011) and identified an interaction between SKAP and EB1 (Tamura et al., 2015; Wang et al., 2012). Despite this, none of these studies documented a plus-end-tracking activity for SKAP in cells. Indeed, we found that long SKAP does not display a robust plus-end-tracking activity in interphase or mitosis (Fig. 3F), possibly due to steric effects or protein instability caused by the N-terminal extension present in long SKAP (Fig. S1A). In contrast, the short SKAP isoform displayed spindle localization and fluorescent speckles along microtubules indicative of microtubule plus-end-tracking. Using live cell imaging, we observed clear localization for short (mitotic) SKAP-GFP to growing microtubule plus ends (Fig. 5A, 5B). In addition, we found that the SKAP and Astrin plus-end signals trailed the extreme tip of the EB1 "comet" in both mitosis and interphase (Fig. 5C and Fig. S3A), in agreement with previous studies for Astrin localization (Dunsch et al., 2011).

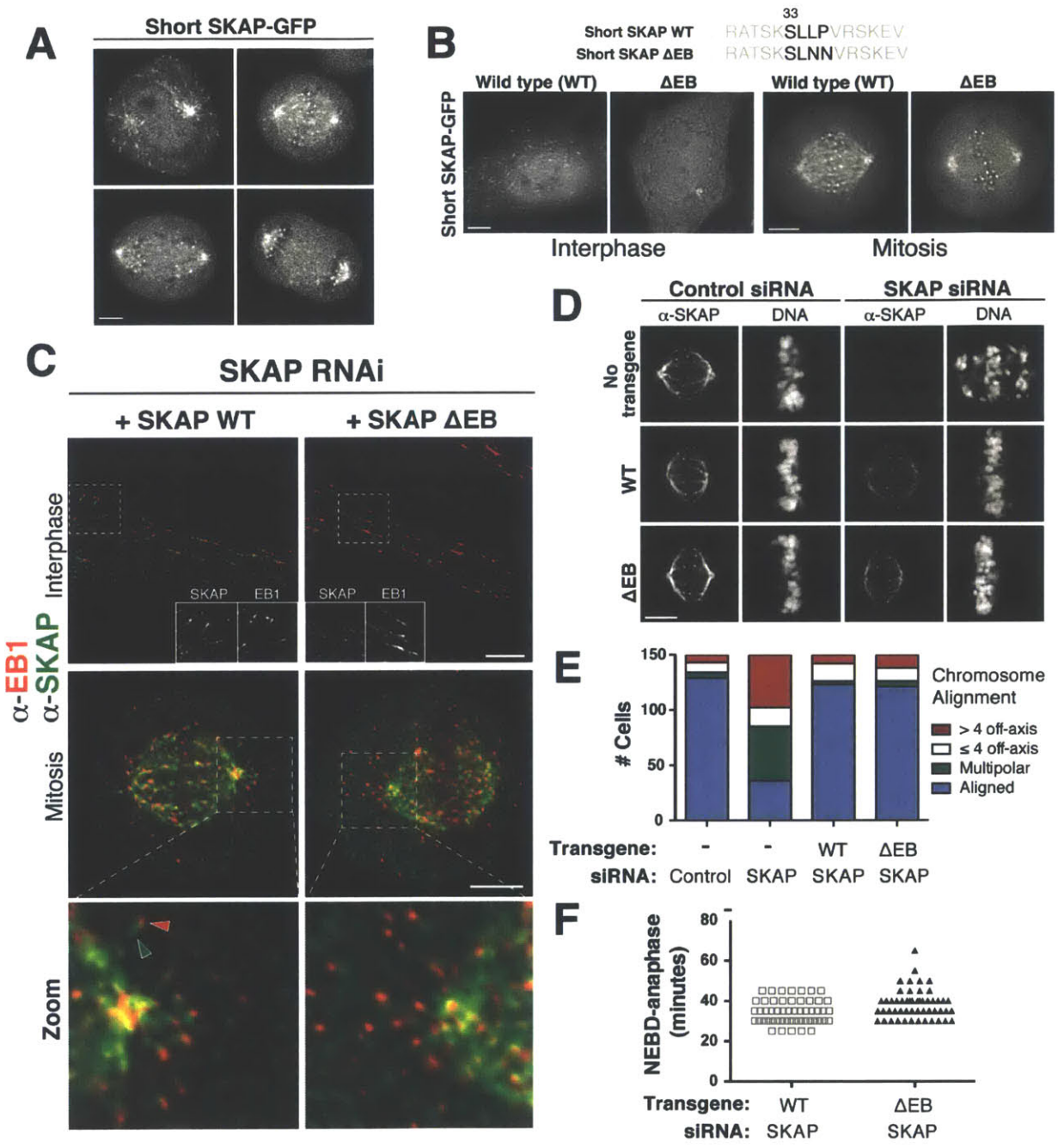

Figure 5. Short SKAP displays a potent EB-motif dependent microtubule plus-end-tracking activity in mitotic cells. (A) Still images from spinning disc confocal movies of short SKAP-GFP. (B) Top: Diagram of SKAP ΔEB mutation. Bottom: Individual fluorescence sections from live cell imaging of mitotic SKAP and SKAP ΔEB mutant GFP-tagged cell lines. (C) Immunofluorescence localization of EB1 and SKAP. Top: SKAP overlaps with the trail of the EB comet, but does not co-localize with the tip. Inset shows a zoomed-in and channel separated view of the boxed region. Bottom: Mitotic cells exhibiting wild-type

(WT) SKAP plus-end-tracking and the ΔEB mutant. Arrows in the zoomed-in image mark SKAP and EB1 on an astral microtubule plus end. (D) Individual fluorescence sections showing SKAP localization for depletion and replacement experiments. DNA is scaled independently for each image. (E) Quantification of mitotic chromosome alignment for SKAP depletion and rescue experiments. Microtubule labeled immunofluorescent cells were quantified by observing DNA and spindle morphology (as in Fig. 3D). (F) Mitotic timing (NEBD-anaphase) quantified from movies (as in Fig. 3E). N = 52 cells/condition. WT rescue data is duplicated from Figure 3E for comparison. Scale bars, 5 μm.

The plus-end-tracking behavior for the Astrin/SKAP complex was dependent upon the EB-binding SKAP Sx[I/L]P motif (Honnappa et al., 2009), as mutation of the SKAP EB-interacting motif from SLLP to SLNN (here termed "SKAP ΔEB") eliminated both SKAP and Astrin plus-end-tracking (Fig. 5B, 5C; Fig. S3A). Importantly, despite eliminating this plus-end-tracking activity, the SKAP ΔEB mutant localized to both kinetochores and microtubules, even in the absence of endogenous SKAP (Fig. 5D). We note that this result for short SKAP localization is different than that reported for long SKAP by others (Tamura et al., 2015), in which an EB mutant also eliminated SKAP microtubule localization. We suspect that long SKAP has reduced capacity to bind and track microtubules, which is consistent with our localization and phenotypic analysis (Fig. 3). Together with our analysis of the SKAP microtubule binding mutants described above, this indicates that SKAP possesses an independent microtubule binding activity in addition to its association with EB family proteins.

To test the role of the SKAP microtubule plus-end-tracking behavior in mitotic cells, we next investigated the functional consequences of replacing endogenous SKAP with the short SKAP ΔEB mutant (Fig. S3B). In contrast to the catastrophic chromosome segregation defects we observed in SKAP mutants that prevent microtubule localization, we found that the SKAP ΔEB mutant was able to rescue the depletion of endogenous SKAP for its ability to facilitate proper

chromosome alignment and segregation (Fig. 5D, E) with normal mitotic timing (Fig. 5F). Therefore, we conclude that Astrin/SKAP plus-end-tracking is not necessary for the key chromosome alignment functions of this complex.

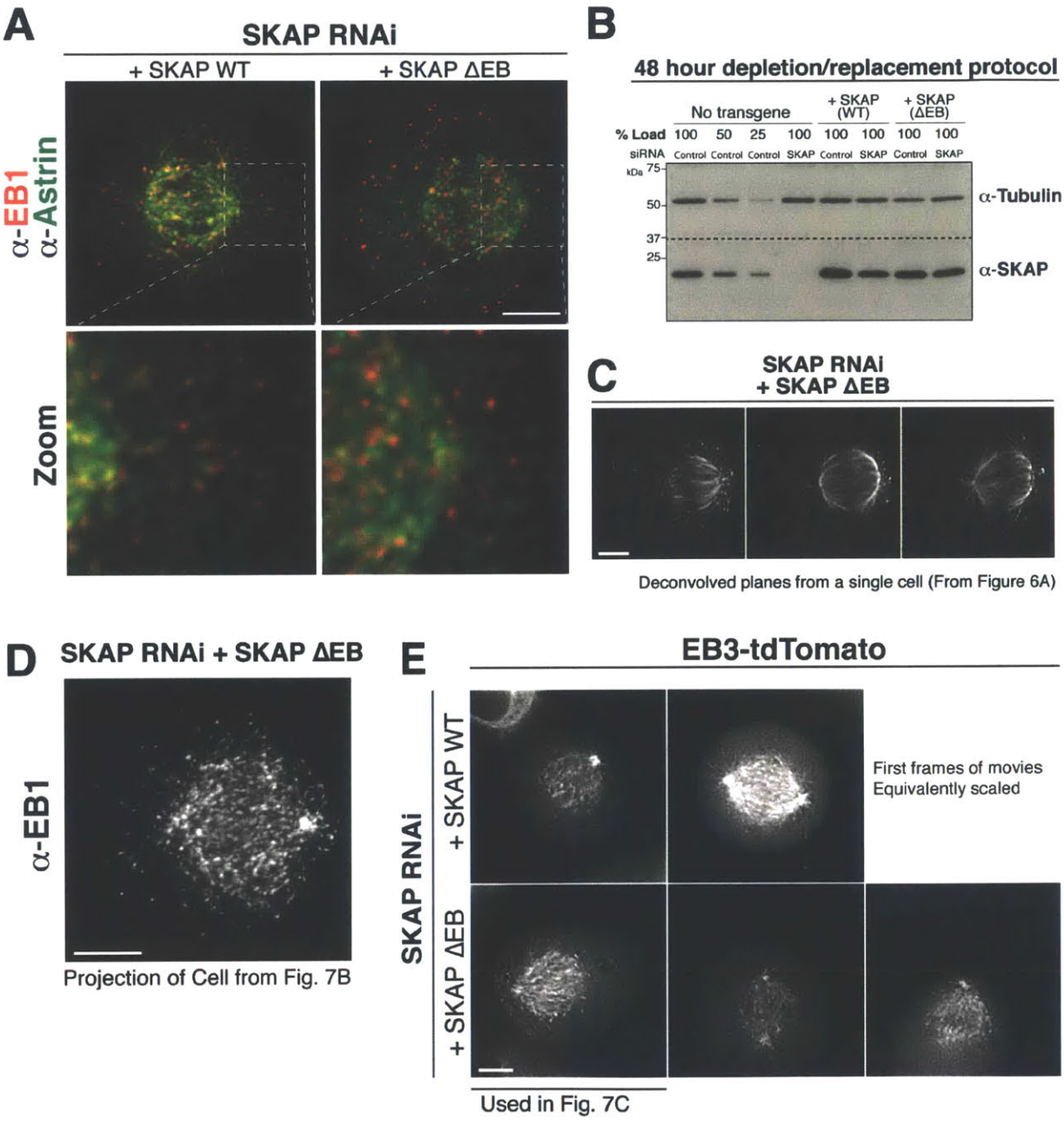

Figure S3. SKAP mitotic plus-end-tracking, validation of the SKAP depletion and SKAP ΔEB mutant replacement protocol, and astral microtubule phenotype. (A) Top: Immunofluorescence of EB1 and Astrin from SKAP WT and SKAP ΔEB cells. Bottom: Zoom of a region near the centrosome showing Astrin plus-end-tracking. (B) Western for the 48 hour depletion and

SKAP replacement protocol for the SKAP ΔEB mutant. Tubulin was used as a loading control. The membrane was cut as indicated by dotted line to probe with each antibody. (C) Deconvolved planes from shifted cell depicted in Fig. 6A. (D) Maximal intensity projection for the cell from Fig. 7B showing the extent of growing microtubule ends along cortex on the right side of the cell and the relative lack of microtubule contact with cortex on the left. (E) Equivalently scaled images for the first frames of the movies used in Fig. 7C and Movie S4. Scale bars, 5 μm.

Astrin/SKAP localization to microtubule plus ends is necessary for proper spindle positioning

Although the SKAP ΔEB mutant was able to and facilitate normal chromosome segregation, during our analysis of chromosome alignment, we unexpectedly observed that many spindles in the SKAP ΔEB mutant were dramatically mispositioned away from the cell mid-zone, often adjacent to or abutting the cell cortex (Fig. 6A). In these extreme cases, cells appeared to have centrosomes and their astral microtubules directly in contact with the cortex (Fig. S3C). In control cells or cells in which wild-type (WT) SKAP rescued endogenous SKAP depletion, we found that the spindle was typically positioned symmetrically within the dividing cells with similar distances between each spindle pole and the cell cortex (mean spindle displacement: Control, 0.62 μm; Rescue, 0.87 μm) (Fig. 6B). In contrast, we found that the spindle was positioned asymmetrically within the cell in SKAP ΔEB mutant cells such that one spindle pole was often much closer to the cell cortex (Fig. 6A, B; mean spindle displacement: ΔEB, 2.1 μm). The quantification of spindle displacement revealed a wide range of spindle positioning in the SKAP ΔEB mutant, including extremely mispositioned spindles (Fig. 6B).

To determine the nature of this defect, we next asked whether the mispositioning we observed in the SKAP ΔEB mutants depended on both components of the spindle positioning pathway: astral microtubules and cortically-localized dynein. Eliminating astral microtubules using low dose

nocodazole treatment prevented spindle mispositioning in the SKAP ΔEB mutant (Fig. 6C, D). Similarly, depletion of LGN, an upstream cortical recruitment factor for dynein that is required for cortical dynein localization in metaphase (Kiyomitsu and Cheeseman, 2012), eliminated the spindle positioning defects observed for the SKAP ΔEB mutant, resulting instead in a central spindle position (Fig. 6E, F). These results demonstrate that aberrant and unbalanced forces generated by astral microtubules and cortical dynein lead to the dramatic spindle positioning defects in the absence of Astrin/SKAP localization to microtubule plus ends.

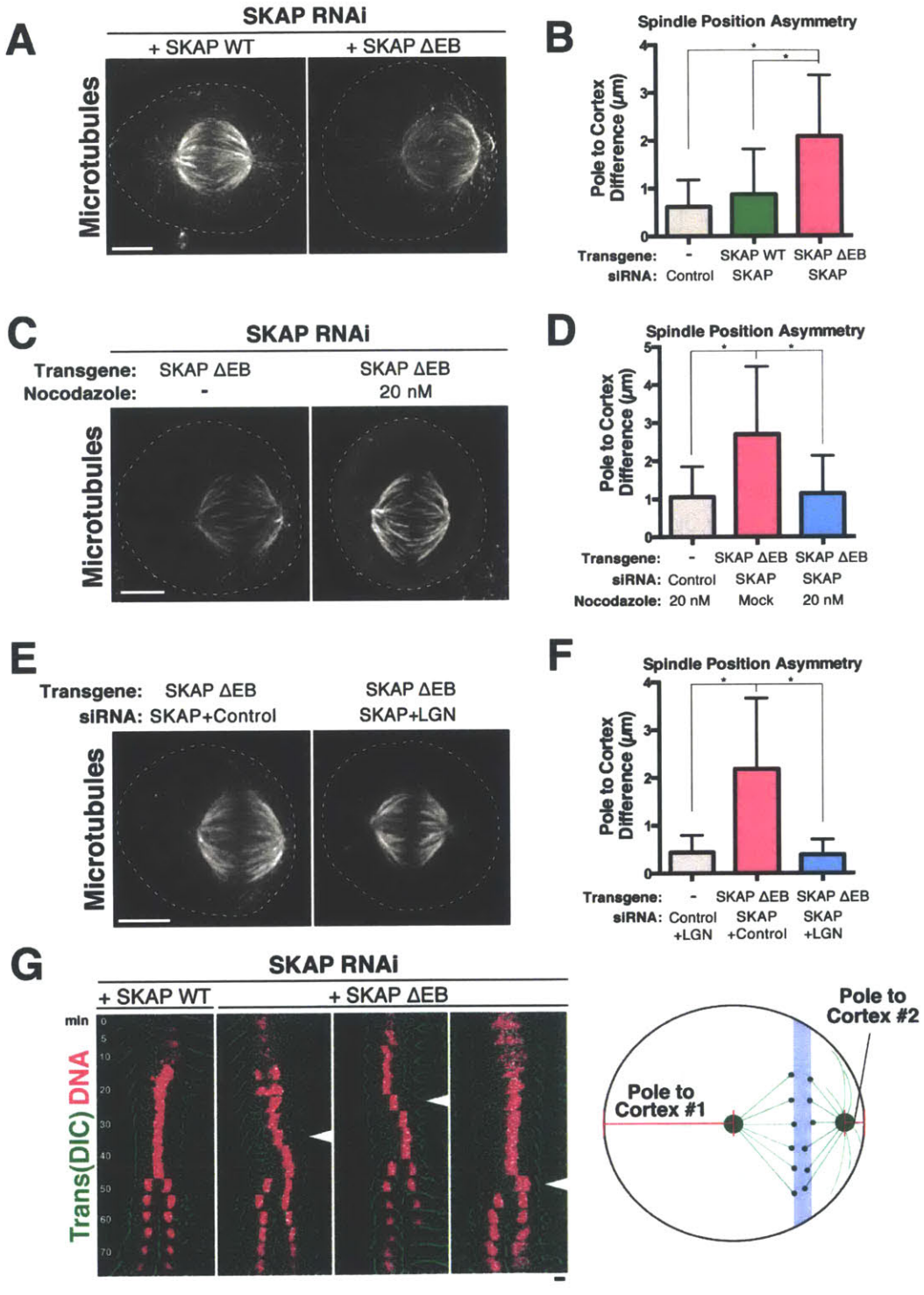

Figure 6. SKAP ΔEB mutant cells display a spindle mispositioning defect (A) Immunofluorescence images showing microtubules in the SKAP ΔEB mutant spindle. Images represent maximal intensity projectsions. The dashed line indicates the cell boundary. (B) Graph showing difference in the distances between each spindle pole and the closest position on the cell cortex (see

diagram at bottom right of the figure). A value of "0" represents spindle positioning in the cell center with equivalent distances to each cell cortex. N = 100 cells per condition collected from 3 independent experiments. Average and standard deviation are plotted. * indicates a significant difference (P value < 0.0001) assessed by an unpaired two-tailed t-test. (C) Maximal intensity projections for microtubule staining show the spindle mispositioning phenotype and its suppression by LGN depletion. (D) Graph showing the pole-cortex difference for LGN experiment (as in Fig. 6B). N = 100 cells per condition collected from 3 independent experiments. * indicates a significant difference (P value < 0.0001) assessed by an unpaired two-tailed t-test. (E) Images showing maximal intensity projections for microtubule staining to show the spindle mispositioning phenotype and its suppression by 20 nM nocodazole. (F) Graph showing the pole-cortex difference (as in Fig. 6B) for the low dose nocozaole experiment. N = 100 cells per condition collected from 2 independent experiments. Average and standard deviation are plotted. * indicates a significant difference (P value < 0.0001) assessed by an unpaired two-tailed t-test. (G) Kymographs of movies from cells in which wild-type (WT) SKAP or the SKAP ΔEB mutant replaces endogenous SKAP. Arrows mark the start of the spindle shift in ΔEB cells. Also see Movie S3.

Based on time-lapse imaging of mitotic cells, SKAP ΔEB mutant cells displayed a directed shift in the position of the metaphase plate towards the cell cortex, usually shortly after chromosome congression (Fig. 6G). These rapid and directed movements are different from the slow spindle oscillations with a narrow amplitude that we have described previously as promoting a central spindle position (Kiyomitsu and Cheeseman, 2012). Such SKAP ΔEB mutant cells entered anaphase with mispositioned spindles, but were able to subsequently position the spindle during early anaphase, consistent with an anaphase correction pathway (Kiyomitsu and Cheeseman, 2013). We note that SKAP depleted cells also exhibit spindle position instability, including side-to-side motions and rotations. However, SKAP depleted cells also have dramatic and pleiotropic defects in chromosome alignment and centrosome stability, which indirectly influence spindle positioning (Kiyomitsu and Cheeseman, 2012), preventing a directed analysis of spindle positioning phenotypes. Thus,

microtubule plus-end-tracking by the Astrin/SKAP complex is necessary for metaphase spindle positioning.

The SKAP plus-end-tracking mutant alters astral microtubule behavior at the cell cortex

As we found that the spindle mispositioning defect in SKAP ΔEB mutant cells was dependent on cortical dynein, it is possible that the spindle shift observed in this mutant could arise from a defect in cortical dynein localization. For instance, the SKAP ΔEB mutant phenotype could be explained by a failure of dynein to delocalize from the cell cortex as the spindle approached (Kiyomitsu and Cheeseman, 2012), leading to enhanced spindle forces on one side of the cell. Therefore, we tested whether SKAP ΔEB mutants displayed a misregulation of cortical dynein localization. Using the dynactin subunit $p150^{Glued}$ as a marker of dynein/dynactin localization (Kiyomitsu, 2015), we did not observe a change in its cortical localization in the SKAP ΔEB mutant. Similar to what we have reported previously for dynein in control cells (Kiyomitsu and Cheeseman, 2013), $p150^{Glued}$ was able to localize to the cell cortex, but when the spindle was significantly shifted to one side of the cell, $p150^{Glued}$ displayed substantially higher localization to the opposite cell cortex (Fig. 7A).

In metaphase, the plus ends of astral microtubules contact the cell cortex, but microtubule-cortical contacts typically persist for only a few seconds before growth ceases and the microtubules depolymerize (Samora et al., 2011). Indeed, we only rarely detected microtubule plus ends in proximity to the cell cortex based on EB1 staining in control cells. In contrast, in SKAP ΔEB mutant cells in which we observed significant spindle shifts, we also observed an accumulation of lateral contacts between growing astral microtubules and the cell cortex (Fig. 7B and Fig. S3D). Based on the imaging of microtubule plus ends marked by

EB3-tdTomato in live cells, we found that in the SKAP ΔEB mutant, astral microtubules often grew along the cell cortex (Fig. 7C, Fig. S3E). This lateral astral microtubule growth increased as the spindle approached the cortex. In cells in which the spindle was substantially shifted, most astral microtubules close to the cortex exhibited lateral cortical growth, whereas astral microtubules on the opposite side were rarely long enough to generate cortical contacts (Fig. 7B, 6C, Fig. S3E). We conclude that Astrin/SKAP complex localization to microtubule plus ends plays an important role in astral microtubule behavior and is required for proper interactions between astral microtubules and cortical dynein to promote spindle positioning.

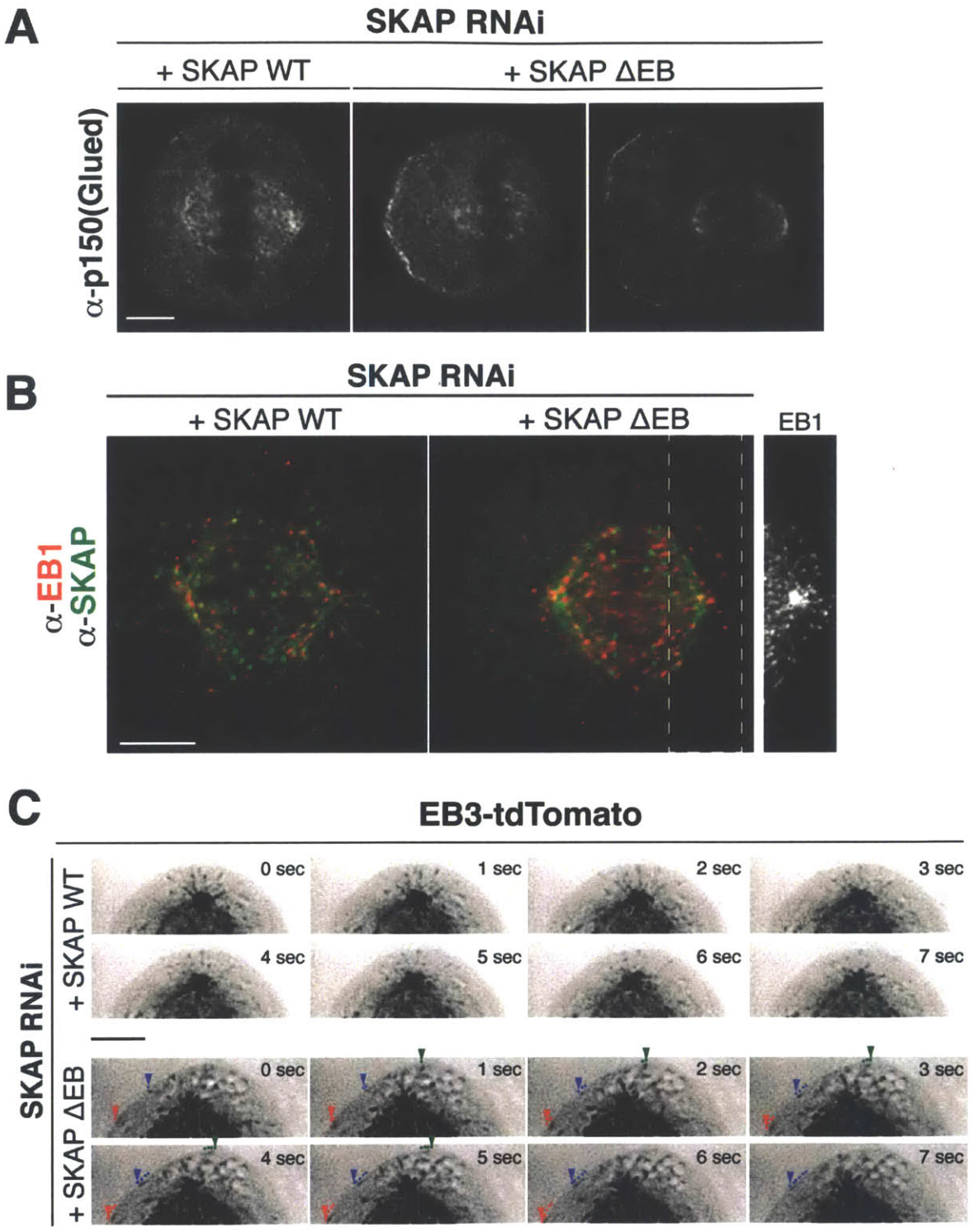

Figure 7. Mispositioned metaphase spindles in SKAP ΔEB mutant cells are accompanied by changes in astral microtubule behavior. (A) Individual sections showing immunofluorescent localization of p150(Glued) as a marker for Dynein/Dynactin from cells in which wild-type (WT) SKAP or the SKAP ΔEB

mutant replaces endogenous SKAP. (B) Immunofluorescence images (deconvolved sections) of EB1 localization in SKAP WT and SKAP ΔEB cells. Far right: EB1 tracks from the SKAP ΔEB mutant cell showing growth along cortex. (C) Still images from a time lapse movie of EB3-tdTomato in SKAP WT and SKAP ΔEB cells. EB3 comets that exhibit clear lateral growth along cortex are marked with color-coded arrows marking the cortical contact site and dots showing lateral growth. Images are scaled individually for clarity. See Fig. S3E for images with identical scaling and Movie S4. Scale bars, 5 μm.

The Astrin/SKAP complex binds and regulates Clasp1 in mitosis

To explore the basis for this unexpected spindle positioning phenotype, we next generated an interaction map by conducting multiple immunoprecipitations of Astrin and SKAP from mitotic cells. We found that the Astrin/SKAP complex interacts with multiple key proteins that function in microtubule organization and spindle positioning, including Clasp1, Plk1, NuMA, and Dynein (Fig. S4A). Previous work found that Clasp1 plays an important role in microtubule-cortex interactions, spindle positioning, and astral microtubule behavior (Ambrose and Wasteneys, 2008; Bird et al., 2013; Mimori-Kiyosue et al., 2005; Samora et al., 2011). Indeed, Samora et al. found similar spindle mispositioning for Clasp1 depletion as described here for the SKAP ΔEB mutant. Therefore, we followed up on our results and previous reports of an interaction between Astrin and Clasp1 (Maffini et al., 2009; Schmidt et al., 2010). We found that the C-terminal domain of Clasp1 (Maiato et al., 2003) localized to the mitotic cell cortex and co-immunoprecipitated with significant amounts of the Astrin/SKAP complex, as well as dynein machinery (Fig. 8A, B). However, affinity purification of the Clasp1 C-terminus did not isolate peptides from endogenous Clasp1, indicating that this construct is not multimerizing and narrowing down the Clasp1 binding region for the Astrin/SKAP complex. Interestingly, we detected significantly enhanced

Clasp1-Astrin/SKAP complex interaction our Clasp1 purifications based on peptide coverage, than in reciprocal Astrin/SKAP purifications (also see (Maffini et al., 2009), suggesting that a much larger percentage of Clasp1 is bound to the Astrin/SKAP complex than vice-versa.

To test requirements for the interaction between the Astrin/SKAP complex and Clasp1, we next tested Clasp1 localization. In control cells, Clasp1 localized to kinetochores, the spindle, and microtubule plus ends during mitosis. In contrast, in the SKAP ΔEB mutant, we observed a reduction in spindle-bound Clasp1 and a reduction of Clasp1 localized to microtubule plus ends (Fig. 8C, D). In interphase, SKAP depletion had no noticeable effect on Clasp1 plus-end binding (Fig. S4B). These results indicate that Astrin/SKAP associates with Clasp1 and contributes to its localization in mitosis, including its robust localization to astral microtubule plus ends. Taken together with the results from Samora et al. (Samora et al., 2011), Astrin/SKAP and Clasp1 play an important role in the connection between astral microtubules and the cell cortex. Misregulation of this plus-end-tracking complex leads to dramatic spindle positioning defects.

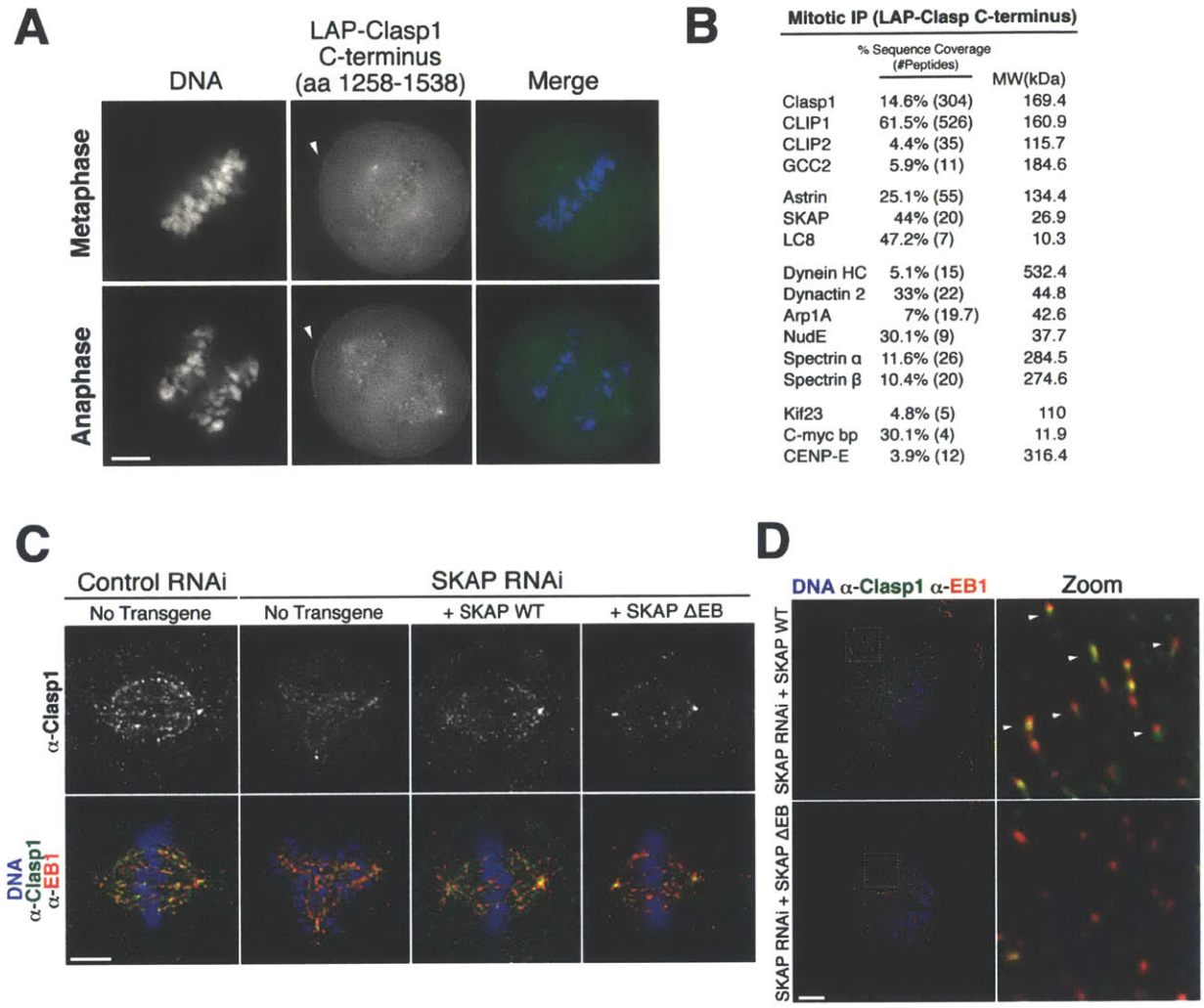

Figure 8. The Astrin/SKAP plus-end-tracking mutant alters Clasp1 localization behavior during mitosis. (A) Localization of LAP-Clasp1 C-terminus in mitosis. Arrows indicate localization to cell cortex. (B) Immunoprecipitation of the LAP-Clasp1 C-terminus from mitotic cells displaying identified peptides with data pooled from two purifications with either 100 mM or 300 mM KCl in the buffer. (C) Immunofluorescence images of mitotic cells (either normal metaphase spindles or cells with a multipolar phenotype) showing the localization of Clasp1 and EB1. Clasp1 spindle and plus-end localization is reduced in the SKAP ΔEB condition. (D) Left: Localization of Clasp1 to microtubule plus ends in early prophase cells in which endogenous SKAP is replaced by with wild-type (WT) SKAP WT or the SKAP ΔEB mutant. Clasp1 localization to plus ends is eliminated in the SKAP ΔEB mutant. Right: Zoom from boxed region on the left images. Clasp1 microtubule plus-end localization is marked by arrows. Scale bars, 5 μm.

A

Mitotic IP (Astrin/SKAP complex)

	% Sequence Coverage (#Peptides)				
	SKAP IP	SKAP (LAP)	Astrin IP	Astrin (LAP)	MW (kDa)
Astrin	84% (920)	37.4% (101)	89.6% (2314)	75.3% (1420)	134.4
SKAP	89.1% (468)	68.1% (223)	84.4% (281)	72.2% (329)	26.9
LC8	89.9% (71)	44.9% (5)	84.3% (66)	52.8% (75)	10.3
Clasp1			2.7% (4)	2.9% (3)	169.4
Clasp2			2.1% (2)	2.3% (3)	164.8
Plk1	4.5% (2)		19.7% (21)	14.8% (21)	68.2
NuMA	9.5% (28)	1.6% (2)	8.6% (21)	5.3% (9)	238.2
CENP-F	1.7% (3)		10.6% (27)	3% (6)	357.5
Dynein HC		4.2% (18)	16.5% (80)	6% (30)	532.4
Dynactin 2		15.3% (4)		14% (6)	44.8
Spectrin α	29% (80)	15.9% (35)	6.6% (11)	8.8% (17)	284.5
Spectrin β	25% (61)	13.2% (36)	5.1% (9)	3.6% (5)	274.6
PRP19	85.3% (431)	49% (281)	4.2% (4)	10.9% (7)	55.1
BCAS2	62.2% (52)	48.4% (40)			26.1
CDC5-like	35% (43)	42.9% (63)		4.1% (2)	92.2
Kif4a			15.4% (28)	8.8% (15)	139.8
Kif11 (Eg5)			8.8% (7)	22.3% (45)	119.1
Kif15			8.3% (9)	24.2% (37)	160.1
Kif23	36.4% (90)	9.9% (14)		18.5% (31)	110
CDK5RAP2	17.6% (44)				215
C-myc bp	78.6% (89)	44.7% (11)	73.8% (38)	78.6% (92)	11.9
TPR	2.7% (5)		8.8% (16)	1.5% (3)	267.2
RANBP2			1.6% (4)	3.8% (12)	358.2
Nup98			2.5% (4)	2% (3)	195.8
Nup107			9.6% (5)	5% (3)	106.3
Nup160			3.8% (3)	7.6% (7)	162.1
Nup210		2% (3)	1.5% (3)		205.1

B

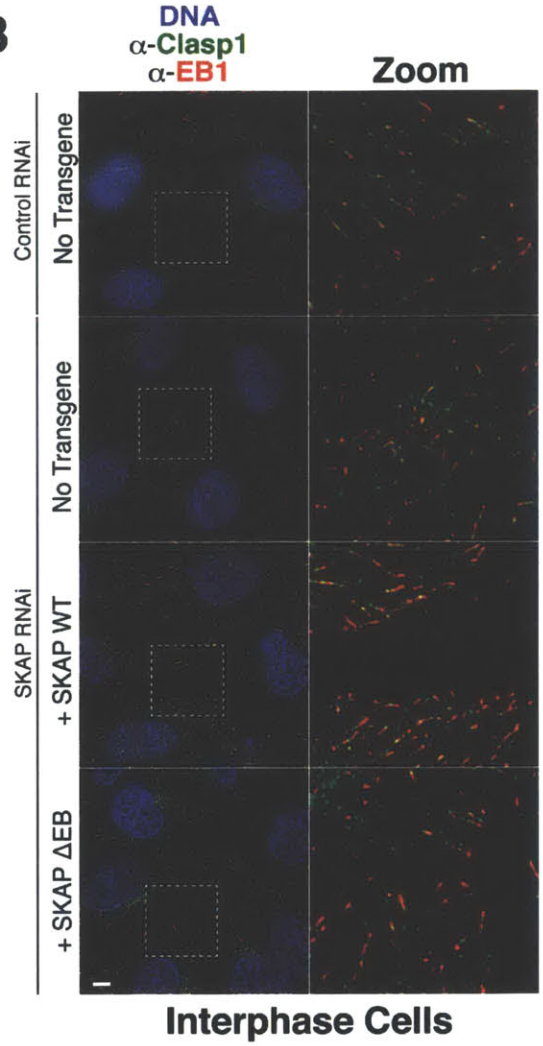

Figure S4. Mitotic interactions of the Astrin/SKAP complex and interphase Clasp1 localization (A) IP-MS of Astrin and SKAP, including GFP tagged protein IPs and direct antibody IPs. For these purifications, the following concentrations of KCl were included in the wash buffer: SKAP antibody IP from HeLa cells (300 mM KCl), SKAP-LAP (100 and 300 mM KCl preps), Astrin antibody IP from HeLa cells (300 mM KCl), LAP-Astrin IPs (two purifications from (Schmidt et al., 2010) at 300 mM KCl; one from this study conducted with 100 mM KCl), LAP-Astrin (aa 458-1193) IP with 300 mM KCl, and a Flp-In Astrin-LAP IP with 200 mM KCl in which Astrin-LAP was induced with 1 µg/mL Doxycyline-induced for 16 hours and the cells were arrested in mitosis with 10 µM STLC. All other preps are from nocodazole-arrested cells. Only proteins with peptides identified in at least two of types of preparations or in the interphase SKAP IPs are depicted here. Proteins that are commonly seen across many unrelated preps were excluded. (B) Interphase localization of Clasp1 to microtubules and plus ends. The boxed

region on the left is presented as a zoomed-in image on the right. Scale bar, 5 μm.

Discussion

Here, we demonstrated that SKAP exists as two distinct transcriptional isoforms and analyzed the novel isoform of SKAP in mitosis, which revealed an unexpected role for SKAP in mitotic spindle positioning. As the testis isoform is only present in eutherian mammals (Fig. S1B), and shows marked sequence divergence even between mammals, it is possible that it has acquired new roles only recently in evolution. For example, it is possible that the N-terminal SKAP extension in testes modifies the structure and behavior of SKAP, and/or facilitates interactions with testis-specific proteins. We note that previous papers from our lab and others have conducted studies on the function of SKAP in mitosis using the longer, testis-specific SKAP isoform (Dunsch et al., 2011; Lee et al., 2014; Schmidt et al., 2010; Tamura et al., 2015; Wang et al., 2012). As this long isoform displays a large reduction or complete loss of microtubule plus-end-tracking activity, a reduction in spindle localization, and is unable to rescue endogenous SKAP depletion (Fig. 3), previous analyses of SKAP mutations and rescue phenotypes should be significantly re-evaluated in the context of this novel mitotic isoform. For example, a prior study identified a recurrent mutation in SKAP in skin cancers based on whole exome sequencing (Lee et al., 2014). However, the identified mutation, S24F, exists in a portion of SKAP that is never translated in mitotic cells, including in the cultured skin cells used for this study, according to the presented Western blots. Although it remains possible that some cancers induce the expression of the long SKAP isoform, this mutation may instead alter short SKAP expression (due to its presence in the 5'UTR), or may

simply reflect a common background mutation due to a UV-sensitive hot spot occurring in skin cancer.

We find that the depletion of SKAP in human cells results in a range of severe defects in mitosis, including problems in chromosome alignment and the establishment and maintenance of a bipolar spindle. This indicates that SKAP, like its binding partner Astrin, functions in diverse mitotic processes, corresponding to its multiple localizations to kinetochores, microtubules, and centrosomes. Our work demonstrates that the microtubule-binding activity of SKAP is critical for localization to microtubules, but not kinetochores, and is required for the core mitotic functions of this complex. In addition to the previously defined roles for the Astrin/SKAP complex during mitosis, our analysis of the SKAP ΔEB mutant revealed a unexpected and unappreciated role for this complex in mitotic spindle positioning. Our work demonstrates that the Astrin/SKAP complex plays an important role at astral microtubule plus ends.

Astral microtubules in metaphase are characterized by transient growth and rapid turnover. Instead of mediating a stable connection with the cell cortex, astral microtubules only occasionally and briefly contact the cortex (Samora et al., 2011). These brief contacts allow cortically-localized dynein to utilize the astral microtubules for transient force generation to drive spindle positioning. This creates a spindle centering system that is rapid and can be quickly regulated by changes in either astral microtubule behavior or cortical dynein recruitment. Interestingly, in the SKAP ΔEB mutant, astral microtubules accumulate lateral, instead of end-on, cortical interactions. We propose that these laterally growing astral microtubules generate more persistent connections with cortical dynein. Due to the persistence of these force-generating interactions, the centrosome closer to the cortex would rapidly obtain a force advantage and the spindle would be pulled to one side of the cell (Fig. 9A, B). As the spindle moves towards one

side of the cell, the astral microtubules from the distal spindle pole would no longer be able to interact with the far cell cortex, preventing cells from correcting this imbalance, even though cortical dynein localization is still properly regulated (also see (Kiyomitsu and Cheeseman, 2012). Thus, we propose that defective astral microtubule interactions with the cell cortex result in the dramatic spindle mispositioning defects that we observed in the SKAP ΔEB mutant. Recent work has described the basis of cortical dynein recruitment and the extrinsic and intrinsic cues that control spindle positioning (Kiyomitsu, 2015). Our work additionally establishes astral microtubule plus-end factors as critical components in spindle positioning.

Astral microtubules have an array of plus-end associated proteins that modify their behavior (Akhmanova and Steinmetz, 2008). Our work definitively adds the Astrin/SKAP complex to the list of bonafide astral microtubule plus-end trackers. SKAP requires its EB-interaction motif for its plus-end localization, but appears to trail the extreme tip of the EB1 comet at microtubule plus ends (Dunsch et al., 2011). In addition to the localization of SKAP to microtubule plus ends, we found that the Astrin/SKAP complex associates with diverse proteins that play roles in spindle positioning, including Clasp1 and Dynein/Dynactin (Duellberg et al., 2014; Maiato et al., 2003; Samora et al., 2011). Here we show that Clasp1 behavior is regulated in mitosis by Astrin/SKAP complex to promote cortical interactions. The combined interactions and activities of these and other proteins may create a modular complex that plays a specific role upon cortical contact. A critical challenge for future work is to define the nature of this astral

microtubule-cortical attachment, including the composition and regulation of the astral microtubule plus ends and the activities required for microtubule-dynein engagement and force generation. These studies will elucidate the process of precise mitotic spindle positioning, which is critical for understanding aspects of human disease and development.

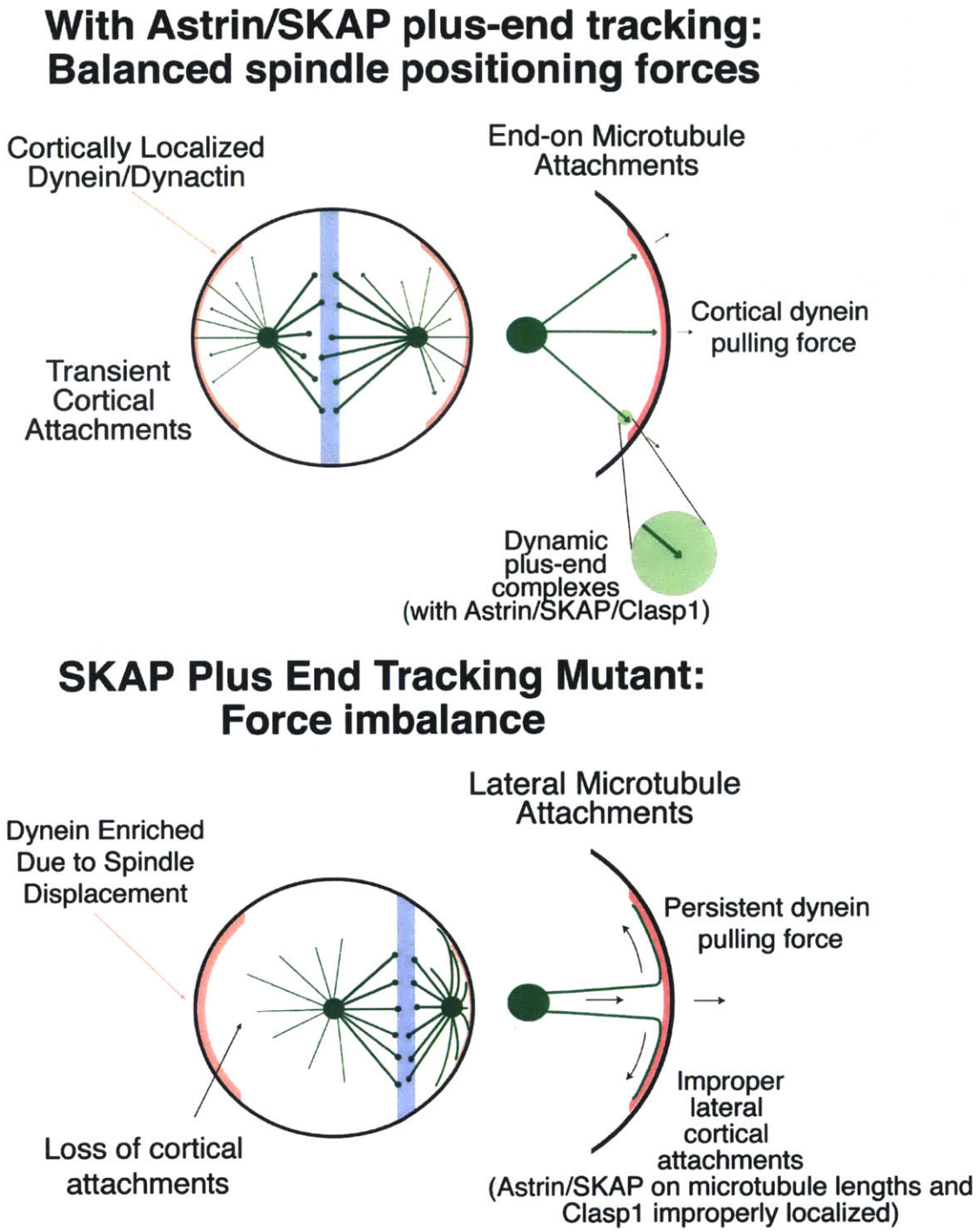

Figure 9. Model for Astrin/SKAP complex plus-end-tracking activity in promoting proper spindle positioning. Schematic of spindle behavior in control cells (top) and SKAP ΔEB mutant cells (bottom). In wild-type cells, the Astrin/SKAP complex localizes to microtubule plus ends along with Clasp1. In these cells, astral microtubules make transient, end-on contacts with the cell

cortex and cortical dynein to generate short bursts of force to position the spindle. In SKAP ΔEB cells, Astrin/SKAP are eliminated from microtubule plus ends. In this condition, metaphase astral microtubules make longer-lasting, lateral contacts with cortex and cortical dynein. These persistent connections lead to significant spindle position shifts from stochastic force imbalances and sustained pulling force from cortical dynein.

Materials and Methods

Cell Line Generation

HeLa Flp-In cells were generated using HeLa LacZeo/TO cells (a gift from S. Taylor, University of Manchester, UK), and pCDNA5-FRT-TO based plasmids (Invitrogen). For untagged SKAP constructs with a GFP expression reporter, we generated a vector by fusing the IRES and eGFP sequences from the pIRES2eGFP vector (Clontech) after the open reading frame of the pCDNA5-FRT-TO based plasmid. Cell lines were made using Flp recombinase–mediated integration based on the manufacturer instructions for the Flp-In TRex System (Invitrogen). Clonal cell lines from retroviral infection were made as described previously (Cheeseman et al., 2004). Cell lines (HeLa, HeLa Flp-In, and 3T3) were maintained in DMEM supplemented with 100 U/ml streptomycin, 100 U/ml penicillin, 2 mM glutamine, and 10% (vol/vol) fetal bovine serum (FBS). Flp-In lines were cultured in HyClone FBS without tetracycline.

Table S1. Cell lines used in this study. Notes: All SKAP cell lines are RNAi resistant. Retroviral cell lines were selected and maintained using Blasticidin. HeLa Flp-In parental line was maintained in Zeocin and Blasticidin. Flp-In lines were selected and maintained using Blasticidin and Hygromycin.

Cell Line	Type	Used	Generated
HeLa	HeLa	Figure 1A, Direct Antibody IPs	Cheeseman Lab HeLa
HeLa Flp-In	HeLa Flp-In	No transgene control, generation of Flp-In Cell lines	Taylor Lab
long SKAP-LAP	HeLa retroviral clonal line	Figure 3	This Study
short SKAP-LAP	HeLa retroviral clonal line	Figures 3, 4, 5, Movie S2, and IP-MS	This Study
short SKAP ΔNT-LAP (aa 89-238)	HeLa retroviral clonal line	Figure 4	This Study
short SKAP 5xD-LAP	HeLa retroviral clonal line	Figure 4	This Study
short SKAP ΔEB-LAP	HeLa retroviral clonal line	Figure 5	This Study
LAP-Astrin	HeLa retroviral clonal line	LAP-Astrin IP-MS	Schmidt et al. 2010
LAP-Astrin (aa 458-1193)	HeLa retroviral clonal line	LAP-Astrin IP-MS	This Study
LAP-Clasp1 (aa 1258-1538)	HeLa retroviral clonal line	Figure 8	This Study
Flp-In long SKAP	HeLa Flp-In IRES eGFP	Figure 3	This Study
Flp-In short SKAP	HeLa Flp-In IRES eGFP	Replacement and rescue experiments	This Study
Flp-In short SKAP ΔNT (89-238)	HeLa Flp-In IRES eGFP	Figure 4	This Study
Flp-In short SKAP 5xD	HeLa Flp-In C-term LAP	Figure 4	This Study
Flp-In short SKAP ΔEB	HeLa Flp-In IRES eGFP	Replacement experiments	This Study
Flp-In Astrin-LAP	HeLa Flp-In C-term LAP	Astrin-LAP IP-MS	This Study

Protein Depletion, Induction, and Transient Transfection

For siRNA transfection, we used Lipofectamine RNAiMAX (Invitrogen) and OptiMEM (Gibco). For protein depletion, we used ON-TARGETplus siRNAs (Dharmacon) against SKAP (5'-AGGCUACAAACCACUGAGUAA-3'; (Dunsch et al., 2011), LGN (5'-GAACUAACAGCACGACUUA-3'; (Kiyomitsu and Cheeseman, 2013), and a non-targeting Control. All siRNAs were used at 40 nM. Double RNAi treatments used 40 nM of each siRNA. We found that neither N-terminal nor C-terminal GFP-tagged, siRNA resistant SKAP constructs were able to fully rescue endogenous protein depletion (data not shown). Therefore, we developed a system using an inducible, siRNA-resistant, and untagged SKAP (with a GFP expression reporter). We note that SKAP (and Astrin) are highly and predominantly expressed in mitosis, with lower levels in interphase cells (Fang et al., 2009; Thiru et al., 2014). Therefore, we induced expression of a substantial amount of exogenous rescue protein at levels comparable to that of the endogenous protein (Fig. S3A and Fig. S4B). This was a achieved by screening for Flp-In cell lines highly responsive to induction and using 2 μg/ mL Doxycycline replaced at 12-16 hour intervals throughout the multi-day protocols (Fig. 3A and Fig. S2C). We note that the expression of long SKAP isoform was slightly less than short SKAP in these assays (Fig. S2A), despite identical constructs and expression conditions. The IRES reporters for each construct were similar therefore the observed expression difference may be due to an inherent instability of the long SKAP protein or the absence of a testis specific binding

partner. For phenotype/mitotic timing movies, filming took place from hour 40 to 48 post siRNA addition. For all other depletion experiments analysis took place at 48 hours post siRNA addition. Transient transfection for EB3-tdTomato (A gift from Erik Dent (Addgene plasmid # 50708; (Merriam et al., 2013) was performed with Effectene (Qiagen) using 0.5 μg of plasmid per dish (see Live Cell Imaging). Transfection was performed two hours after the second media change (see Fig. 3A) and left on cells for six hours.

Antibody Generation

The antibody to detect the Mouse long SKAP N-terminus was raised against GST-mouse long SKAP (aa 1-78), affinity purified using the same protein, and depleted for GST-specific antibodies using a GST column. The affinity purified human Astrin antibody used for IP-MS and IF was raised against Astrin (aa 955-1193-His) and purified using (aa 965-1193-His). Affinity purification was carried out as described previously (Desai et al., 2003).

Immunofluorescence and Westerns

Immunofluorescence and Westerns were conducted using antibodies against human SKAP (Schmidt et al., 2010) (1:2000 for IF, 1:4000 for Western), mouse SKAP N-terminus (1:400 IF, 1:1000 Western), tubulin (DM1α, Sigma, 1:1000 for IF, 1:2000 for Western, for human cell experiments), tubulin (T5186, Sigma 1:1000 for IF, 1:2000 for Western, for mouse cell experiments), Centrin2 (Backer

et al., 2012) (1:12,000 for IF) human Astrin (1:2000 for IF), EB1 (5/EB1, BD Transduction Laboratories, 1:250), Clasp1 (Xorbit) (1:2000 for IF) (Hannak and Heald, 2006), p150(Glued) (1/p150Glued (RUO), BD Transduction Laboratories, 1:250), and centromeres (ACA, Antibodies Incorporated, 1:100). For immunofluorescence, cells were plated on glass coverslips coated with poly-L-lysine (Sigma-Aldrich). For Nocodazole experiments, the indicated concentration of Nocodazole (Sigma-Aldrich) or vehicle control were added to cells for 1 hour prior to fixation (47 hours post-siRNA addition). Fixation conditions were as follows: for IF with SKAP visualized (Fig. 2A, 3C, 4D, Fig. S3B), cells were first pre-extracted for 5 minutes in 0.1% Triton X-100 in PHEM buffer (60 mM PIPES, 25 mM HEPES, 10 mM EGTA, 4 mM $MgSO_4$, pH 7), followed by fixation for 10 minutes in 4% formaldehyde in PHEM buffer. For IF with microtubules visualized, cells were fixed for 10 minutes in 4% formaldehyde in PHEM buffer. For IF with EB1 or Centrin 2 antibodies, cells were fixed for 5 minutes in methanol at -20°C. All other fixation steps were carried out at room temperature immediately following removal from 37°C incubator. Blocking and primary antibody dilution were performed using AbDil (20 mM Tris, 150 mM NaCl, 0.1% Triton X-100, 3% BSA, 0.1% NaN_3, pH 7.5). Washing and secondary antibody dilution steps were performed in PBS + 0.1% Triton X-100 (PBS-TX). Cy2-, Cy3-, and Alexa Fluor 647-conjugated secondary antibodies (Jackson ImmunoResearch Laboratories) were used at 1:300. DNA was visualized by incubating cells in 1 µg/ml Hoechst-33342 (Sigma) in PBS-TX for 2 minutes followed by PBS-TX rinsing. Coverslips

were mounted using PPDM (0.5% p-phenylenediamine and 20 mM Tris-Cl, pH 8.8, in 90% glycerol).

SKAP models and phylogeny

The SKAP gene model (Fig. 2B) was generated using the Integrated Genomics Viewer (Robinson et al., 2011) with data from Human BodyMap 2.0 (Illumina). SKAP proteins were aligned and visualized using Jalview software (Robinson et al., 2011). Phylogenetic tree was made using data from TimeTree (Hedges et al., 2006).

Live and Fixed Cell Imaging

Fixed-cell and live cell images were acquired on a DeltaVision Core microscope (Applied Precision) equipped with a CoolSnap HQ2 CCD camera (Photometrics). Images were deconvolved and planes projected (maximum intensity) as noted in the figure legends. Paired images are scaled equivalently unless otherwise noted. Fixed cells were imaged using a 100×, 1.4 NA U-PlanApo objective (Olympus). For live-cell imaging, cells were plated on 35-mm glass bottom microwell dishes (MatTek) and imaged in CO_2-independent media (Invitrogen) with 100 ng/ml Hoechst-33342 (Sigma) at 37°C. For mitotic timing/phenotype movies, to assess the IRES GFP reporter, points were selected and imaged prior to movie start. For movie imaging, points were imaged with 3 Z-sections 5 um apart using fluorescent and transmitted light at the lowest level usable for data

collection. Images were collected at 5-minute intervals for 8 hours using a using an Olympus 40×, 1.35 NA U-PlanApo objective. For EB3-tdTomato movies, GFP-positive (transgene expressing) cells were selected and the 100× objective was used to collect images every 1 s for 30 s with a 50 ms exposure time. Spinning disc confocal movies were taken with a Nikon Ti-E inverted microscope using an Andor Revolution laser system using a Nikon Apo 100× TIRF objective (NA 1.49) and an Andor iXon 897E EMCCD camera in a 37°C chamber. Images were collected every 0.5 s for 30 s with a 240 ms exposure time. Images and movies were processed using Softworx (Applied Precision), Metamorph (Molecular Devices), ImageJ/Fiji, and Adobe software. Measurements for quantifications were made using Softworx and then plotted and analyzed using Prism (GraphPad).

Mouse Immunostaining

Wild-type 129S2/SvPasCrl mice were purchased from Charles River Laboratories. All animals were housed at the Whitehead Institute for Biomedical Research and maintained according to protocols approved by the Massachusetts Institute of Technology Committee on Animal Care. Adult male mice (60-70 day old) were euthanized in CO_2, and the testes removed. For histological analysis, testes were fixed in Bouin's solution or 4% paraformaldehyde overnight, processed into paraffin wax, and 10 µm sections cut and mounted on Superfrost slides. For immunohistology, tissues were rehydrated and blocked in 5% normal

donkey serum. Primary antibodies (Mouse SKAP N-terminus) were applied in PBS with 5% normal donkey serum overnight at 4°C. Immunolocalization was performed by fluorescence using a FITC-conjugated donkey anti-rabbit (Jackson ImmunoResearch Laboratories) and mounted using Prolong mounting media with DAPI (Molecular Probes); or colorimetrically using ImmPRESS HRP anti-Rabbit detection and developed with a DAB substrate kit (Vector Laboratories), counterstained with Harris' haematoxylin and mounted using Permount (Fisher Scientific).

Immunoprecipitations and Mass Spectrometry

For direct antibody IPs (Fig. S2D and Fig. S4A) indicated antibodies were coupled to beads as described previously (Cheeseman and Desai, 2005). For mitotic IPs, unless otherwise noted, cells were arrested with nocodazole (Sigma-Aldrich) at 330 nM for 14 hours and harvested by shake-off. For interphase IPs, mitotic cells were removed by shake off and the remaining cells harvested. GFP^{LAP} tagged proteins or endogenous proteins were isolated from HeLa cells as described previously (Cheeseman and Desai, 2005). Salt concentrations for bead binding and washing are indicated in figure legends. Purified proteins were identified by mass LTQ XL Ion trap mass spectrometer (Thermo Fisher Scientific) using MudPIT and SEQUEST software as described previously (Washburn et al., 2001). For the mouse testis IP, testes were collected as described above from one 3 month old mouse. Testes were then de-tunicated, and re-suspended in

HeLa Lysis Buffer (Cheeseman and Desai, 2005) to a final volume of ~2 mL. For protease inhibition, 1/2 of a Complete Mini, EDTA-free tablet (Roche) and 1 mM PMSF were added. This mix was subjected to Dounce homogenizer strokes until a suspension was achieved (as determined by light microscope). This mix was used with our standard LAP protocol (Cheeseman and Desai, 2005) using wash buffer with 150 mM KCl.

Acknowledgements

We thank Tomomi Kiyomitsu, Terry Orr-Weaver and members of Cheeseman, Page, and Burge Labs for their support and constructive comments, the Bioinformatics and Research Computing (BaRC) group at Whitehead for assistance with the analysis of SKAP isoforms, Wendy Salmon and the W. M. Keck Microscopy Facility at Whitehead, Dirk de Rooij for help with testis staging and identifying meitoic spindles, Corinne Grey and Bernard de Massy for discussions and sharing results prior to publication, and Rebecca Heald for suggesting and providing the Xorbit/Clasp1 antibody. PKN is a Hope Funds for Cancer Research Fellow supported by the Hope Funds for Cancer Research (HFCR-15-06-06) and recipient of an Early Career Fellowship (GNT1053776, NH&MRC, Australia). This work was supported by a Scholar award to IMC from the Leukemia & Lymphoma Society, a grant from the NIH/National Institute of General Medical Sciences to IMC (GM088313), and a Research Scholar Grant to IMC (121776) from the American Cancer Society.

References

Akhmanova, A., and Steinmetz, M.O. (2008). Tracking the ends: a dynamic protein network controls the fate of microtubule tips. Nat Rev Mol Cell Biol *9*, 309-322.

Ambrose, J.C., and Wasteneys, G.O. (2008). CLASP modulates microtubule-cortex interaction during self-organization of acentrosomal microtubules. Mol Biol Cell *19*, 4730-4737.

Backer, C.B., Gutzman, J.H., Pearson, C.G., and Cheeseman, I.M. (2012). CSAP localizes to polyglutamylated microtubules and promotes proper cilia function and zebrafish development. Mol Biol Cell *23*, 2122-2130.

Bird, S.L., Heald, R., and Weis, K. (2013). RanGTP and CLASP1 cooperate to position the mitotic spindle. Mol Biol Cell *24*, 2506-2514.

Cheeseman, I.M., and Desai, A. (2005). A combined approach for the localization and tandem affinity purification of protein complexes from metazoans. Sci STKE *2005*, pl1.

Cheeseman, I.M., Niessen, S., Anderson, S., Hyndman, F., Yates, J.R., III, Oegema, K., and Desai, A. (2004). A conserved protein network controls assembly of the outer kinetochore and its ability to sustain tension. Genes Dev *18*, 2255-2268.

Collins, E.S., Balchand, S.K., Faraci, J.L., Wadsworth, P., and Lee, W.L. (2012). Cell cycle-regulated cortical dynein/dynactin promotes symmetric cell division by differential pole motion in anaphase. Mol Biol Cell *23*, 3380-3390.

Desai, A., Rybina, S., Muller-Reichert, T., Shevchenko, A., Shevchenko, A., Hyman, A., and Oegema, K. (2003). KNL-1 directs assembly of the microtubule-binding interface of the kinetochore in C. elegans. Genes Dev *17*, 2421-2435.

Duellberg, C., Trokter, M., Jha, R., Sen, I., Steinmetz, M.O., and Surrey, T. (2014). Reconstitution of a hierarchical +TIP interaction network controlling microtubule end tracking of dynein. Nat Cell Biol *16*, 804-811.

Dunsch, A.K., Linnane, E., Barr, F.A., and Gruneberg, U. (2011). The astrin-kinastrin/SKAP complex localizes to microtubule plus ends and facilitates chromosome alignment. J Cell Biol *192*, 959-968.

Fang, L., Seki, A., and Fang, G. (2009). SKAP associates with kinetochores and promotes the metaphase-to-anaphase transition. Cell Cycle *8*, 2819-2827.

Fink, J., Carpi, N., Betz, T., Betard, A., Chebah, M., Azioune, A., Bornens, M., Sykes, C., Fetler, L., Cuvelier, D., *et al.* (2011). External forces control mitotic spindle positioning. Nat Cell Biol *13*, 771-778.

Gonczy, P. (2008). Mechanisms of asymmetric cell division: flies and worms pave the way. Nat Rev Mol Cell Biol *9*, 355-366.

Green, R.A., Wollman, R., and Kaplan, K.B. (2005). APC and EB1 function together in mitosis to regulate spindle dynamics and chromosome alignment. Mol Biol Cell *16*, 4609-4622.

Gruber, J., Harborth, J., Schnabel, J., Weber, K., and Hatzfeld, M. (2002). The mitotic-spindle-associated protein astrin is essential for progression through mitosis. J Cell Sci *115*, 4053-4059.

Hannak, E., and Heald, R. (2006). Xorbit/CLASP links dynamic microtubules to chromosomes in the Xenopus meiotic spindle. J Cell Biol *172*, 19-25.

Hedges, S.B., Dudley, J., and Kumar, S. (2006). TimeTree: a public knowledge-base of divergence times among organisms. Bioinformatics *22*, 2971-2972.

Hendricks, A.G., Lazarus, J.E., Perlson, E., Gardner, M.K., Odde, D.J., Goldman, Y.E., and Holzbaur, E.L. (2012). Dynein tethers and stabilizes dynamic microtubule plus ends. Curr Biol *22*, 632-637.

Honnappa, S., Gouveia, S.M., Weisbrich, A., Damberger, F.F., Bhavesh, N.S., Jawhari, H., Grigoriev, I., van Rijssel, F.J., Buey, R.M., Lawera, A., *et al.* (2009). An EB1-binding motif acts as a microtubule tip localization signal. Cell *138*, 366-376.

Kiyomitsu, T. (2015). Mechanisms of daughter cell-size control during cell division. Trends Cell Biol *25*, 286-295.

Kiyomitsu, T., and Cheeseman, I.M. (2012). Chromosome- and spindle-pole-derived signals generate an intrinsic code for spindle position and orientation. Nat Cell Biol *14*, 311-317.

Kiyomitsu, T., and Cheeseman, I.M. (2013). Cortical dynein and asymmetric membrane elongation coordinately position the spindle in anaphase. Cell *154*, 391-402.

Knoblich, J.A. (2010). Asymmetric cell division: recent developments and their implications for tumour biology. Nat Rev Mol Cell Biol *11*, 849-860.

Kotak, S., Busso, C., and Gonczy, P. (2012). Cortical dynein is critical for proper spindle positioning in human cells. J Cell Biol *199*, 97-110.

Laan, L., Pavin, N., Husson, J., Romet-Lemonne, G., van Duijn, M., Lopez, M.P., Vale, R.D., Julicher, F., Reck-Peterson, S.L., and Dogterom, M. (2012). Cortical dynein controls microtubule dynamics to generate pulling forces that position microtubule asters. Cell *148*, 502-514.

Lee, C.S., Bhaduri, A., Mah, A., Johnson, W.L., Ungewickell, A., Aros, C.J., Nguyen, C.B., Rios, E.J., Siprashvili, Z., Straight, A., *et al.* (2014). Recurrent point mutations in the kinetochore gene KNSTRN in cutaneous squamous cell carcinoma. Nat Genet *46*, 1060-1062.

Mack, G.J., and Compton, D.A. (2001). Analysis of mitotic microtubule-associated proteins using mass spectrometry identifies astrin, a spindle-associated protein. Proc Natl Acad Sci U S A *98*, 14434-14439.

Maffini, S., Maia, A.R., Manning, A.L., Maliga, Z., Pereira, A.L., Junqueira, M., Shevchenko, A., Hyman, A., Yates, J.R., 3rd, Galjart, N., *et al.* (2009). Motor-independent targeting of CLASPs to kinetochores by CENP-E promotes microtubule turnover and poleward flux. Curr Biol *19*, 1566-1572.

Maiato, H., Fairley, E.A., Rieder, C.L., Swedlow, J.R., Sunkel, C.E., and Earnshaw, W.C. (2003). Human CLASP1 is an outer kinetochore component that regulates spindle microtubule dynamics. Cell *113*, 891-904.

Manning, A.L., Bakhoum, S.F., Maffini, S., Correia-Melo, C., Maiato, H., and Compton, D.A. (2010). CLASP1, astrin and Kif2b form a molecular switch that regulates kinetochore-microtubule dynamics to promote mitotic progression and fidelity. EMBO J *29*, 3531-3543.

McNally, F.J. (2013). Mechanisms of spindle positioning. J Cell Biol *200*, 131-140.

Merriam, E.B., Millette, M., Lumbard, D.C., Saengsawang, W., Fothergill, T., Hu, X., Ferhat, L., and Dent, E.W. (2013). Synaptic regulation of microtubule dynamics in dendritic spines by calcium, F-actin, and drebrin. J Neuroscience. *33*, 16471-16482.

Mimori-Kiyosue, Y., Grigoriev, I., Lansbergen, G., Sasaki, H., Matsui, C., Severin, F., Galjart, N., Grosveld, F., Vorobjev, I., Tsukita, S., *et al.* (2005). CLASP1 and CLASP2 bind to EB1 and regulate microtubule plus-end dynamics at the cell cortex. J Cell Biol *168*, 141-153.

Robinson, J.T., Thorvaldsdottir, H., Winckler, W., Guttman, M., Lander, E.S., Getz, G., and Mesirov, J.P. (2011). Integrative genomics viewer. Nat Biotechnol *29*, 24-26.

Rogers, S.L., Rogers, G.C., Sharp, D.J., and Vale, R.D. (2002). Drosophila EB1 is important for proper assembly, dynamics, and positioning of the mitotic spindle. J Cell Biol *158*, 873-884.

Samora, C.P., Mogessie, B., Conway, L., Ross, J.L., Straube, A., and McAinsh, A.D. (2011). MAP4 and CLASP1 operate as a safety mechanism to maintain a stable spindle position in mitosis. Nat Cell Biol *13*, 1040-1050.

Schmidt, J.C., Kiyomitsu, T., Hori, T., Backer, C.B., Fukagawa, T., and Cheeseman, I.M. (2010). Aurora B kinase controls the targeting of the Astrin-SKAP complex to bioriented kinetochores. J Cell Biol *191*, 269-280.

Siller, K.H., and Doe, C.Q. (2009). Spindle orientation during asymmetric cell division. Nat Cell Biol *11*, 365-374.

Tamura, N., Simon, J.E., Nayak, A., Shenoy, R., Hiroi, N., Boilot, V., Funahashi, A., and Draviam, V.M. (2015). A proteomic study of mitotic phase-specific interactors of EB1 reveals a role for SXIP-mediated protein interactions in anaphase onset. Biol Open *4*, 155-169.

Thein, K.H., Kleylein-Sohn, J., Nigg, E.A., and Gruneberg, U. (2007). Astrin is required for the maintenance of sister chromatid cohesion and centrosome integrity. J Cell Biol *178*, 345-354.

Thiru, P., Kern, D.M., McKinley, K.L., Monda, J.K., Rago, F., Su, K.C., Tsinman, T., Yarar, D., Bell, G.W., and Cheeseman, I.M. (2014). Kinetochore genes are coordinately up-regulated in human tumors as part of a FoxM1-related cell division program. Mol Biol Cell *25*, 1983-1994.

Wang, X., Zhuang, X., Cao, D., Chu, Y., Yao, P., Liu, W., Liu, L., Adams, G., Fang, G., Dou, Z., *et al.* (2012). Mitotic regulator SKAP forms a link between kinetochore core complex KMN and dynamic spindle microtubules. J Biol Chem *287*, 39380-39390.

Washburn, M.P., Wolters, D., and Yates, J.R., 3rd (2001). Large-scale analysis of the yeast proteome by multidimensional protein identification technology. Nat Biotechnol *19*, 242-247.

Chapter IV: Discussion and Future Directions

Key conclusions of this thesis

Nematode KNL-1 forms a defined oligomer in vitro, but does not play a major role in kinetochore structure and function

The initial aim of the KNL-1 oligomerization project was to test if KNL-1 plays a conserved structural role in organizing the KMN network of the outer kinetochore (Cheeseman et al., 2006). We found that KNL-1 oligomerizes in vitro for two species of nematodes, *C. elegans* and *C. remanei (Kern et al., 2015)*. The oligomers formed at physiological concentrations, especially considering the in vivo clustering of KNL-1 that occurs at a kinetochore. We were able to obtain AUC and EM data to show that the oligomers have a defined structure and are composed of approximately 10 subunits. Finally, we found that removal or mutation of a small hydrophic region was sufficient to ablate oligomerization activity.

However, the region involved in KNL-1 oligomerization is not conserved in other organisms. Furthermore, we observed no major defects when we replaced wild-type KNL-1 with mutants defective for oligomerization in *C. elegans*. Therefore, we concluded that the oligomerization does not play a major role in kinetochore organization. The location of the oligomerization domain, within the "MELT"-repeat domains of KNL-1, hints that the oligomer may instead organize the N-terminal checkpoint and phosphatase signaling domains of KNL-1 (Vleugel et al., 2015). Since nematode kinetochores coat the entire chromosome, the creation of localized signaling clusters may be more important in these organisms

and there may be redundant pathways to achieve this goal. In other organisms, checkpoint proteins have been proposed to cluster themselves, and KNL-1 is a putative dimer (Petrovic et al., 2014). The work presented here is one of only a couple attempts to express, purify, and conduct biochemical analysis on the potentially unstructured MELT-repeat region of KNL-1 (Espeut et al., 2012). We found unique properties for the oligomer, such as high expression, solubility, and gel formation at high concentrations. These may be a glimpse into the properties and behavior of KNL-1 in vivo.

SKAP has a testis-expressed and a novel mitotic isoform

In this work, we found that the isoform of SKAP used by our lab and others in studies of mitosis was, in fact, only expressed in testes. The true mitotic form is actually a shorter protein, which is made by an alternative transcriptional start site generating an in-frame truncation of the testis-specific isoform. Since both proteins share the much of the same sequence, and the testis protein is longer, the mitotic isoform had remained hidden. However, the testis isoform had appeared more recently evolutionarily in eutherian (placental) mammals, whereas the sequence of the mitotic isoform is conserved in all vertebrates we have investigated. We found that testis SKAP is highly expressed in elongating spermatids and more modestly expressed on spindles of meiotic cells in the testis. The mitotic form, expressed in all tissues and tissue culture cells, was able to rescue siRNA depletion of SKAP.

SKAP depletion leads to pleotropic defects in chromosome segregation, centrosome stability, and spindle stability

Multiple previous studies have studied SKAP depletion, but none had rescued this depletion (Dunsch et al., 2011; Fang et al., 2009; Schmidt and Cheeseman, 2011). Therefore, the reported phenotypes, which were not all in agreement, had the caveat of potential off-target effects. We developed a system in which untagged siRNA-resistant mitotic SKAP, when expressed at a high level mimicking the endogenous, could rescue a thorough SKAP depletion. Therefore, the phenotypes we observed in our depletions, including chromosome mis-segregation, a mitotic delay, multipolarity, and spindle instability, were all due to the reduction of SKAP protein. In SKAP depleted cells, chromosomes often have difficulty aligning and remaining on the metaphase plate. Furthermore, many cells exhibit multipolarity during mitosis. Importantly, this is not due to centrosomal material fragmenting during a prolonged mitosis or additional centrosomes, because in the multipolar cells we observed a centriole at each pole. This indicates that the multipolarity is due to premature centriole disengagement in mitosis, and argues for an Astrin/SKAP complex role in centrosome stability. Finally, we observed many disorganized and improperly oriented spindles in our depletions. However, due to these pleiotropic phenotypes, it was difficult to separate these observations into specific roles for the Astrin/SKAP complex without further mutations.

SKAP microtubule binding is necessary for Astrin/SKAP complex spindle localization and function

The Astrin/SKAP complex localizes to the mitotic spindle, and previous studies had suggested that Astrin and SKAP have microtubule binding ability (Dunsch et al., 2011; Schmidt and Cheeseman, 2011; Wang et al., 2012). We localized the major microtubule binding activity for the Astrin/SKAP complex to the N-terminus of SKAP, specifically a small region of positive charge. We investigated two SKAP microtubule binding mutants in vivo, an N-terminal truncation and a charge swap mutation, which each removed SKAP spindle localization. When wild-type SKAP was replaced with these mutants, we observed phenotypes very similar to SKAP depletion alone. This indicates that SKAP microtubule binding is essential for Astrin/SKAP complex function.

The Astrin/SKAP complex is a plus-end tracker that localizes to astral microtubule plus ends

Previous reports on the Astrin/SKAP complex described plus-end-tracking, but these reports were largely devoid of mitotic in vivo data proving the activity (Dunsch et al., 2011; Tamura et al., 2015). We had not observed clear mitotic plus-end-tracking with the testis-specific long form of SKAP. However, when we tagged the mitotic isoform of SKAP with GFP, we observed striking localization to mitotic plus ends. We confirmed this result with rescue experiments and

immunofluorescence data showing both Astrin and SKAP on mitotic plus ends, including astral microtubules. Furthermore, a EB-protein binding motif had been described by other labs in SKAP's N-terminus. We showed that by mutating this motif, the Astrin/SKAP complex was specifically removed from microtubule plus ends, but importantly still localized to both the mitotic spindle and kinetochores. When we replaced wild-type SKAP with the SKAP ΔEB mutant, we found that the defects in chromosome segregation and centrosome stability were rescued, indicating that plus-end-tracking was not necessary for these Astrin/SKAP roles. However, we noticed that many spindles were dramatically mispositioned with this mutant.

The Astrin/SKAP complex plus-end-tracking is needed for metaphase spindle positioning

We found that many cells lacking Astrin/SKAP plus-end-tracking contained mispositioned metaphase spindles. In extreme cases, spindles were smashed against one side of the cell, with astral microtubules making many lateral connections with cell cortex. When we quantified cells in this condition we found that cells were mispositioned away from center more often, and at greater distances, than in the control or rescue cases. In live cell experiments, we observed that spindles often were moved away from the cell center in a single sweeping motion post chromosome alignment. Spindles remained mispositioned until anaphase, where they were generally corrected through early anaphase.

Using LGN depletion and low dose nocodazole, we found that the metaphase spindle mispositioning we observed in the SKAP ΔEB mutants requires both cortical dynein and astral microtubules. This placed the Astrin/SKAP complex, specifically through its plus-end localization, as a potential regulator of the spindle-positioning pathway (Kiyomitsu, 2015).

The Astrin/SKAP complex interacts with multiple other spindle positioning proteins and regulates Clasp1 localization in mitosis

In our proteomic efforts, we generated a list of Astrin and SKAP interacting proteins using both tagged and endogenous immunoprecipitation strategies. Among the interactors, we found dynein, NuMA Plk1, and Clasp1, all proteins that have been implicated in mitotic spindle positioning (Kiyomitsu and Cheeseman, 2012; Samora et al., 2011). We found that the SKAP ΔEB mutant did not affect localization of the dynein/dynactin complex to the cortex, or its regulation by off-axis spindles. However, when we tested for Clasp1 localization, we found that it was dramatically reduced on the spindle and at astral microtubule plus ends. Importantly, we saw no affect on Clasp1 localization in SKAP depletions in interphase cells or by expressing wild-type SKAP ectopically in interphase. Only when we ectopically expressed the SKAP ΔEB mutant did we see a reduction in interphase Clasp1 localization to plus ends. Clasp1 had previously been implicated in side-to-side spindle mispositioning using depletions (Samora et al., 2011). Our data indicate that the Astrin/SKAP complex regulates

Clasp1 localization to plus ends during mitosis. We hypothesize that Clasp1 and the Astrin/SKAP complex interact at astral microtubule plus ends to form a docking mechanism for cortical dynein. Perturbation of these proteins can lead to aberrant astral microtubule interactions with the cortex, imbalanced spindle positioning forces, and ultimately dramatically mispositioned metaphase spindles.

Unanswered questions and future directions

What is the structural role of KNL-1 within the kinetochore?

We did not find a major role for KNL-1 oligomerization in KMN network organization. However, multiple studies from other labs have established KNL-1's role in nucleating the spindle assembly checkpoint, specifically through Bub1/3 binding to the MELT repeats and KI-motifs in KNL-1 (Bolanos-Garcia et al., 2009; Kiyomitsu et al., 2007; Krenn et al., 2014). Further studies have established that these repeats are phosphorylated by the checkpoint kinase Mps1 to initiate the formation of a checkpoint complex docking site at the kinetochore (Yamagishi et al., 2012; Krenn et al., 2012; Vleugel et al., 2015). Recently, two groups showed that Mps1 docks on the Ndc80 complex in a process that is negatively regulated by microtubule attachment (Hiruma et al., 2015; Ji et al., 2015). A third group proposed a model where spatial separation between Ndc80 localized Mps1 and its KNL-1 substrate controls checkpoint activity (Aravamudhan et al., 2015). These checkpoint models establish KNL-1 and its behavior to be critical.

Therefore establishing the biochemical behavior of KNL-1's N-terminus, a region predicted and observed to be largely unstructured, is important. For instance, the KNL-1 N-terminal region is potentially clustered by multiple dimeric checkpoint proteins, including Bub1 (Krenn et al., 2012). Is this region of KNL-1 an interconnected cluster or is KNL-1 extended out towards microtubules? Does the KNL-1 N-terminus have spring-like properties? How does a large, mostly unstructured, protein fit into a complex responsible for conducting a precise cellular process? These biophysical and cell biological questions must be answered in order to understand the true role of KNL-1.

What are the organizing principles governing outer kinetochore architecture?

It is formally possible that the outer kinetochore has no overriding organization. However the conserved number of proteins found per microtubule attachment site, as well as the precise nature of the complex, argue against this point (Joglekar et al., 2006; Joglekar et al., 2008; Johnston et al., 2010; Suzuki et al., 2014; Wan et al., 2009). One possible structural factor is the Ndc80 complex itself, which has been proposed to form low affinity oligomeric arrays on microtubules (Alushin et al., 2012; Alushin et al., 2010). The kinetochore is made up of many tethered molecules. Therefore, local concentration effects can be powerful and can enhance even weak oligomeric affinities to physiologically relevant levels. Thus, it is possible that Ndc80 oligomerization, potentially aided

by other proteins, may organize the outer kinetochore around microtubules (Powers et al., 2009). This hypothesis has yet to be thoroughly tested in vivo, largely due to the difficulty of the question and obtaining a specific mutant, but remains an interesting possibility. Furthermore, organization may arise from the base of the outer kinetochore, a structure including the inner kinetochore proteins of the CCAN and their centromeric DNA binding site (McKinley and Cheeseman, 2015). Many studies have suggested a structured array of inner kinetochore proteins and DNA (Ribeiro et al., 2010), and any structure that influences the placement of CENP-C and CENP-T would affect the organization of the outer kinetochore. Answering this question will be complex, as it necessitates reconstruction of the kinetochore on its DNA substrate. However, kinetochore reconstitution is an important goal for answering many questions and is worth pursuing.

What is the role of the testis isoform of SKAP?

We found that SKAP has a testis-specific isoform in eutherian mammals which localizes to meiotic spindles and elongating spermatids. Astrin has also been proposed to play roles in testes and sperm (Shao et al., 2001) (Xue et al., 2002). Thus, it is an interesting question what this mitotic, kinetochore localized complex may be doing late in spermatogenesis. Specifically answering this question will require a mouse knockout of the long form of SKAP and a thorough investigation of the testis phenotypes. However, the low conservation in SKAP's N-terminal tail may indicate that this protein plays new or different roles in humans. Looking for

Astrin or SKAP mutations in human males with fertility defects may shed some light on the human role of this complex in testes.

Is the Astrin/SKAP complex a mitotic stabilizing factor at centrosomes and kinetochores?

The phenotypes for Astrin and SKAP depletions include centrosome instability and chromosome misalignment, corresponding with the Astrin/SKAP complex localizing to centrosomes and kinetochores in mitosis. The complex arrives at centrosomes when it is highly expressed in the G2/M phase transition (Thiru et al., 2014), and this localization is maintained through mitosis (Schmidt and Cheeseman, 2011). Both SKAP depletion and SKAP microtubule binding mutant replacement, which each reduce the complex localization to centrosomes, led to premature centriole disengagement and spindle multipolarity. Besides possessing microtubule-binding activity and localizing to the centrosome, we find here that Astrin and SKAP have multiple binding partners implicated in centrosome structure and maintenance, including Plk1 and CDK5RAP2 (Kodani et al., 2015). Both of these proteins appear to be upstream of Astrin/SKAP localization, as each play major roles in centrosomal structure (Conduit et al., 2015), but it is possible that the Astrin/SKAP complex is playing a more direct role in regulating these proteins or holding together centrosomal elements. Answering these questions will be fruitful for understanding the maintenance of centriole tethering and the regulation of centriole disengagement.

Astrin/SKAP kinetochore localization is intriguing, as the complex arrives just before the rapid and crucial separation of chromosomes at anaphase onset. This approximate localization timing is shared by only one other protein, the phosphatase PP1, and both of these molecules are regulated by the kinetochore-localized, tension-sensing kinase Aurora B (Liu et al., 2010). PP1's critical role at the kinetochore is to remove phosphorylation by Aurora B and other kinases to promote stable microtubule attachments and the removal of the spindle assembly checkpoint (Meadows et al., 2011; Rosenberg et al., 2011). Could the Astrin/SKAP complex be playing a role in stabilizing kinetochore-microtubule attachments? Besides localization timing, the chromosome segregation defect and dependence on SKAP microtubule binding suggest that this stabilizing role is a possibility. More experiments need to be conducted to establish how the Astrin/SKAP complex gets to kinetochores and how this interaction is regulated. Specific kinetochore binding mutants of Astrin/SKAP could isolate its kinetochore role, helping us understand this unique activity.

What is the mechanism of astral microtubule and cortical dynein force generation?

In this thesis, we present data that the Astrin/SKAP complex, along with its interacting partner Clasp1, localize to astral microtubule plus ends to mediate spindle positioning. The mechanism of dynein motility has been extensively studied as has its localization to the cell cortex, however the study of how astral microtubules dock on cortical dynein is just beginning. One possibility is that

multiple other plus-end-tracking proteins, such as the EB-proteins themselves or the depolymerizing kinesin MCAK, could play a role in controlling astral microtubule behavior at cell cortex. The study of what controls the composition of the mitotic plus end is both interesting and difficult due to the transient nature of plus ends and difficulty working with the dynamically unstable microtubule polymer. However, working out these questions will reveal what differentiates distinct microtubule populations and more about how the mitotic spindle is constructed. Working out what happens upon microtubule contact with the cortex is also very difficult and will likely require sophisticated in vivo microscopy, in vitro reconstitution, and a sophisticated single molecule setup to answer. However, careful study of another plus-end attachment site, the kinetochore, has uncovered and answered many questions, and undoubtedly the study of the cortical docking site will as well.

Concluding remarks

The work presented in this thesis expands our knowledge of that happens at two mitotic microtubule attachment sites: the kinetochore and the cell cortex. Additionally, it uncovers the true mitotic form of the SKAP protein, helping characterize the previously proposed mitotic roles for the Astrin/SKAP complex in chromosome segregation and centrosome stability. Revealing these two isoforms also opens up new areas of study for the Astrin/SKAP complex in the mammalian testis and in mitotic spindle positioning. Hopefully, all of these areas will be fruitful grounds for future studies in understanding the essential process of mitosis, the

growth and development of an organism, and the role of mitotic abnormalities in cancer.

References

Alushin, G.M., V. Musinipally, D. Matson, J. Tooley, P.T. Stukenberg, and E. Nogales. 2012. Multimodal microtubule binding by the Ndc80 kinetochore complex. *Nature Structural & Molecular Biology*. 19:1161-1167.

Alushin, G.M., V.H. Ramey, S. Pasqualato, D.A. Ball, N. Grigorieff, A. Musacchio, and E. Nogales. 2010. The Ndc80 kinetochore complex forms oligomeric arrays along microtubules. *Nature*. 467:805-810.

Aravamudhan, P., A.A. Goldfarb, and A.P. Joglekar. 2015. The kinetochore encodes a mechanical switch to disrupt spindle assembly checkpoint signalling. *Nature Cell Biology*. 17:868-879.

Bolanos-Garcia, V.M., T. Kiyomitsu, S. D'Arcy, D.Y. Chirgadze, J.G. Grossmann, D. Matak-Vinkovic, A.R. Venkitaraman, M. Yanagida, C.V. Robinson, and T.L. Blundell. 2009. The crystal structure of the N-terminal region of BUB1 provides insight into the mechanism of BUB1 recruitment to kinetochores. *Structure*. 17:105-116.

Cheeseman, I.M., J.S. Chappie, E.M. Wilson-Kubalek, and A. Desai. 2006. The Conserved KMN Network Constitutes the Core Microtubule-Binding Site of the Kinetochore. *Cell*. 127:983-997.

Conduit, P.T., A. Wainman, and J.W. Raff. 2015. Centrosome function and assembly in animal cells. *Nature Reviews Molecular Cell Biology*. 16:611-624.

Dunsch, A.K., E. Linnane, F.A. Barr, and U. Gruneberg. 2011. The astrin-kinastrin/SKAP complex localizes to microtubule plus ends and facilitates chromosome alignment. *The Journal of Cell Biology*. 192:959-968.

Espeut, J., D.K. Cheerambathur, L. Krenning, K. Oegema, and A. Desai. 2012. Microtubule binding by KNL-1 contributes to spindle checkpoint silencing at the kinetochore. *The Journal of Cell Biology*. 196:469-482.

Fang, L., A. Seki, and G. Fang. 2009. SKAP associates with kinetochores and promotes the metaphase-to-anaphase transition. *Cell cycle*. 8:2819-2827.

Hiruma, Y., C. Sacristan, S.T. Pachis, A. Adamopoulos, T. Kuijt, M. Ubbink, E. von Castelmur, A. Perrakis, and G.J. Kops. 2015. Competition between MPS1 and microtubules at kinetochores regulates spindle checkpoint signaling. *Science*. 348:1264-1267.

Ji, Z., H. Gao, and H. Yu. 2015. Kinetochore attachment sensed by competitive Mps1 and microtubule binding to Ndc80C. *Science*. 348:1260-1264.

Joglekar, A.P., D.C. Bouck, J.N. Molk, K.S. Bloom, and E.D. Salmon. 2006. Molecular architecture of a kinetochore-microtubule attachment site. *Nature Cell Biology*. 8:581-585.

Joglekar, A.P., E.D. Salmon, and K.S. Bloom. 2008. Counting kinetochore protein numbers in budding yeast using genetically encoded fluorescent proteins. *Methods in cell biology*. 85:127-151.

Johnston, K., A. Joglekar, T. Hori, A. Suzuki, T. Fukagawa, and E.D. Salmon. 2010. Vertebrate kinetochore protein architecture: protein copy number. *The Journal of Cell Biology*. 189:937-943.

Kern, D.M., T. Kim, M. Rigney, N. Hattersley, A. Desai, and I.M. Cheeseman. 2015. The outer kinetochore protein KNL-1 contains a defined oligomerization domain in nematodes. *Molecular Biology of the Cell.* 26:229-237.

Kiyomitsu, T. 2015. Mechanisms of daughter cell-size control during cell division. *Trends in Cell Biology.* 25:286-295.

Kiyomitsu, T., and I.M. Cheeseman. 2012. Chromosome- and spindle-pole-derived signals generate an intrinsic code for spindle position and orientation. *Nature Cell Biology.* 14:311-317.

Kiyomitsu, T., C. Obuse, and M. Yanagida. 2007. Human Blinkin/AF15q14 is required for chromosome alignment and the mitotic checkpoint through direct interaction with Bub1 and BubR1. *Developmental Cell.* 13:663-676.

Kodani, A., T.W. Yu, J.R. Johnson, D. Jayaraman, T.L. Johnson, L. Al-Gazali, L. Sztriha, J.N. Partlow, H. Kim, A.L. Krup, A. Dammermann, N.J. Krogan, C.A. Walsh, and J.F. Reiter. 2015. Centriolar satellites assemble centrosomal microcephaly proteins to recruit CDK2 and promote centriole duplication. *eLife.* 4.

Krenn, V., K. Overlack, I. Primorac, S. van Gerwen, and A. Musacchio. 2014. KI motifs of human Knl1 enhance assembly of comprehensive spindle checkpoint complexes around MELT repeats. *Current Biology.* 24:29-39.

Krenn, V., A. Wehenkel, X. Li, S. Santaguida, and A. Musacchio. 2012. Structural analysis reveals features of the spindle checkpoint kinase Bub1-kinetochore subunit Knl1 interaction. *The Journal of Cell Biology.* 196:451-467.

Liu, D., M. Vleugel, C.B. Backer, T. Hori, T. Fukagawa, I.M. Cheeseman, and M.A. Lampson. 2010. Regulated targeting of protein phosphatase 1 to the outer kinetochore by KNL1 opposes Aurora B kinase. *The Journal of Cell Biology.* 188:809-820.

McKinley, K.L., and I.M. Cheeseman. 2015. The molecular basis for centromere identity and function. *Nature Reviews Molecular Cell Biology.*

Meadows, J.C., L.A. Shepperd, V. Vanoosthuyse, T.C. Lancaster, A.M. Sochaj, G.J. Buttrick, K.G. Hardwick, and J.B. Millar. 2011. Spindle checkpoint silencing requires association of PP1 to both Spc7 and kinesin-8 motors. *Developmental Cell.* 20:739-750.

Petrovic, A., S. Mosalaganti, J. Keller, M. Mattiuzzo, K. Overlack, V. Krenn, A. De Antoni, S. Wohlgemuth, V. Cecatiello, S. Pasqualato, S. Raunser, and A. Musacchio. 2014. Modular assembly of RWD domains on the Mis12 complex underlies outer kinetochore organization. *Molecular Cell.* 53:591-605.

Powers, A.F., A.D. Franck, D.R. Gestaut, J. Cooper, B. Gracyzk, R.R. Wei, L. Wordeman, T.N. Davis, and C.L. Asbury. 2009. The Ndc80 kinetochore complex forms load-bearing attachments to dynamic microtubule tips via biased diffusion. *Cell.* 136:865-875.

Ribeiro, S.A., P. Vagnarelli, Y. Dong, T. Hori, B.F. McEwen, T. Fukagawa, C. Flors, and W.C. Earnshaw. 2010. A super-resolution map of the vertebrate kinetochore. *Proceedings of the National Academy of Sciences of the United States of America.* 107:10484-10489.

Rosenberg, J.S., F.R. Cross, and H. Funabiki. 2011. KNL1/Spc105 recruits PP1 to silence the spindle assembly checkpoint. *Current Biology.* 21:942-947.

Samora, C.P., B. Mogessie, L. Conway, J.L. Ross, A. Straube, and A.D. McAinsh. 2011. MAP4 and CLASP1 operate as a safety mechanism to maintain a stable spindle position in mitosis. *Nature Cell Biology*. 13:1040-1050.

Schmidt, J.C., and I.M. Cheeseman. 2011. Chromosome segregation: keeping kinetochores in the loop. *Current Biology*. 21:R110-112.

Shao, X., J. Xue, and F.A. van der Hoorn. 2001. Testicular protein Spag5 has similarity to mitotic spindle protein Deepest and binds outer dense fiber protein Odf1. *Molecular Reproduction and Development*. 59:410-416.

Suzuki, A., B.L. Badger, X. Wan, J.G. DeLuca, and E.D. Salmon. 2014. The architecture of CCAN proteins creates a structural integrity to resist spindle forces and achieve proper Intrakinetochore stretch. *Developmental Cell*. 30:717-730.

Tamura, N., J.E. Simon, A. Nayak, R. Shenoy, N. Hiroi, V. Boilot, A. Funahashi, and V.M. Draviam. 2015. A proteomic study of mitotic phase-specific interactors of EB1 reveals a role for SXIP-mediated protein interactions in anaphase onset. *Biology Open*. 4:155-169.

Thiru, P., D.M. Kern, K.L. McKinley, J.K. Monda, F. Rago, K.C. Su, T. Tsinman, D. Yarar, G.W. Bell, and I.M. Cheeseman. 2014. Kinetochore genes are coordinately up-regulated in human tumors as part of a FoxM1-related cell division program. *Molecular Biology of the Cell*. 25:1983-1994.

Vleugel, M., M. Omerzu, V. Groenewold, M.A. Hadders, S.M. Lens, and G.J. Kops. 2015. Sequential multisite phospho-regulation of KNL1-BUB3 interfaces at mitotic kinetochores. *Molecular Cell*. 57:824-835.

Wan, X., R.P. O'Quinn, H.L. Pierce, A.P. Joglekar, W.E. Gall, J.G. DeLuca, C.W. Carroll, S.T. Liu, T.J. Yen, B.F. McEwen, P.T. Stukenberg, A. Desai, and E.D. Salmon. 2009. Protein architecture of the human kinetochore microtubule attachment site. *Cell*. 137:672-684.

Wang, X., X. Zhuang, D. Cao, Y. Chu, P. Yao, W. Liu, L. Liu, G. Adams, G. Fang, Z. Dou, X. Ding, Y. Huang, D. Wang, and X. Yao. 2012. Mitotic regulator SKAP forms a link between kinetochore core complex KMN and dynamic spindle microtubules. *The Journal of Biological Chemistry*. 287:39380-39390.

Xue, J., H.A. Tarnasky, D.E. Rancourt, and F.A. van Der Hoorn. 2002. Targeted disruption of the testicular SPAG5/deepest protein does not affect spermatogenesis or fertility. *Molecular and Cellular Biology*. 22:1993-1997.

Yamagishi, Y., C.H. Yang, Y. Tanno, and Y. Watanabe. 2012. MPS1/Mph1 phosphorylates the kinetochore protein KNL1/Spc7 to recruit SAC components. *Nature Cell Biology*. 14:746-752.

Appendix:

Kinetochore Structure: Pulling Answers from Yeast

Reprinted from Cell Press (Current Biology Preview):

David M. Kern and Iain M. Cheeseman. **Kinetochore Structure: Pulling Answers from Yeast**

2012. Current Biology 22 (19), R842-R844

Despite the identification of multiple kinetochore proteins, their structure and organization has remained unclear. New work utilizes electron microscopy to visualize isolated budding yeast kinetochore particles and reveal the kinetochore structure on microtubules.

The kinetochore is a complex macromolecular structure that mediates chromosome-microtubule interactions to direct the dynamic process of chromosome segregation. Despite the discovery of a large number of kinetochore components, the basic structure of this complex remains unknown [1] [2]. In this respect, the kinetochore structure has lagged significantly behind other large complexes such as the ribosome [3] or the nuclear pore [4]. Indeed, the kinetochore is often depicted as a set of interconnected shapes that lack molecular or structural detail. A major limitation in studying kinetochore structure has been that, at least until recently, it was not possible to isolate kinetochore assemblies from cells. Defining the structure and organization of the kinetochore represents a major goal for understanding the mechanisms that ensure the faithful distribution of the genetic material. Now, new work by Gonen et al. helps to bridge the gap between the structure of individual kinetochore components and a model for the entire kinetochore complex by directly visualizing isolated kinetochore particles [5].

The kinetochore connects the centromere of a chromosome to microtubules from the mitotic spindle. Early structural data from electron microscopy of vertebrate cells established a trilaminar model for the kinetochore [6]. An electron dense region of the kinetochore near the chromosomal DNA was

termed the "inner kinetochore" and a second electron dense region near the microtubule was termed the "outer kinetochore". These images have remained useful structural references while researchers elucidated the molecular composition of the kinetochore. However, the vertebrate kinetochore is an extremely large structure that connects to multiple different microtubule polymers suggesting that this trilaminar arrangement is likely formed by multiple interlinked repeats of a smaller underlying kinetochore units. In contrast, the budding yeast kinetochore is much smaller and thus simpler, connecting to just a single microtubule [7]. Visualizing this minimal structure would be an ideal way to define the organization of the kinetochore proteins that form the microtubule attachment. Unfortunately, due in part to its small size, it has not been possible to observe the kinetochore in intact yeast cells by electron microscopy [8].

Despite the differences in size between the vertebrate and budding yeast kinetochores, there are significant similarities in their molecular composition. The inner kinetochore is composed of several DNA binding proteins including the conserved histone variant CENP-A^{Cse4} and a set of sub-complexes termed the centromere-associated network (CCAN) [9]. These proteins provide a platform for the outer kinetochore, which contains the conserved microtubule binding Ndc80 complex and additional associated proteins including KNL1 and the Mis12 complex, which together form the KMN network. In yeast, the Dam1 complex contributes an additional microtubule binding element. High resolution fluorescence imaging has established the general distribution of these many

proteins within the kinetochore [10] [11] as well as provided details on their relative stoichiometries [12]. These studies have indicated that, although kinetochore size varies, the number of protein molecules per bound microtubule remains conserved between yeast and vertebrates.

To achieve chromosome segregation, the kinetochore must couple the force of microtubule polymerization and depolymerization to chromosome movement. How this is achieved is a major question that is closely linked to mysteries of kinetochore structure. There are two major, non-exclusive models for how a kinetochore remains attached to a microtubule during mitosis [13]. The first model, termed biased diffusion, suggests that multiple weak attachments from the kinetochore form a moving interface with a depolymerizing microtubule. This model necessitates a multivalent attachment, a role potentially performed by the Ndc80 complex. The second model, termed "forced walk", suggests that curling protofilaments displace a more tightly associated microtubule binding protein down the microtubule lattice allowing the kinetochore to capture the force from microtubule depolymerization. A ring-like structure, such as has been identified in vitro for the budding yeast Dam1 complex [14] could act in this way to remain attached even as a microtubule shrinks. The budding yeast kinetochore is unique in that it binds to only one microtubule per centromere, whereas human kinetochores bind to ~15-20 microtubules [15]. This places a unique challenge on the budding yeast kinetochore because it cannot disassociate from this lone microtubule without chromosome loss. The strict requirement for Dam1 in

budding yeast and its lack of conservation in higher eukaryotes may reflect this important functional difference [16].

A key challenge in the kinetochore field has been to analyze kinetochore function biochemically. One approach for such studies has been a "bottom up" approach to reconstitute individual kinetochore proteins and complexes to analyze their associations and activities. In an elegant alternative approach to isolate intact kinetochore particles, the Biggins lab previously developed one-step purifications to pull out the structure from budding yeast cells. For these studies, they utilized FLAG-tagged Dsn1, a member of the Mis12 complex that bridges the inner and outer kinetochore, as a "handle" [17]. When Dsn1 is affinity purified under low stringency conditions, the majority of the defined components of the budding yeast kinetochore co-purify. The choice of lower salt conditions was extremely important, as higher stringency purifications have been shown to isolate individual sub-complexes.

These isolated kinetochore particles have provided a powerful tool for a range of studies on kinetochore function. In addition to defining kinetochore components [17], the Biggins lab has previously collaborated with the Asbury lab to analyze the microtubule binding behavior of these kinetochore particles [18]. They found that the particles displayed many properties of native kinetochores, including microtubule binding activity and the ability to track with depolymerizing microtubule ends. The particles also exhibited an intriguing catch-bond property

in the presence of force, in which the connection with microtubules was enhanced with increased force.

Now, the Biggins group has collaborated with the Gonen lab to directly visualize the kinetochore particles by electron microscopy [5]. This work revealed that they are 126 nm in diameter with a dense central domain and globular outer domains. In the presence of increased salt, these particles appeared more extended, which could indicate conformational flexibility of the proteins. The number of globular outer domains present in each particle ranged from five to seven. The authors hypothesized that each of these globular domains represents a KMN network unit. This result suggests that a component of the particle's central hub dictates the stoichiometry and organization of the particle. This organizational player could be an oligomeric protein or a DNA-based structure.

When the authors mixed the isolated kinetochore particles with stabilized microtubules, they observed structures decorating the microtubules. As predicted by the earlier biophysical work, the particles were capable of associating with microtubules in both side-on and end-on configurations. When they observed side-on attachments, they were able to visualize a structure that appeared to be an extended Ndc80 complex gripping the microtubule. Most strikingly, when they observed end-on attachments, they also observed a ring around the microtubule that likely corresponds to the Dam1 complex (Figure 1). This ring was attached to the main particle by elongated, Ndc80-like structures. Importantly, the ring was observed even though Dam1 complex was not present at stoichiometric

concentrations in the kinetochore affinity purifications. This result supports the model that Dam1 ring formation is a cooperative process aided by both microtubules and the Ndc80 complex [19]. Gonen et al. also made tomographic reconstructions that show that the isolated kinetochore assembly encircles the microtubule and that the ring is contacted at regular intervals by protrusions from the kinetochore particle. Finally, deletion of key subunits from the Dam1 and Ndc80 complex almost completely abolished rings and attachment, respectively. Although this is not a definitive identification of the complexes, these results are consistent with current models.

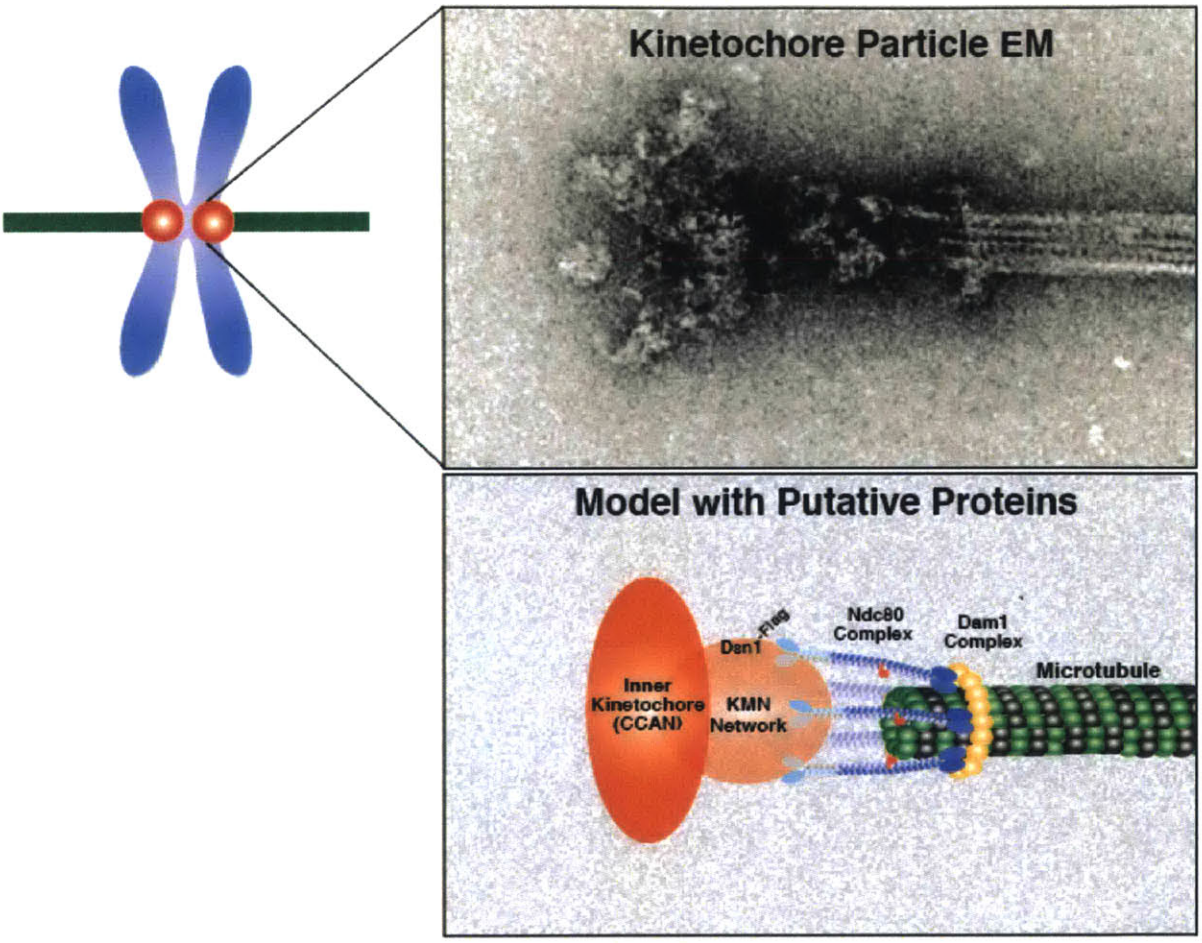

Figure 1. Electron microscopy of isolated kinetochore particles. (A) Electron microscope image of an isolated kinetochore particle with an end-on attachment to a microtubule. The particle is composed of a central density with surrounding globular structures. There is a clear ring around the microtubule that is connected to the kinetochore particle through elongated structures. (B) A model of the predicted proteins that correspond to the visualized EM density. Gonen et al. propose that the globular domains represent KMN network components (red spheres). The central density (red oval) likely contains inner kinetochore components. The extended molecules that contact the microtubule are proposed to be the Ndc80 complex. Finally, the ring is represented as an oligomer of the Dam1 complex. The image in (A) was kindly provided by Tamir Gonen.

The work from Gonen et al. presents thought-provoking images and enhances our knowledge of kinetochore structure. The observations of an oligomeric structure, the multivalent attachment site with microtubules, and the formation of a ring for end-on attachments all support models of kinetochore function. Specific identification of the proteins within this structure is an important next step for this work. Protein labels, specific truncations, and mutations will be interesting additions to the experiment. This work opens the question of whether the kinetochore in higher eukaryotes will emerge as a tessellation of the yeast kinetochore, or whether the structure will be fundamentally different. Collectively, these experiments provide a face for the yeast kinetochore and a foundation for future studies.

References

1. Welburn, J. P. I., and Cheeseman, I. M. (2008). Toward a molecular structure of the eukaryotic kinetochore. Developmental Cell *15*, 645–655.

2. Alushin, G., and Nogales, E. (2011). Visualizing kinetochore architecture. Curr Opin Struct Biol. 21, 661-669.

3. Ben-Shem, A., Garreau de Loubresse, N., Melnikov, S., Jenner, L., Yusupova, G., and Yusupov, M. (2011). The structure of the eukaryotic ribosome at 3.0 Å resolution. Science *334*, 1524–1529.

4. Bilokapic, S., and Schwartz, T. U. (2012). 3D ultrastructure of the nuclear pore complex. Current Opinion in Cell Biology *24*, 86–91.

5. Gonen, S., Akiyoshi, B., Iadanza, M.G., Shi D., Duggan N., Biggins S., Gonen T. (2012) The structure of purified kinetochores reveals multiple microtubule attachment sites. Nature Structure and Molecular Biology Sep;19(9):925-9.

6. McEwen, B. F., and Dong, Y. (2010). Contrasting models for kinetochore microtubule attachment in mammalian cells. Cell. Mol. Life Sci. *67*, 2163–

2172.

7. Westermann, S., Drubin, D. G., and Barnes, G. (2007). Structures and functions of yeast kinetochore complexes. Annu. Rev. Biochem. *76*, 563–591.

8. Müller-Reichert, T., Sassoon, I., O'Toole, E., Romao, M., Ashford, A. J., Hyman, A. A., and Antony, C. (2003). Analysis of the distribution of the kinetochore protein Ndc10p in Saccharomyces cerevisiae using 3-D modeling of mitotic spindles. Chromosoma *111*, 417–428.

9. Perpelescu, M., and Fukagawa, T. (2011). The ABCs of CENPs. Chromosoma *120*, 425–446.

10. Joglekar, A. P., Bloom, K., and Salmon, E. D. (2009). In vivo protein architecture of the eukaryotic kinetochore with nanometer scale accuracy. Curr. Biol. *19*, 694–699.

11. Wan, X., O'Quinn, R. P., Pierce, H. L., Joglekar, A. P., Gall, W. E., DeLuca, J. G., Carroll, C. W., Liu, S.-T., Yen, T. J., McEwen, B. F., et al. (2009). Protein architecture of the human kinetochore microtubule attachment site. Cell *137*, 672–684.

12. Lawrimore, J., Bloom, K. S., and Salmon, E. D. (2011). Point centromeres contain more than a single centromere-specific Cse4 (CENP-A) nucleosome. J. Cell Biol. *195*, 573–582.

13. Joglekar, A. P., Bloom, K. S., and Salmon, E. D. (2010). Mechanisms of force generation by end-on kinetochore-microtubule attachments. Current Opinion in Cell Biology *22*, 57–67.

14. Miranda, J. J. L., De Wulf, P., Sorger, P. K., and Harrison, S. C. (2005). The yeast DASH complex forms closed rings on microtubules. Nat. Struct. Mol. Biol. *12*, 138–143.

15. McEwen, B. F., Chan, G. K., Zubrowski, B., Savoian, M. S., Sauer, M. T., and Yen, T. J. (2001). CENP-E is essential for reliable bioriented spindle attachment, but chromosome alignment can be achieved via redundant mechanisms in mammalian cells. Mol. Biol. Cell *12*, 2776–2789.

16. Burrack, L. S., Applen, S. E., and Berman, J. (2011). The requirement for the Dam1 complex is dependent upon the number of kinetochore proteins and microtubules. Curr. Biol. *21*, 889–896.

17. Akiyoshi, B., Nelson, C. R., Ranish, J. A., and Biggins, S. (2009). Quantitative proteomic analysis of purified yeast kinetochores identifies a

PP1 regulatory subunit. Genes Dev. *23*, 2887–2899.

18. Akiyoshi, B., Sarangapani, K. K., Powers, A. F., Nelson, C. R., Reichow, S. L., Arellano-Santoyo, H., Gonen, T., Ranish, J. A., Asbury, C. L., and Biggins, S. (2010). Tension directly stabilizes reconstituted kinetochore-microtubule attachments. Nature *468*, 576–579.

19. Tien, J. F., Umbreit, N. T., Gestaut, D. R., Franck, A. D., Cooper, J., Wordeman, L., Gonen, T., Asbury, C. L., and Davis, T. N. (2010). Cooperation of the Dam1 and Ndc80 kinetochore complexes enhances microtubule coupling and is regulated by aurora B. J. Cell Biol. *189*, 713–723.